UNIVERSIDADE FEDERAL DE MINAS GERAIS
Faculdade de Odontologia
Colegiado de Pós-Graduação em Odontologia

Jader Oliva Jorge

COMPARAÇÃO ENTRE AS PROPRIEDADES FÍSICAS E MECÂNICAS DE ALINHADORES ORTODÔNTICOS CONFECCIONADOS POR TERMOFORMAGEM E POR IMPRESSÃO TRIDIMENSIONAL DIRETA (3D): *UMA REVISÃO SISTEMÁTICA E METANÁLISE*

Belo Horizonte
2025

Jader Oliva Jorge

COMPARAÇÃO ENTRE AS PROPRIEDADES FÍSICAS E MECÂNICAS DE ALINHADORES ORTODÔNTICOS CONFECCIONADOS POR TERMOFORMAGEM E POR IMPRESSÃO TRIDIMENSIONAL DIRETA (3D): *UMA REVISÃO SISTEMÁTICA E METANÁLISE*

Dissertação apresentada ao Colegiado de Pós-Graduação em Odontologia da Faculdade de Odontologia da Universidade Federal de Minas Gerais, como requisito parcial à obtenção do grau de Mestre em Odontologia – área de concentração Clínica Odontológica

Orientador (a): Prof (a) Soraia Macari
Coorientador (a): Prof (a) Lucas Guimarães Abreu

Belo Horizonte
2025

Ficha Catalográfica

J82c 2025 MP

Jorge, Jader Oliva.
Comparação entre as propriedades físicas e mecânicas de alinhadores ortodônticos confeccionados por termoformagem e por impressãotridimensional direta (3d): uma revisão sistemática e metanálise / Jader Oliva Jorge. -- 2025.

154 f. : il.

Orientadora: Soraia Macari .
Coorientador: Lucas Guimarães Abreu.

Dissertação (Mestrado) -- Universidade Federal de Minas Gerais, Faculdade de Odontologia.

1. Ortodontia. 2. Aparelhos ortodônticos removíveis. 3. Revisão sistemática. 4. Testes mecânicos. 5. Precisão da medição dimensional. I. Macari , Soraia . II. Abreu, Lucas Guimarães. III. Universidade Federal de Minas Gerais. Faculdade de Odontologia. IV. Título.

BLACK - D047

Elaborada por: Miriam Cândida de Jesus - CRB 6/2727.

UNIVERSIDADE FEDERAL DE MINAS GERAIS

FACULDADE DE ODONTOLOGIA

COLEGIADO DO CURSO DE PÓS-GRADUAÇÃO EM ODONTOLOGIA

FOLHA DE APROVAÇÃO

COMPARAÇÃO ENTRE AS PROPRIEDADES FÍSICAS E MECÂNICAS DE ALINHADORES ORTODÔNTICOS CONFECCIONADOS POR TERMOFORMAGEM E POR IMPRESSÃO TRIDIMENSIONAL DIRETA (3D): *UMA REVISÃO SISTEMÁTICA E METANÁLISE*

JADER OLIVA JORGE

Dissertação submetida à Banca Examinadora designada pelo Colegiado do Programa de Pós-Graduação em ODONTOLOGIA, como requisito para obtenção do grau de Mestre em ODONTOLOGIA, área de concentração CLÍNICA ODONTOLÓGICA.

Aprovada em 31 de julho de 2025, pela banca constituída pelos membros:

Profa. Soraia Macari - Orientadora
Faculdade de Odontologia da UFMG

Profa. Cristiane Canavarro Rodrigues Martins
Universidade Estadual do Rio de janeiro - UERJ

Profa. Carina Cristina Montalvany Antonucci
UFMG

Belo Horizonte, 31 de julho de 2025.

Documento assinado eletronicamente por **Carina Cristina Montalvany Antonucci**, **Usuária Externa**, em 31/07/2025, às 10:54, conforme horário oficial de Brasília, com fundamento no art. 5º do Decreto nº 10.543, de 13 de novembro de 2020.

Documento assinado eletronicamente por **Cristiane Canavarro Rodrigues Martins**, **Usuária Externa**, em 31/07/2025, às 10:54, conforme horário oficial de Brasília, com fundamento no art. 5º do Decreto nº 10.543, de 13 de novembro de 2020.

Documento assinado eletronicamente por **Soraia Macari**, **Professora do Magistério Superior**, em 31/07/2025, às 10:54, conforme horário oficial de Brasília, com fundamento no art. 5º do Decreto nº 10.543, de 13 de novembro de 2020.

A autenticidade deste documento pode ser conferida no site https://sei.ufmg.br/sei/controlador_externo.php?acao=documento_conferir&id_orgao_acesso_externo=0, informando o código verificador **4352696** e o código CRC **7B8CC30B**.

AGRADECIMENTOS

Gostaria de expressar minha mais sincera gratidão à minha orientadora, Profª Dra. Soraia Macari, por sua orientação excepcional, paciência e incentivo ao longo de toda a realização deste trabalho. Sua sabedoria, dedicação e apoio foram fundamentais para o desenvolvimento deste estudo, e sou imensamente grato pela oportunidade de aprender com você.

Ao meu coorientador, Prof. Dr. Lucas Guimarães Abreu, registro meu profundo agradecimento pela valiosa contribuição científica, pelas sugestões criteriosas e pelo constante apoio acadêmico ao longo de toda minha jornada. Sua escuta atenta, olhar analítico e disponibilidade foram essenciais para a construção crítica deste trabalho e para o meu crescimento como pesquisador.

À minha família, meu sincero agradecimento. A força e a motivação que vocês me oferecem são a base do meu esforço constante. Em especial, quero dedicar um agradecimento a minha mãe, Lourdes, que sempre esteve ao meu lado, acreditando em meu potencial, e a todos os membros da minha família que, de maneira direta ou indireta, me incentivaram e acompanharam cada passo.

Aos meus amigos, especialmente àqueles que estiveram comigo em todos os momentos, compartilhando risadas, desafios e conquistas. O apoio, as conversas e as amizades sinceras de cada um de vocês foram essenciais para que eu chegasse até aqui.

Por fim, agradeço à Coordenação de Aperfeiçoamento de Pessoal de Nível Superior (CAPES) pelo apoio financeiro, que permitiu a minha dedicação ao mestrado. Estendo o agradecimento às demais agências de fomento pelo papel fundamental no fortalecimento da pesquisa científica no país.

.

"Fazer ciência é, acima de tudo, ter a coragem de questionar o desconhecido."

Marie Curie

RESUMO

Alinhadores ortodônticos estéticos são dispositivos removíveis, confeccionados em material polimérico, amplamente utilizados na correção de má oclusões dentárias. Esses alinhadores podem ser fabricados por termoformagem (AOCT) ou por impressão tridimensional direta (AOCITD). As diferentes tecnicas de aquisição conferem características distintas aos dispositivos e podem influenciar seu desempenho clínico. Esta revisão sistemática objetivou comparar as propriedades físicas e mecânicas de AOCT e AOCID. Foi realizada uma busca abrangente em seis bases eletrônicas (maio/2025), incluindo estudos laboratoriais *in vitro* que avaliaram comparativamente AOCT e AOCID. A seleção dos estudos, a extração de dados e a avaliação do risco de viés foram conduzidas por dois revisores independentes. Quando possível, os dados foram combinados em metanálises. Um total de 23 estudos foi incluído na revisão, dos quais 4 atingiram os critérios para uma metanálise. Os AOCID apresentaram desempenho superior em diversos parâmetros. Observou-se redução significativa da espessura nos AOCT (−39,76%, DP=14,09) e aumento nos AOCID (+11,02%, DP=21,43; p<0,001). A acurácia geométrica favoreceu os AOCID (p<0,001), que também apresentaram menor temperatura de transição vítrea (42,3 °C), maior recuperação de forma (p<0,001), maior força em tração vertical (p<0,005), melhor adaptação marginal e menor adesão bacteriana (p<0,005). Os AOCT, por sua vez, mostraram maior estabilidade dos módulos de armazenamento (p<0,005), maior microdureza (p<0,005), maior resistência à flexão (p<0,05) e maior estabilidade sob compressão cíclica. Quanto à rugosidade superficial, os AOCID apresentaram valores mais elevados de Sa (SMD=2,73; IC95%: 2,14–3,31; p<0,00001) e Sz após uso (SMD=1,70; IC95%: 0,67–2,74; p=0,001), enquanto os AOCT mostraram valores superiores de Sv (SMD=–1,19; IC95%: –2,29 a –0,08; p=0,04) e menores de Sa após uso (SMD=–1,07; IC95%: –2,12 a –0,02; p=0,04). Não houve diferença significativa entre a espessura planejada e a real (SMD=1,48; IC95%: –7,26 a 4,30; p=0,62). A heterogeneidade metodológica que os estudos incluídos apresentaram limiataram análises adicionais. **Conclusão:** Os AOCID apresentaram vantagens físicas, mecânicas e comportamentais em relação aos AOCT. Entretanto, a falta de padronização metodológica entre os estudos e a ausência de validação clínica limitam a robustez das evidências, destacando a necessidade de protocolos experimentais uniformes e de investigações clínicas futuras para orientar a prática ortodôntica baseada em evidências.

Palavras-chave: ortodontia; aparelhos ortodônticos removíveis; revisão sistemática; testes mecânicos; precisão da medição dimensional.

ABSTRACT

Comparison between the physical and mechanical properties of orthodontic aligners made by thermoforming and direct three-dimensional (3d) printing: a systematic review and meta-analysis

Aesthetic orthodontic aligners are removable polymer-based devices widely used for the correction of dental malocclusions. These aligners can be fabricated using thermoforming (AOCT) or direct three-dimensional printing (AOCID). The different manufacturing techniques impart distinct characteristics to the devices, which may influence their clinical performance. This systematic review aimed to compare the physical and mechanical properties of AOCT and AOCID. A comprehensive search was performed in six electronic databases (May/2025), including in vitro laboratory studies that directly compared AOCT and AOCID. Study selection, data extraction, and risk of bias assessment were independently conducted by two reviewers. When feasible, data were synthesized through meta-analyses. A total of 23 studies met the inclusion criteria, of which 4 were eligible for meta-analysis. AOCID demonstrated superior performance across multiple parameters. AOCT showed a significant reduction in thickness (−39.76%, SD=14.09), whereas AOCID exhibited an increase (+11.02%, SD=21.43; $p<0.001$). Geometric accuracy favored AOCID ($p<0.001$), which also presented a lower glass transition temperature (42.3 °C), greater shape recovery ($p<0.001$), higher vertical tensile forces ($p<0.005$), improved marginal adaptation, and reduced bacterial adhesion ($p<0.005$). Conversely, AOCT demonstrated greater storage modulus stability ($p<0.005$), higher microhardness ($p<0.005$), greater flexural strength ($p<0.05$), and better stability under cyclic compression. Regarding surface roughness, AOCID exhibited higher Sa values (SMD=2.73; 95%CI: 2.14–3.31; $p<0.00001$) and Sz after use (SMD=1.70; 95%CI: 0.67–2.74; $p=0.001$), while AOCT showed higher Sv (SMD=−1.19; 95%CI: −2.29 to −0.08; $p=0.04$) and lower Sa after use (SMD=−1.07; 95%CI: −2.12 to −0.02; $p=0.04$). No significant difference was observed between planned and actual thickness (SMD=1.48; 95%CI: −7.26 to 4.30; $p=0.62$). Methodological heterogeneity among the included studies limited additional analyses. AOCID presented physical, mechanical, and behavioral advantages over AOCT. However, methodological variability and the lack of clinical validation weaken the strength of current evidence, highlighting the need for standardized experimental protocols and future clinical investigations to guide evidence-based orthodontic practice.

Keywords: orthodontics; orthodontic appliances, removable; systematic review; mechanical tests; dimensional measurement accuracy.

LISTA DE FIGURAS

ARTIGO

LISTA DE TABELAS

ARTIGO

LISTA DE ABREVIATURAS E SIGLAS

AOCID - Alinhador Ortodôntico Confeccionado por Impressão Tridimensional Direta

AOCT - Alinhador Ortodôntico Confecionado por Termoformagem

CLSM - Microscopia Confocal de Varredura a Laser (Confocal Laser Scanning Microscopy)

DLP - Processamento Digital de Luz (Digital Light Processing)

DLP - Processamento Digital de Luz (Digital Light Processing)

DMA - Análise Mecânica Dinâmica (Dynamic Mechanical Analysis)

DSC - Calorimetria Diferencial de Varredura (Differential Scanning Calorimetry)

IIT - Indentação Instrumentada (Instrumented Indentation Test)

MEV - Microscopia Eletrônica de Varredura (Scanning Electron Microscopy)

PC - Policarbonato (Polycarbonate)

PETG - Polietileno Tereftalato Glicol (Polyethylene Terephthalate Glycol)

PP - Polipropileno (Polypropylene)

PU - Poliuretano (Polyurethane)

Sa - Amplitude Média Absoluta da Superfície (Surface Arithmetic Average)

SLA - Estereolitografia (Stereolithography)

SLS - Sinterização Seletiva a Laser (Selective Laser Sintering)

SLS - Sinterização Seletiva a Laser (Selective Laser Sintering)

Sq - Desvio Quadrático Médio da Altura da Superfície (Surface Root Mean Square)

Sv - Profundidade Máxima dos Vales (Maximum Valley Depth)

Sz - Amplitude Total Entre Picos e Vales Extremos (Total Height of Surface Profile

Tg - Temperatura de Transição Vitrificada (Glass Transition Temperature)

VHN - Dureza Vickers (Vickers Hardness Number)

SUMÁRIO

1 CONSIDERAÇÕES INICIAIS

A qualidade de vida é um processo dinâmico e continuamente construído, envolvendo fatores objetivos e subjetivos, além das expectativas individuais (Allison, Locker *et al.,* 1997; Abreu 2018; Göranson, Sonesson *et al.,* 2023). Esses aspectos impactam diretamente diversas áreas da saúde, incluindo a odontologia (ElNaghy, Hasanin 2023). Na ortodontia, a maloclusão pode comprometer funções orais, prejudicar a estética facial e influenciar negativamente o desenvolvimento psicológico (Kiyak 2008; Ribeiro, Antunes *et al.,* 2023). Nesse contexto, a busca por alternativas aos bráquetes ortodônticos tradicionais tem aumentado consideravelmente (Zheng, Liu *et al.,* 2017; Flores-Mir, Brandelli *et al.,* 2018)

Tradicionalmente, o tratamento ortodôntico é realizado com bráquetes metálicos, que dificultam a higienização, aumentam o risco de acúmulo de biofilme e lesões nos tecidos moles, além de causarem desconforto estético e social (Allison, Locker *et al.,* 1997; Di Spirito, D'Ambrosio *et al.,* 2023). Como alternativa, os alinhadores ortodônticos estéticos surgem como opção eficaz, proporcionando maior aceitação estética, menor desconforto, melhor controle periodontal e menor tempo clínico (Levrini, Mangano *et al.,* 2015; Borda, Garfinkle *et al.,* 2020). Entretanto, esses dispositivos também apresentam limitações, incluindo dificuldades na realização de determinados movimentos dentoalveolares, dependência da colaboração do paciente e custos mais elevados. Apesar disso, estudos indicam que mais de 90% dos jovens adultos preferem alinhadores aos bráquetes convencionais quando submetidos a tratamento ortodôntico (Gao, Yan *et al.,* 2022).

A confecção de alinhadores ortodônticos estéticos pode ocorrer por meio de dois métodos principais: termoformagem (AOCT) ou impressão tridimensional direta (AOCID). No processo de termoformagem, uma lâmina termoplástica é aquecida e moldada sobre um modelo dentário, o que pode gerar alterações geométricas e comprometer a espessura final do alinhador. Por outro lado, os AOCID são produzidos camada a camada por impressão 3D, permitindo maior precisão e controle dimensional (Papadopoulou 2019). Essas diferenças nos métodos de fabricação influenciam diretamente propriedades físicas e mecânicas, como resistência à flexão, recuperação de forma, estabilidade térmica e rugosidade superficial, podendo impactar o desempenho clínico dos alinhadores (Gao, Yan *et al.,* 2022). Apesar do crescente uso dos AOCID, a literatura ainda carece de

evidências científicas robustas que comparem suas propriedades físico-mecânicas em relação aos alinhadores termoformados, configurando uma lacuna de conhecimento que motiva a presente investigação.

2 REVISAO DE LITERATURA

O avanço tecnológico na ortodontia tem sido contínuo ao longo das últimas décadas, proporcionando melhorias significativas nos processos terapêuticos e na redução do tempo necessário para alcançar resultados clínicos satisfatórios. A crescente demanda por alternativas menos invasivas estimulou o desenvolvimento de dispositivos capazes de corrigir efetivamente as posições dentárias, oferecendo simultaneamente conforto e melhor estética aos pacientes (Boyd 2008). Diversas opções surgiram como substitutas parciais dos aparelhos fixos convencionais, incluindo aparelhos cerâmicos, ortodontia lingual e, mais recentemente, alinhadores estéticos transparentes (Srivastava, Jyoti *et al.,* 2017; Zinelis, Panayi *et al.,* 2022).

O mecanismo de ação dos alinhadores pode seguir duas abordagens principais: abordagem de movimento dirigido**,** na qual as placas são projetadas para posicionar gradualmente os dentes até a posição desejada; e abordagem de forças direcionadas, em que o alinhador exerce forças contínuas, auxiliado por recursos adicionais, como attachments de resina, permitindo movimentos dentários unitários ou em bloco. Os sistemas contemporâneos frequentemente combinam ambas as abordagens para otimizar a eficiência biomecânica do tratamento (Dasy, Dasy *et al.,* 2015; Lombardo, Arreghini *et al.,* 2017).

Historicamente, o conceito de alinhadores ortodônticos foi introduzido por Kesling (1945), que utilizou placas de borracha flexível para o refinamento e contenção pós-tratamento com aparelhos fixos. Posteriormente, Ponitz (1971) apresentou o “retentor invisível”, confeccionado a partir de modelos em cera, ainda limitado em termos de amplitude de movimento dentário. Em 1994, Sheridan e colaboradores propuseram uma técnica que associava a redução interproximal do esmalte à utilização de placas sucessivas para alinhamento gradual (Phan, Ling 2007). Apesar de suas limitações, essa abordagem foi utilizada por anos, demandando novos modelos de setup e moldagens a cada consulta, o que acarretava maior desconforto ao paciente e elevado tempo clínico (Kesling 1945; Joffe 2003).

A consolidação dos alinhadores ocorreu em 1997, na Califórnia (EUA), com a criação do sistema Invisalign® pela empresa Align Technology, disponibilizado comercialmente em 1999. O método incorporou o processamento digital das impressões das arcadas dentárias, permitindo a confecção seriada de

placas transparentes personalizadas, representando um marco no uso clínico dos alinhadores estéticos (Bichu, Alwafi *et al.,* 2023).

Bichu *et al.,* (2023) abordaram em seu estudo as diferentes gerações de alinhadores ortodônticos, com suas respectivas características, estudadas na literatura por diversos pesquisadores ao longo dos anos. A partir da observação desses dados, é possível classificar os alinhadores em oito fases distintas (Hennessy, Al-Awadhi 2016; Ganta, Cheruvu *et al.,* 2021; Moshiri, Kravitz *et al.,* 2021; Wajekar, Pathak *et al.,* 2022; Bichu, Alwafi *et al.,* 2023).

Os alinhadores ortodônticos de primeira geração não possuíam quaisquer elementos de auxílio para movimentação dentoalveolar, além de seu arcabouço plástico termoformado. Esse material, conhecido como Proceed30 (PC30), era formado por uma mistura de polímeros que se mostrou ineficiente na correção de má oclusões, devido às suas propriedades físicas e mecânicas inadequadas (Condo, Pazzini *et al.,* 2018).

Haja vista as desvantagens dos alinhadores de primeira geração, pesquisadores incorporaram aos tratamentos o uso de attachments fixados à superfície do esmalte dentário, além de elásticos intermaxilares e recursos tecnológicos de planejamento digital, como o SmartForce™ e o Power Ridge™, que otimizaram a velocidade e o controle do tratamento ortodôntico, dando início à segunda geração de alinhadores ortodônticos. O material utilizado para confecção também foi alterado para um polímero de camada única conhecido por Exceed30 (EX30), que apresentava propriedades físicas e mecânicas superiores ao PC30 (Eliades, Bourauel 2005).

A partir do ano de 2010, a Invisalign Technology introduziu em seus alinhadores avanços tecnológicos ligados diretamente ao software de planejamento ortodôntico, como os recursos SmartForce™ e Power Ridge. Tais inovações possibilitavam a introdução automática de attachments personalizados e indentações na placa alinhadora em locais específicos, melhorando o controle ortodôntico em movimentos complexos como rotação e torque, surgiu assim os alinhadores de terceira geração (Moshiri, Kravitz *et al.,* 2021).

No ano seguinte, houve a criação dos alinhadores de quarta geração, onde foi acrescentada ao software planejador a possibilidade de utilização da tecnologia de attachments G4, que facilitava os movimentos ortodônticos para correção de mordidas abertas, uma vez que permitia acrescentar attachments em

múltiplos dentes anteriores para realizar movimentos multiplanares em um só momento (Moshiri, Kravitz *et al.,* 2021).

Em 2013, um novo material polimérico para termoformagem dos alinhadores foi oficialmente lançado: o SmartTrack™ (LD30)**,** composto por múltiplas camadas de poliuretano/co-poliéster aromático. As vantagens sobre o EX30 são diversas, como melhor ajuste e encaixe, sentido tanto pelo ortodontista quanto pelo paciente, maior controle nos movimentos, forças mais previsíveis, além de maior elasticidade (Bräscher, Zuran *et al.,* 2016).

Os alinhadores de quinta geração surgiram entre 2013 e 2014, com aprimoramentos tecnológicos voltados para correção de mordidas profundas, por meio do acréscimo de rampas e áreas de pressão na superfície lingual dos incisivos superiores (Blundell, Weir *et al.,* 2022).

No final do ano seguinte, foram lançados os alinhadores de sexta geração, que apresentaram como novidade o planejamento de casos ortodônticos complexos com necessidade de exodontia de pré-molares. Esta geração introduziu o design SmartStage™, aliado aos recursos SmartForce™**,** garantindo movimentação dentária com paralelismo radicular (Blundell, Weir *et al.,* 2022).

Os alinhadores de sétima geração**,** lançados em 2016, foram voltados ao tratamento ortodôntico de adolescentes, com ênfase no controle dos incisivos laterais superiores e na prevenção de recidivas de mordida aberta anterior (Moshiri, Kravitz *et al.,* 2021).

Por fim, entre 2020 e 2021, a tecnologia de alinhadores termoformados alcançou seu ápice com os alinhadores de oitava geração, com melhorias voltadas ao tratamento e prevenção de recidiva de mordida profunda e controle mais preciso da coroa dos molares em movimentos de expansão dentoalveolar. Esses dispositivos utilizam a tecnologia SmartForce™ para intrusão anterior e controle de potenciais rotações das coroas dentárias. Houve também um avanço significativo no software de controle ortodôntico, que passou a permitir o nivelamento da curva de Spee (Moshiri, Kravitz *et al.,* 2021).

Houve também uma evolução nos materiais empregados na fabricação das placas. Os primeiros alinhadores eram produzidos com o polímero vulcanite**;** atualmente, utilizam-se predominantemente polietileno tereftalato glicol (PETG)**,** poliuretano (PU)**,** polipropileno ou policarbonato (Hahn, Engelke *et al.,* 2010; Rossini, Parrini *et al.,* 2015; Condo, Pazzini *et al.,* 2018). Na termoformagem, o processo

inicia-se pelo escaneamento intraoral da arcada dentária, seguido de manipulação digital dos dentes via software e adaptação de lâminas termoplásticas sob pressão de ar ou vácuo (Weir 2017; Koenig, Choi *et al.,* 2022). Apesar de proporcionar ganhos estéticos expressivos em relação à aparatologia fixa, o método é trabalhoso e apresenta custos relativamente elevados (Zinelis, Panayi *et al.,* 2022).

Com o avanço dos materiais e das tecnologias digitais, surgiram os AOCID (Alinhadores Ortodônticos Confeccionados por Impressão Direta), os quais também utilizam dados de scanners intraorais para manipulação tridimensional dos elementos dentários e confecção do alinhador (Maspero, Tartaglia 2020; Nakornnoi, Srirodjanakul *et al.,* 2024). Fabricados majoritariamente com resinas epóxi e fotopolímeros, esses alinhadores apresentam vantagens adicionais, como redução do tempo laboratorial, menor custo, diminuição da geração de resíduos e propriedades físico-mecânicas superiores quando comparados aos AOCT (Alhasyimi, Ayub *et al.,* 2024).

A literatura relata que a produção dos alinhadores por impressão tridimensional direta impacta diretamente na praticidade e facilidade do ortodontista em exercer sua função com qualidade e competência, de modo que os AOCID diminuem a cadeia de suprimentos para a produção dos aparelhos, reduzindo o prazo de entrega das placas aos pacientes e os custos, especialmente quando fabricadas pelo próprio ortodontista. A tendência atual é a redução de resíduos tóxicos e prejudiciais ao meio ambiente, e os AOCID se mostraram mais aceitáveis e menos prejudiciais do que os AOCT (Bichu, Alwafi *et al.,* 2023).

Um fator que precisa ser considerado é a possibilidade de desvios na produção em camadas dos AOCID, com consequentes alterações na precisão dimensional dos movimentos ortodônticos. Jindal *et al.,* (2019) identificaram que a orientação de impressão do equipamento utilizado, o tempo e principalmente a temperatura de cura do alinhador pós-impressão são fatores determinantes nas alterações físicas e mecânicas, como resistência à carga e compressão das placas alinhadoras (Jindal, Juneja *et al.,* 2019).

Outra preocupação que surge ao se trabalhar com materiais impressos em 3D refere-se à toxicidade das resinas. Autores identificaram em suas pesquisas que essa toxicidade reduz gradualmente após a polimerização e o processo de pós-cura do material. Por essa razão, uma impressão controlada, com protocolos

específicos e detalhados, deve ser sempre seguida para a aquisição segura de AOCID (FayyazAhamed, Kumar *et al.,* 2020).

Kumar (2019) realizou um estudo comparativo com o objetivo de avaliar a citotoxicidade de diversos alinhadores ortodônticos, termoformados e impressos em 3D. Seus resultados evidenciaram que o alinhador que apresentou menor potencial citotóxico foi o Invisalign®, seguido pela resina Dental LT utilizada para impressão tridimensional, ressaltando que, na época deste estudo, essa resina ainda não estava licenciada para produção de AOCID. FayyazAhamed *et al.,* (2020) realizaram uma pesquisa semelhante, que confirmou os achados de Kumar (2019), demonstrando, por meio de análises in vitro de viabilidade celular, que o Invisalign® apresenta maior biocompatibilidade que os AOCID (Kumar 2019; FayyazAhamed, Kumar *et al.,* 2020),

A grande inovação na tecnologia de impressão direta de alinhadores ocorreu em 2021 com o lançamento de uma resina idealizada especificamente para alinhadores ortodônticos, produzida pela empresa sul-coreana Graphy. Essa resina apresenta como principal característica sua capacidade de memória de forma a temperaturas intraorais, o que garante um controle de forças contínuo e preciso durante o uso do alinhador. Outra novidade apresentada pela fabricante foi a compatibilidade da resina com qualquer marca e modelo de impressoras 3D, garantindo rápida disseminação do produto (Lee, Kim *et al.,* 2022).

Os alinhadores Graphy são confeccionados com propriedades físicas e mecânicas únicas, que permitem, por exemplo, a desinfecção completa da placa por meio de escovação, além de suportarem temperaturas de até 100 °C por até dois minutos (Lee, Kim *et al.,* 2022).

A biocompatibilidade é um requisito essencial para os alinhadores ortodônticos, uma vez que permanecem em contato direto com o esmalte e as mucosas bucais por, no mínimo, 22 horas diárias (Raszewski, Chojnacka *et al.,* 2022). Embora os materiais termoplásticos empregados sejam considerados seguros, não são quimicamente inertes e sofrem alterações estruturais e físico-químicas quando expostos ao ambiente bucal, calor, umidade e forças mastigatórias (Di Spirito, D'Ambrosio *et al.,* 2023). Alinhadores impressos em 3D, especificamente, necessitam de pós-cura controlada para assegurar suas propriedades de biocompatibilidade (Safavi, Bordbar-Khiabani *et al.,* 2022).

2.1 Propriedades Mecânicas dos Alinhadores Ortodônticos Estéticos

Apesar dos avanços tecnológicos e da evolução dos métodos de tratamento das más oclusões, os alinhadores ortodônticos estéticos ainda apresentam limitações biomecânicas que comprometem, ou dificultam, a execução de determinados movimentos dentários complexos. Movimentos como extrusão e rotação, por exemplo, apresentam as menores taxas de precisão quando comparados a outros tipos de deslocamentos dentários (Rossini, Parrini *et al.,* 2015; Haouili, Kravitz *et al.,* 2020). Nessas situações, frequentemente é necessária a utilização de recursos auxiliares, como acessórios ortodônticos e dispositivos de bioancoragem, para garantir um refinamento e finalização mais previsíveis dos casos clínicos (Fang, Li *et al.,* 2020).

Diversos estudos têm investigado essas alterações físicas e mecânicas dos alinhadores ortodonticos. Dalaie *et al.,* (2021) avaliaram os efeitos da termoformagem e do envelhecimento artificial em alinhadores confeccionados em polietileno tereftalato glicol (PETG), utilizando ciclos térmicos e testes mecânicos, incluindo ensaios de flexão em três pontos e dureza Vickers. Os resultados demonstraram redução significativa do módulo de elasticidade após a termoformagem, embora o envelhecimento térmico não tenha produzido alterações estatisticamente relevantes (Dalaie, Behnia *et al.,* 2021).

De forma semelhante, Fang *et al.,* (2020) conduziram um estudo *in vivo* com alinhadores Invisalign fabricados em LD30, Smart Track, submetendo-os a ensaios mecânicos antes e após duas semanas de uso clínico. Apesar de terem sido detectadas alterações físicas e microdefeitos na superfície dos alinhadores por meio de microscopia eletrônica de varredura (MEV), as mudanças não foram estatisticamente significativas (Fang, Li *et al.,* 2020).

Alexandropoulos *et al.,* (2015) compararam diferentes marcas comerciais, A+, Clear Aligner, Essix ACE e Invisalign, avaliando propriedades químicas e físicas. Os alinhadores de PETG, como A+, Clear Aligner, Essix ACE, apresentaram menor módulo de elasticidade e dureza, porém melhor desempenho em testes de fluência quando comparados aos de poliuretano, Invisalign. Em concordância, Ryu *et al.,* (2018) realizaram testes de transparência, absorção de água, solubilidade, dureza e módulo elástico em materiais termoformados, Duran, Essix A+, Essix ACE, eCligner, submetidos a termociclagem, constatando que a absorção de água e a transparência

diminuíram com o envelhecimento, enquanto o módulo de tensão e flexão variou de acordo com a espessura das amostras (Alexandropoulos, Al Jabbari *et al.,* 2015; Ryu, Kwon *et al.,* 2018).

Pesquisas recentes também analisaram AOCID. Can *et al.,* (2022) investigaram alinhadores confeccionados em resina TC-85DAC, da Graphy, após uma semana de uso in vivo e observaram que as propriedades mecânicas se mantiveram estáveis, embora o material avaliado não seja amplamente utilizado comercialmente. Milovanović *et al.,* (2021), por sua vez, avaliaram o polímero Dental LT Clear V1 (base de éster acrílico) e encontraram manutenção das propriedades mecânicas, como tração, tensão e flexão, após sete dias de envelhecimento. Jindal *et al.,* (2019) compararam AOCT e AOCID, concluindo que estes últimos apresentaram maior estabilidade estrutural e resistência mecânica (Jindal, Juneja *et al.,* 2019; Milovanović, Sedmak *et al.,* 2021; Can, Panayi *et al.,* 2022).

Em outra linha de pesquisa, Fang *et al.,* (2020) analisaram quatro materiais termoplásticos, F22 Aligner, Duran, Erkoloc-Pro, Durasoft, e identificaram uma rápida liberação de estresse nas primeiras oito horas de uso, seguida de estabilização até 24 horas. Um estudo subsequente ampliou o tempo de observação para 14 dias e adicionou o material F22 Evoflex, confirmando o mesmo comportamento (Fang, Li *et al.,* 2020; Albertini, Colombo *et al.,* 2022).

A microscopia eletrônica de varredura tem sido amplamente empregada para avaliar alterações morfológicas nos alinhadores. Condò *et al.,* (2021) compararam dois polímeros de poliuretano, Smart Track e Exceed30, antes e após duas semanas de uso clínico. Foram observadas fissuras e trincas, mais pronunciadas no Exceed30, embora a estabilidade química global tenha sido mantida. Linjawi *et al.,* (2022), utilizando MEV, demonstraram que o ajuste adaptativo dos alinhadores melhora com o tempo, apresentando melhores resultados após 15 dias de uso (Condò, Mampieri *et al.,* 2021; Linjawi, Abushal 2022).

Considerando esses achados, ainda não há consenso na literatura sobre a estabilidade física e mecânica dos materiais utilizados para a confecção de alinhadores ortodônticos estéticos, especialmente sob condições intraorais prolongadas. As evidências disponíveis são mais robustas para estudos *in vitro*, enquanto investigações clínicas *in vivo* permanecem limitadas, reforçando a

necessidade de pesquisas adicionais para compreender o comportamento mecânico e os possíveis subprodutos liberados por esses dispositivos durante o uso.

3. OBJETIVOS

3.1 Objetivo geral

- Avaliar e comparar as alterações nas propriedades físicas e mecânicas de alinhadores ortodônticos confeccionados por termoformagem e por impressão tridimensional direta (3D).

3.2 Objetivos específicos

- Analisar as propriedades físicas dos alinhadores ortodônticos confeccionados por termoformagem e impressão tridimensional direta, incluindo aspectos como espessura, densidade e resistência ao desgaste.

-Avaliar as propriedades mecânicas dos alinhadores, incluindo a resistência à flexão, módulo de elasticidade e força de atuação, comparando os diferentes métodos de fabricação.

- Investigar as propriedades térmicas dos alinhadores, como sua resposta à temperatura corporal e sua estabilidade sob diferentes condições térmicas, considerando os processos de termoformagem e impressão 3D.

- Examinar os métodos de teste utilizados para avaliar as propriedades dos alinhadores, comparando sua aplicabilidade, reprodutibilidade e relevância para a prática clínica.

4. METODOLOGIA EXPANDIDA

4.1 Protocolo e Registro

Esta revisão sistemática foi conduzida de acordo com as diretrizes do Preferred Reporting Items for Systematic Reviews and Meta-Analyses (PRISMA) (Moher, Liberati *et al.,* 2009). O protocolo foi registrado na plataforma Open Science Framework (OSF) sob o identificador: https://doi.org/10.17605/OSF.IO/BT98F.

4.2 Critérios de Elegibilidade

Foram incluídos exclusivamente estudos *in vitro* que compararam as alterações nas propriedades físicas e mecânicas de alinhadores ortodônticos confeccionados por termoformagem a vácuo, ou pressão, versus alinhadores produzidos por impressão tridimensional (3D). Os critérios de exclusão foram estudos *in vitro* que avaliaram propriedades físicas e mecânicas sem grupo controle comparativo entre os dois métodos de confecção, estudos cujo texto completo estava indisponível ou incompleto e estudos que não apresentavam delineamento *in vitro*. A pergunta da revisão foi estruturada segundo o modelo PICO:

P (Population): Não aplicável;

I (Intervention): Alinhadores ortodônticos estéticos confeccionados por termoformagem a vácuo ou pressão;

C (Comparison): Alinhadores ortodônticos estéticos confeccionados por impressão tridimensional (3D);

O (Outcome): Qualquer desfecho físico ou mecânico avaliado nos estudos incluídos.

Não foram aplicadas restrições quanto a idioma, data de publicação ou população investigada.

4.3 Fontes de Informação

A busca eletrônica foi realizada nas seguintes bases de dados: PubMed, MEDLINE (Wolters Kluwer), Web of Science (Clarivate Analytics), Scopus (Elsevier), LILACS, e EMBASE (Excerpta Medica database).

Além disso, foi feita uma busca manual nas listas de referências dos estudos incluídos para identificar artigos adicionais não localizados nas buscas eletrônicas. Também foi conduzida uma busca no Google Acadêmico, limitada às 200 primeiras citações recuperadas.

As buscas foram realizadas desde o início da indexação de cada base até dezembro de 2024, com uma atualização adicional realizada em maio de 2025. Quando um artigo não pôde ser recuperado, os autores foram contatados por e-mail para tentativa de obtenção do texto completo.

4.4 Busca

Em cada base, foram elaboradas estratégias específicas de busca adaptadas às suas características. No PubMed, os seguintes termos foram utilizados: Invisalign OR clear aligner OR vacuum thermoforming aligner OR thermoformed aligners OR in-office aligner OR in-house aligner OR TFA AND Graphy Aligner OR 3D Aligner OR three-dimensional impression Aligner OR 3D-printed clear aligners OR 3-dimensional printed aligners OR direct printed aligners OR DPA

Para as demais bases, os descritores foram adaptados conforme os operadores de busca disponíveis em cada plataforma. A estratégia combinou palavras-chave e descritores MeSH, associados por operadores booleanos “AND” e “OR”.

As estratégias completas de busca utilizadas em cada base de dados estão apresentadas na Tabela 1. Todas as referências foram organizadas e triadas utilizando o software Rayyan (https://www.rayyan.ai), desenvolvido para auxiliar revisões sistemáticas.

4.5 Seleção dos estudos

A seleção dos estudos foi conduzida por dois revisores independentes (J.O.J. e B.R.B.) em duas etapas. Na primeira fase, foi realizada a triagem por título

e resumo, em que os títulos e resumos foram lidos e os duplicados eliminados pelo software gerenciador. Estudos que atendiam aos critérios de elegibilidade foram incluídos, enquanto os que não atendiam foram excluídos. Em caso de divergência entre os revisores, um terceiro avaliador (S.M.) foi consultado para decisão por consenso. Quando o resumo não continha informações suficientes, o artigo completo foi recuperado. Na segunda fase, os artigos selecionados foram lidos integralmente pelos mesmos avaliadores, seguindo os critérios previamente definidos. Novamente, discordâncias foram resolvidas com mediação do terceiro revisor. A concordância entre os avaliadores foi medida pelo coeficiente kappa de Cohen (Landis, Koch 1977).

4,6 Extração de dados

Dois autores (J.O.J. e B.R.B.) realizaram a extração dos dados de forma independente. Um terceiro autor (S.M.) revisou os dados para garantir a consistência e precisão.

4.7 Itens a serem extraídos

Na etapa de extração de dados, os seguintes itens foram extraídos: nome do autor principal, ano de publicação, tamanho e características da amostra, métodos laboratoriais utilizados, desfechos avaliados e principais resultados.

4.8 Risco de viés em estudos individuais

A avaliação do risco de viés foi conduzida por dois revisores (J.O.J. e B.R.B.), com mediação do terceiro (S.M.) em caso de discordâncias. Utilizou-se uma adaptação da ferramenta do Joanna Briggs Institute (JBI) para estudos experimentais (Iliadi, Koletsi *et al.,* 2020; Dos Reis-Prado, Abreu *et al.,* 2021; Dos Reis-Prado, Abreu *et al.,* 2023).

Cada item foi pontuado como:

- 1: Relatado e adequado (baixo risco de viés);

- 0: Não relatado ou inadequado (alto risco de viés).

4.9 Resumo das medidas

Foram consideradas medidas estatísticas que comparassem as alterações nas propriedades físicas, mecânicas e de acurácia dos alinhadores, incluindo: média, desvio-padrão e valores de significância (p-valor).

4.10 Síntese dos resultados

Quando os dados foram considerados homogêneos e apropriados, procedeu-se à meta-análise. Em casos de heterogeneidade metodológica, elaborou-se uma síntese qualitativa. As diferenças entre os estudos incluíram tipo de alinhador avaliado, presença de grupo controle, testes laboratoriais aplicados e métodos estatísticos utilizados.

4.11 Risco de viés entre os estudos

A avaliação de viés entre estudos considerou os mesmos parâmetros utilizados na análise do viés individual.

4.12 Análises adicionais

Análises adicionais foram consideradas conforme a disponibilidade e compatibilidade dos dados.

5. ARTIGO

Physical and mechanical properties of thermoformed vs. 3D-printed aligners: systematic review and meta-analysis

ABSTRACT

Aesthetic orthodontic aligners are removable polymer-based devices increasingly used for correcting dental malocclusions. These appliances can be fabricated by thermoforming (AOCT) or direct three-dimensional printing (AOCID), with each manufacturing approach imparting distinct physical and mechanical characteristics that may influence clinical performance. **Objective:** This systematic review and meta-analysis aimed to compare the physical, mechanical, geometric, and behavioral properties of AOCT and AOCID. **Methods:** A comprehensive search was conducted in six electronic databases (May/2025), identifying in vitro laboratory studies that directly compared AOCT and AOCID. Two independent reviewers performed study selection, data extraction, and risk of bias assessment. When appropriate, data were pooled through meta-analyses. **Results:** Twenty-three studies met the inclusion criteria, with four eligible for meta-analysis. AOCID demonstrated superior performance across multiple parameters. AOCT showed a significant mean thickness reduction (−39.76%, SD=14.09), whereas AOCID exhibited an increase (+11.02%, SD=21.43; $p<0.001$). Geometric accuracy favored AOCID ($p<0.001$), which also presented a lower glass transition temperature (42.3 °C), greater shape recovery ($p<0.001$), higher vertical tensile forces ($p<0.005$), improved marginal adaptation, and reduced bacterial adhesion ($p<0.005$). Conversely, AOCT demonstrated greater storage modulus stability ($p<0.005$), higher microhardness ($p<0.005$), greater flexural strength ($p<0.05$), and better stability under cyclic compression. Regarding surface roughness, AOCID exhibited higher Sa values (SMD=2.73; 95%CI: 2.14–3.31; $p<0.00001$) and Sz after use (SMD=1.70; 95%CI: 0.67–2.74; $p=0.001$), while AOCT showed higher Sv (SMD=−1.19; 95%CI: −2.29 to −0.08; $p=0.04$) and lower Sa after use (SMD=−1.07; 95%CI: −2.12 to −0.02; $p=0.04$). No significant difference was found between planned and actual thickness (SMD=1.48; 95%CI: −7.26 to 4.30; $p=0.62$). Methodological heterogeneity among studies limited further analyses. **Conclusion:** AOCID demonstrated physical,

mechanical, and behavioral advantages over AOCT. Nevertheless, the lack of standardized experimental protocols and clinical validation limits the strength of current evidence, underscoring the need for future research to guide evidence-based orthodontic practice.

Registration: https://doi.org/10.17605/OSF.IO/BT98F
Conflict of interest: none

Key words: Orthodontics; Orthodontic Appliances; Clear Aligner Appliances; Systematic Review; Mechanical Tests; Mechanical Phenomena

•

Introduction

Aesthetic orthodontic aligners are removable devices made from polymeric materials, designed to promote controlled dental movements through sequential tray changes(Papadopoulou 2019; Al-Nadawi, Kravitz *et al.,* 2021; Monisha, Peter 2024). These devices represent an aesthetic and comfortable alternative to traditional fixed orthodontic appliances.

Aligners are fabricated using two main methods: thermoforming and three-dimensional (3D) printing. With advancements in material technology, sophisticated polymers have been increasingly used for aligner production, such as glycol-modified polyethylene terephthalate (PETG), polyurethane (PU), polypropylene (PP), and polycarbonate (PC), which offer better clinical performance. Currently, multi-layered polyurethane aligners, such as Smart Trak from Invisalign, are prominent in the market(Al-Nadawi, Kravitz *et al.,* 2021; Monisha, Peter 2024; Nakornnoi, Srirodjanakul *et al.,* 2024).

In the thermoforming technique, the process begins with obtaining a physical model of the dental arch, typically from an intraoral scan, followed by digital manipulation of the orthodontic treatment stages. The trays are then molded over the models using heat and pressure, either through vacuum or compressed air(Weir 2017; Shirey, Mendonca *et al.,* 2023). Although this technique has become established in clinical practice due to its excellent aesthetic and functional performance, it has drawbacks, such as high production costs, environmental impact after disposal, and the leaching of greater amounts of harmful substances into the patient's saliva (Shirey, Mendonca *et al.,* 2023; Arslan Avan, Bodur *et al.,* 2025).

With advances in digital dentistry and material engineering, 3D-printed orthodontic aligners have emerged. In this method, there is no need for printing physical models to fabricate the trays, as aligners are generated directly from digital files. The primary materials used in direct printing are photopolymers and modified epoxy resins, with properties designed to withstand the oral environment (Maspero, Tartaglia 2020; Ko, Bloomstein *et al.,* 2021).

Despite the variety of materials and fabrication methods, orthodontic aligners still face limitations related to their physical and mechanical properties. Changes such as loss of elasticity, surface degradation, moisture absorption, and permanent deformations may compromise the effectiveness of dental movement (Rossini, Parrini *et al.,* 2015; Raszewski, Chojnacka *et al.,* 2022).

Furthermore, constant exposure to the challenges of the oral environment, such as temperature variations, humidity, pH, and masticatory forces, directly affects the structural and functional stability of polymeric materials, leading to exponential declines in their physicochemical and mechanical properties during clinical use (Papadopoulou 2015; Eslami, Kopp *et al.,* 2024).

Therefore, understanding how different manufacturing methods impact the durability and clinical performance of aligners is essential for guiding evidence-based therapeutic choices.

The aim of this systematic review was to assess and compare the changes in the physical and mechanical properties of orthodontic aligners fabricated by thermoforming and direct three-dimensional printing.

Materials and methods

Protocol and Registration

This systematic review was conducted following the guidelines of the Preferred Reporting Items for Systematic Reviews and Meta-Analyses (PRISMA) (Moher, Liberati *et al.,* 2009). The protocol was registered on the Open Science Framework (OSF) platform under the identifier: https://doi.org/10.17605/OSF.IO/BT98F.

Eligibility Criteria

Only in vitro studies were included that compared the changes in the physical, mechanical, and accuracy properties of orthodontic aligners fabricated by thermoforming versus aligners produced by three-dimensional (3D) printing. The exclusion criteria were in vitro studies that evaluated physical, mechanical, or accuracy properties without a control group comparing the two fabrication methods, studies with unavailable or incomplete full texts, and studies that did not present an in vitro design.

The review question was structured according to the PICO model:

P (Population): Not applicable;

I (Intervention): Aesthetic orthodontic aligners made by vacuum or pressure thermoforming;

C (Comparison): Aesthetic orthodontic aligners fabricated by direct 3D printing;

O (Outcome): Any physical or mechanical outcome evaluated in the included studies.

No restrictions were applied regarding language, publication date, or the population under investigation.

Databases and search strategy

The electronic search was conducted in the following databases: PubMed, MEDLINE (Wolters Kluwer), Web of Science (Clarivate Analytics), Scopus (Elsevier), LILACS, and EMBASE (Excerpta Medica database).Additionally, a manual search of the reference lists of included studies was performed to identify additional articles not found through the electronic searches. A search was also conducted on Google Scholar, limited to the first 200 citations retrieved.

The searches were conducted from the inception of each database's indexing, specifically: 1996; 1971; 2004; 2004; 1982; and 1947, respectively, until December 2024, with an additional update carried out in May 2025. When an article could not be retrieved, the authors were contacted via email in an attempt to obtain the full text.

The strategy combined keywords and MeSH descriptors, connected by the boolean operators “AND” and “OR.” Specific search strategies were developed for each database, adapted to their characteristics. In PubMed, the following terms were used: Invisalign OR clear aligner OR vacuum thermoforming aligner OR thermoformed aligners OR in-office aligner OR in-house aligner OR TFA AND Graphy Aligner OR 3D Aligner OR three-dimensional impression Aligner OR 3D-printed clear aligners OR 3-dimensional printed aligners OR direct printed aligners OR DPA.

For other databases, the descriptors were adapted according to the available search operators in each platform.

The full search strategies used in each database are presented in Table 1. All references were organized and screened using the Rayyan software (https://www.rayyan.ai), developed to assist systematic reviews

Screening procedure

The study selection was conducted by two independent reviewers (J.O.J. and B.R.B.) in two stages. In the first stage, a title and abstract screening was performed, where the titles and abstracts were read, and duplicates were eliminated using reference management software. Studies meeting the eligibility criteria were included, while those not meeting the criteria were excluded. In cases of disagreement between the reviewers, a third evaluator (L.G.A.) was consulted to reach a consensus decision. When the abstract did not contain sufficient information, the full article was retrieved. In the second stage, the selected articles were read in full by the same evaluators, following the previously defined criteria. Again, disagreements were resolved with mediation from the third reviewer. Inter-rater agreement was measured using Cohen's kappa coefficient (Landis, Koch 1977).

Data Extraction

Two authors (J.O.J. and B.R.B.) independently performed the data extraction. A third author (L.G.A.) reviewed the data to ensure consistency and accuracy.

The following items were extracted during the data extraction phase: the name of the lead author, year of publication, sample size and characteristics, laboratory methods used, outcomes evaluated, and key results.

Risk of Bias in Individual Studies

The risk of bias assessment was conducted by two reviewers (J.O.J. and B.R.B.), with mediation by the third reviewer (L.G.A.) in case of disagreements. An adaptation of the Joanna Briggs Institute (JBI) tool for experimental studies was used (Iliadi, Koletsi *et al.,* 2020; Dos Reis-Prado, Abreu *et al.,* 2021; Dos Reis-Prado, Abreu *et al.,* 2023).

Each item was scored as:

- 1: Reported and adequate (low risk of bias);
- 0: Not reported or inadequate (high risk of bias).

Summary of Measures

Statistical measures that compared changes in the physical, mechanical, and accuracy properties of the aligners were considered, including: mean, standard deviation, and significance values (p-value).

Synthesis of Results

For studies with similar methodologies, the data were combined in a meta-analysis of continuous outcomes. The analysis was conducted using the Review Manager (RevMan) software, version 5.4, following the criteria established by the Cochrane Collaboration (2020). The mean, standard deviation (SD), and number of participants were considered. The findings were expressed as standardized mean difference (SMD), with 95% confidence intervals (CI). A random-effects model was used, and heterogeneity between studies was assessed using the I^2 index.

In cases of methodological heterogeneity, a qualitative synthesis was developed. The differences between the studies included the type of aligner evaluated, presence of a control group, laboratory tests applied, and statistical methods used.

Assessment of the Strength of Evidence

The GRADE tool is not applicable in systematic reviews consisting solely of in vitro studies, as it was developed to assess the quality of clinical evidence and the strength of recommendations based on patient outcomes (Schünemann HB 2013).

Results

Study Selection

The search in electronic databases, grey literature, and article references resulted in 1,323 studies identified. After removing duplicates (n = 556), 767 titles and abstracts remained for screening (Phase 1). Of these, 20 studies were included directly, and 720 were excluded. An additional 27 titles/abstracts did not provide sufficient data for an immediate decision, and the full articles were analyzed in Phase 2. After this analysis, 3 studies met the inclusion criteria, and 24 were excluded. Therefore, 23 studies were included in the review. The reasons for exclusion are

described in Supplemental Material 1. The PRISMA flowchart of the selection process is shown in Figure 1.

Characteristics of the Studies

The 23 included studies were published in English between 2019 and 2025. The sample size varied from 1 to 34 per group. Five studies were conducted in Germany (Atta, Bourauel *et al.,* 2024; Eslami, Kopp *et al.,* 2024; Sayahpour, Zinelis *et al.,* 2024; Sharifa, Bourauela *et al.,* 2024; Wendl, Wendl *et al.,* 2025), three in South Korea (Lee, Kim *et al.,* 2022; Park, Choi *et al.,* 2023; Bae, Kim *et al.,* 2025), two in Croatia (Bandić, Vodanović *et al.,* 2024; Šimunović, Čekalović Agović *et al.,* 2024), three in Italy (Cremonini, Brucculeri *et al.,* 2024; Cremonini, Cappelletti *et al.,* 2025; Cremonini, Cappelletti *et al.,* 2025), five in the United States (Hertan, McCray *et al.,* 2022; Koenig, Choi *et al.,* 2022; Shirey, Mendonca *et al.,* 2023; Souman 2023; Spangler, Ammoun *et al.,* 2023), two in India (Jindal, Juneja *et al.,* 2019; Jindal, Worcester *et al.,* 2020), one in Switzerland (Koletsi, Panayi *et al.,* 2023), one in France (Kuntz, Aranda *et al.,* 2024), and one in Turkey (Sarı, Camcı *et al.,* 2025).

Among the thermoformed aligners, the CA Pro (Scheu-Dental) stands out, used in 4 studies (Atta, Bourauel *et al.,* 2024; Bandić, Vodanović *et al.,* 2024; Sarı, Camcı *et al.,* 2025; Wendl, Wendl *et al.,* 2025). The Zendura A material was employed in 2 studies (Atta, Bourauel *et al.,* 2024; Bandić, Vodanović *et al.,* 2024), while Zendura FLX appeared in 6 publications (Koenig, Choi *et al.,* 2022; Atta, Bourauel *et al.,* 2024; Bandić, Vodanović *et al.,* 2024; Cremonini, Brucculeri *et al.,* 2024; Sharifa, Bourauela *et al.,* 2024; Cremonini, Cappelletti *et al.,* 2025). The Suresmile Essix ACE was cited in 2 studies (Koenig, Choi *et al.,* 2022; Kuntz, Aranda *et al.,* 2024).

Other thermoformed aligners include Angel Aligner and Accusmile/Fas, both used in one study each (Kuntz, Aranda *et al.,* 2024). The Gaxeta Easy-Vac was used by Lee *et al.,* (2022)(Lee, Kim *et al.,* 2022), while Scheu-Dental single-layer and multilayer aligners were reported by Park *et al.,* (2023)(Park, Choi *et al.,* 2023), each in one study.

Invisalign, one of the most widely used systems, was present in 8 studies (Koletsi, Panayi *et al.,* 2023; Shirey, Mendonca *et al.,* 2023; Alhasyimi, Ayub *et al.,* 2024; Eslami, Kopp *et al.,* 2024; Kuntz, Aranda *et al.,* 2024; Sayahpour, Zinelis *et al.,* 2024; Šimunović, Čekalović Agović *et al.,* 2024; Sarı, Camcı *et al.,* 2025). The

ClearCorrect system was mentioned in 1 study(Šimunović, Čekalović Agović *et al.,* 2024), as was the SMP aligner (Wendl, Wendl *et al.,* 2025) and the 3A GS030 model (Bae, Kim *et al.,* 2025).

Among the thermoformed aligners, the Duran+ aligner appeared in 5 studies (Jindal, Juneja *et al.,* 2019; Jindal, Worcester *et al.,* 2020; Bandić, Vodanović *et al.,* 2024; Cremonini, Brucculeri *et al.,* 2024; Sayahpour, Zinelis *et al.,* 2024), while Duransoft was used in 1 (Jindal, Worcester *et al.,* 2020). The Invisacryl Ultra is cited in 1 article (Spangler, Ammoun *et al.,* 2023). Additionally, the materials Erkodur and Erkoloc-Pro were analyzed in 2 and 1 studies, respectively (Bandić, Vodanović *et al.,* 2024; Wendl, Wendl *et al.,* 2025). The F22 aligner was used in 1 study (Cremonini, Cappelletti *et al.,* 2025), as well as the ATMOS aligners (Hertan, McCray *et al.,* 2022) and PET-G (Souman 2023).

In the 3D-printed aligner group, the Graphy system stands out, present in 15 studies (Iliadi, Koletsi *et al.,* 2020; Hertan, McCray *et al.,* 2022; Koenig, Choi *et al.,* 2022; Lee, Kim *et al.,* 2022; Park, Choi *et al.,* 2023; Alhasyimi, Ayub *et al.,* 2024; Atta, Bourauel *et al.,* 2024; Cremonini, Brucculeri *et al.,* 2024; Eslami, Kopp *et al.,* 2024; Kuntz, Aranda *et al.,* 2024; Sayahpour, Zinelis *et al.,* 2024; Sharifa, Bourauela *et al.,* 2024; Šimunović, Čekalović Agović *et al.,* 2024; Bae, Kim *et al.,* 2025; Sarı, Camcı *et al.,* 2025; Wendl, Wendl *et al.,* 2025).

Other 3D-printed aligners include Clear-A (Šimunović, Čekalović Agović *et al.,* 2024), Envisiontec X, not yet commercially available (Shirey, Mendonca *et al.,* 2023), OD-Clear TF Tough and Foldable (Shirey, Mendonca *et al.,* 2023), and Digiline (Souman 2023), each present in only 1 study.

The Dental LT material was used in 3 studies (Jindal, Juneja *et al.,* 2019; Jindal, Worcester *et al.,* 2020; Spangler, Ammoun *et al.,* 2023), while NextDent appears in 1 (Bandić, Vodanović *et al.,* 2024). Lastly, the Noxi aligner, also 3D-printed, was cited in 3 studies (Cremonini, Brucculeri *et al.,* 2024; Cremonini, Cappelletti *et al.,* 2025; Cremonini, Cappelletti *et al.,* 2025).

Table 2 classifies the orthodontic aligner systems found in the literature, highlighting materials, manufacturers and frequency of use in clinical studies.

Table 2 - Classification and Utilization Frequency of Orthodontic Aligners in Clinical Studies

Aligner Type	Aligner brand	Articles	Number of

			articles
Thermoplastics	CA Pro (Scheu-Dental)	Atta *et al.,* (2024); Bandić *et al.,* (2024); Sarı *et al.,* (2025); Wendl *et al.,* (2025)	4
	Zendura A	Atta *et al.,* (2024); Bandić *et al.,* (2024)	2
	Zendura FLX	Koenig *et al.,* (2022); Atta *et al.,* (2024); Bandić *et al.,* (2024); Cremonini *et al.,* (2024); Sharifa *et al.,* (2024); Cremonini *et al.,* (2025)	6
	Suresmile Essix ACE	Koenig *et al.,* (2022); Kuntz *et al.,* (2024)	2
	Angel Aligner	Kuntz *et al.,* (2024)	1
	Accusmile/Fas	Kuntz *et al.,* (2024)	1
	Gaxeta Easy-Vac	Lee *et al.,* (2022)	1
	Scheu-Dental (single/multi)	Park *et al.,* (2023)	1
	Duran+	Jindal *et al.,* (2019, 2020); Bandić *et al.,* (2024); Cremonini *et al.,* (2024); Sayahpour *et al.,* (2024)	5
	Duransoft	Jindal *et al.,* (2020)	1
	Invisacryl Ultra	Spangler *et al.,* (2023)	1
	Erkodur	Bandić *et al.,* (2024); Wendl *et al.,* (2025)	2
	Erkoloc-Pro	Wendl *et al.,* (2025)	1
	F22	Cremonini *et al.,* (2025)	1
	ATMOS	Hertan *et al.,* (2022)	1
	PET-G	Souman (2023)	1
	Invisalign	Koletsi *et al.,* (2023); Shirey *et al.,* (2023); Alhasyimi *et al.,* (2024); Eslami *et al.,* (2024); Kuntz *et al.,* (2024); Sayahpour *et al.,* (2024); Šimunović *et al.,* (2024); Sarı *et al.,* (2025)	8
	ClearCorrect	Šimunović *et al.,* (2024)	1
	SMP	Wendl *et al.,* (2025)	1
	3A GS030	Bae *et al.,* (2025)	1
3D printed	Graphy	Iliadi *et al.,* (2020); Hertan *et al.,* (2022); Koenig *et al.,* (2022); Lee *et al.,* (2022); Park *et al.,* (2023); Alhasyimi *et al.,* (2024); Atta *et al.,* (2024); Cremonini *et al.,* (2024); Eslami *et al.,* (2024); Kuntz *et al.,* (2024); Sayahpour *et al.,* (2024); Sharifa *et al.,* (2024); Šimunović *et al.,* (2024); Bae *et al.,* (2025); Sarı *et al.,* (2025); Wendl *et al.,* (2025)	15
	Clear-A	Šimunović *et al.,* (2024)	1
	Envisiontec X	Shirey *et al.,* (2023)	1
	OD-Clear TF Tough/Foldable	Shirey *et al.,* (2023)	1
	Digiline	Souman (2023)	1

The studies included in this systematic review assessed thermal properties using Differential Scanning Calorimetry (DSC) and Dynamic Mechanical Analysis

(DMA), including tests at various temperature ranges and operational modes. The mechanical properties were investigated through tensile, compression, three-point bending, tensile strength, stress relaxation, creep, elasticity modulus, as well as shape recovery and shape memory tests. Vickers microhardness, Instrumented Indentation Test (IIT), and cyclic loading tests were also conducted. Surface morphology was examined using Scanning Electron Microscopy (SEM), roughness, and porosity via Confocal Laser Scanning Microscopy (CLSM) and optical profilometry. Optical evaluations included measuring translucency by spectrophotometry and analyzing color change using ΔE parameters (total color difference in the CIELab color space) and the National Bureau of Standards (NBS) classification. The adaptation and thickness of the aligners were analyzed using direct measurements with a digital caliper, electronic micrometer, methods with high-resolution micro-computed tomography (micro-CT), 3D visualization of the marginal gap, and overlay of digital files in STL (Standard Tessellation Language) format. Additionally, the behavior of the aligners after accelerated thermal aging was monitored in different cycles of hot and cold immersion. Finally, three-dimensional digital models were employed for computational simulations using Finite Element Method (FEM), allowing the analysis of forces, moments, and displacements generated by the aligners under different usage conditions (Jindal, Juneja *et al.,* 2019; Jindal, Worcester *et al.,* 2020; Hertan, McCray *et al.,* 2022; Koenig, Choi *et al.,* 2022; Lee, Kim *et al.,* 2022; Koletsi, Panayi *et al.,* 2023; Park, Choi *et al.,* 2023; Shirey, Mendonca *et al.,* 2023; Souman 2023; Spangler, Ammoun *et al.,* 2023; Atta, Bourauel *et al.,* 2024; Bandić, Vodanović *et al.,* 2024; Cremonini, Brucculeri *et al.,* 2024; Eslami, Kopp *et al.,* 2024; Kuntz, Aranda *et al.,* 2024; Sayahpour, Zinelis *et al.,* 2024; Sharifa, Bourauela *et al.,* 2024; Šimunović, Čekalović Agović *et al.,* 2024; Bae, Kim *et al.,* 2025; Cremonini, Cappelletti *et al.,* 2025; Cremonini, Cappelletti *et al.,* 2025; Sarı, Camcı *et al.,* 2025; Wendl, Wendl *et al.,* 2025)

Table 3 summarizes the main methodologies used to evaluate the thermomechanical, optical and adaptation properties of aligners, with examples of representative studies.

Table 3 - Different tests used to study clear aligners

Evaluation Category	Specific Techniques	Key Parameters Assessed	Studies

Thermal Analysis	Differential Scanning Calorimetry (DSC), Dynamic Mechanical Analysis (DMA)	Glass transition temperature (Tg), melting points, thermal stability	Jindal *et al.,* (2019, 2020); Spangler *et al.,* (2023); Atta *et al.,* (2024)
Mechanical Characterization	Tensile/compression testing, 3-point bending, stress relaxation, creep compliance	Elastic modulus, yield strength, viscoelastic behavior	Koenig *et al.,* (2022); Lee *et al.,* (2022); Cremonini *et al.,* (2024, 2025)
Surface Topography	SEM, CLSM, optical profilometry	Surface roughness (Ra, Rz), pore distribution, wear patterns	Park *et al.,* (2023); Bandić *et al.,* (2024); Šimunović *et al.,* (2024)
Optical Properties	Spectrophotometry, CIELab color space analysis	Translucency parameter (TP), ΔE values, NBS classification	Shirey *et al.,* (2023); Kuntz *et al.,* (2024); Wendl *et al.,* (2025)
Dimensional Accuracy	Micro-CT, STL overlay analysis, digital caliper/ micrometer measurements	Marginal gap width, thickness uniformity, fit precision	Hertan *et al.,* (2022); Eslami *et al.,* (2024); Sarı *et al.,* (2025)
Aging Resistance	Accelerated thermal cycling (hot/cold immersion)	Material degradation, property retention	Souman (2023); Bae *et al.,* (2025); Cremonini *et al.,* (2025)
Computational Modeling	Finite Element Analysis (FEA)	Stress distribution, force vectors, displacement patterns	Koletsi *et al.,* (2023); Sayahpour *et al.,* (2024); Sharifa *et al.,* (2024)

The characteristics of the studies included are described in Table 4.

Risk of Bias Assessment

A total of 23 studies were assessed according to 16 methodological quality criteria, with a maximum score of 16 points, where higher scores indicate lower risk of bias. The final scores ranged from 10 to 14 points, reflecting varying levels of experimental rigor among the studies.

It was observed that all the included studies clearly stated their research objectives, demonstrating alignment between the experimental planning and the investigative proposal (Jindal, Juneja *et al.,* 2019; Jindal, Worcester *et al.,* 2020; Hertan, McCray *et al.,* 2022; Koenig, Choi *et al.,* 2022; Lee, Kim *et al.,* 2022; Koletsi, Panayi *et al.,* 2023; Park, Choi *et al.,* 2023; Shirey, Mendonca *et al.,* 2023; Souman 2023; Spangler, Ammoun *et al.,* 2023; Atta, Bourauel *et al.,* 2024; Bandić, Vodanović *et al.,* 2024; Cremonini, Brucculeri *et al.,* 2024; Eslami, Kopp *et al.,* 2024; Kuntz,

Aranda *et al.,* 2024; Sayahpour, Zinelis *et al.,* 2024; Sharifa, Bourauela *et al.,* 2024; Šimunović, Čekalović Agović *et al.,* 2024; Bae, Kim *et al.,* 2025; Cremonini, Cappelletti *et al.,* 2025; Cremonini, Cappelletti *et al.,* 2025; Sarı, Camcı *et al.,* 2025; Wendl, Wendl *et al.,* 2025). However, only seven studies justified the sample size used, which represents a limitation in terms of statistical power and sample planning (Hahn, Engelke *et al.,* 2010; Koenig, Choi *et al.,* 2022; Eslami, Kopp *et al.,* 2024; Sayahpour, Zinelis *et al.,* 2024; Bae, Kim *et al.,* 2025; Cremonini, Cappelletti *et al.,* 2025; Cremonini, Cappelletti *et al.,* 2025; Sarı, Camcı *et al.,* 2025).

Regarding sample homogeneity, equivalence in the number of units per experimental group was observed in only twelve studies (Jindal, Juneja *et al.,* 2019; Hertan, McCray *et al.,* 2022; Koenig, Choi *et al.,* 2022; Koletsi, Panayi *et al.,* 2023; Park, Choi *et al.,* 2023; Alhasyimi, Ayub *et al.,* 2024; Cremonini, Brucculeri *et al.,* 2024; Eslami, Kopp *et al.,* 2024; Sayahpour, Zinelis *et al.,* 2024; Sharifa, Bourauela *et al.,* 2024; Cremonini, Cappelletti *et al.,* 2025; Cremonini, Cappelletti *et al.,* 2025; Sarı, Camcı *et al.,* 2025), with imbalance in the others. Nevertheless, all studies ensured similar baseline conditions between groups concerning the aligner brand and usage condition, whether new or recovered (Jindal, Juneja *et al.,* 2019; Jindal, Worcester *et al.,* 2020; Hertan, McCray *et al.,* 2022; Koenig, Choi *et al.,* 2022; Lee, Kim *et al.,* 2022; Koletsi, Panayi *et al.,* 2023; Park, Choi *et al.,* 2023; Shirey, Mendonca *et al.,* 2023; Souman 2023; Atta, Bourauel *et al.,* 2024; Bandić, Vodanović *et al.,* 2024; Cremonini, Brucculeri *et al.,* 2024; Eslami, Kopp *et al.,* 2024; Kuntz, Aranda *et al.,* 2024; Sayahpour, Zinelis *et al.,* 2024; Sharifa, Bourauela *et al.,* 2024; Šimunović, Čekalović Agović *et al.,* 2024; Bae, Kim *et al.,* 2025; Sarı, Camcı *et al.,* 2025; Wendl, Wendl *et al.,* 2025).

The lack of blinding of the evaluators and operators was one of the most frequent limitations. No study reported blinding of the operators, and only one explicitly stated that the evaluators were blinded to group allocation and outcome analysis (Šimunović, Čekalović Agović *et al.,* 2024). The other studies did not describe any form of blinding during the conduction or assessment of the tests, which represents a risk of observational bias, especially in measurements with subjective elements.

In contrast, all studies clearly described their experimental protocols, indicating methodological transparency. Likewise, all applied experimental procedures similarly between groups and used the same outcome measurement

criteria (Jindal, Juneja *et al.,* 2019; Jindal, Worcester *et al.,* 2020; Hertan, McCray *et al.,* 2022; Koenig, Choi *et al.,* 2022; Lee, Kim *et al.,* 2022; Koletsi, Panayi *et al.,* 2023; Park, Choi *et al.,* 2023; Shirey, Mendonca *et al.,* 2023; Souman 2023; Spangler, Ammoun *et al.,* 2023; Atta, Bourauel *et al.,* 2024; Bandić, Vodanović *et al.,* 2024; Cremonini, Brucculeri *et al.,* 2024; Eslami, Kopp *et al.,* 2024; Kuntz, Aranda *et al.,* 2024; Sayahpour, Zinelis *et al.,* 2024; Sharifa, Bourauela *et al.,* 2024; Šimunović, Čekalović Agović *et al.,* 2024; Bae, Kim *et al.,* 2025; Cremonini, Cappelletti *et al.,* 2025; Cremonini, Cappelletti *et al.,* 2025; Sarı, Camcı *et al.,* 2025; Wendl, Wendl *et al.,* 2025).

Regarding data completeness, all studies presented results in their entirety and without gaps, except for a few that did not clearly report all the data or presented results partially described (Jindal, Worcester *et al.,* 2020; Lee, Kim *et al.,* 2022; Kuntz, Aranda *et al.,* 2024; Bae, Kim *et al.,* 2025). Most of the studies employed appropriate statistical analyses,while some publications did not specify the tests used, limiting the critical evaluation of the robustness of the findings (Spangler, Ammoun *et al.,* 2023; Bae, Kim *et al.,* 2025).

The studies with higher scores, such as (14/16)(Šimunović, Čekalović Agović *et al.,* 2024), (13/16) (Sarı, Camcı *et al.,* 2025), (13/16) (Sayahpour, Zinelis *et al.,* 2024), (13/16) (Sharifa, Bourauela *et al.,* 2024), and (13/16) (Cremonini, Cappelletti *et al.,* 2025), demonstrated higher methodological rigor. On the other hand, those with lower scores (10/16) were mainly due to the lack of blinding, absence of sample justification, and limited presentation of results (Jindal, Worcester *et al.,* 2020; Lee, Kim *et al.,* 2022; Atta, Bourauel *et al.,* 2024; Kuntz, Aranda *et al.,* 2024; Bae, Kim *et al.,* 2025). The mean score obtained among the evaluated studies ranged from 11 to 13 points, representing an overall moderate risk of bias.

The details of the risk of bias analysis are provided in Table 5 and Supplemental Material 2.

Results of individual studies

This systematic review included 23 in vitro laboratory studies that compared orthodontic aligners fabricated through thermoforming and 3D printing, focusing on the evaluation of their physical and mechanical, thermal, geometric, structural, and behavioral properties

Table 6 - Test Classification by Physical and Mechanical Properties

Category	Type of Test	Classification
Geometric Properties and Thickness Variation	Thickness measurement, geometric accuracy, gap analysis	Physical
Thermal Properties (DSC)	Differential Scanning Calorimetry (DSC) – Glass Transition Temperature	Physical
Color Change and Translucency	Spectrophotometry, colorimetry (ΔE*), translucency analysis	Physical
Surface Roughness and Finish	Optical profilometry, porosity parameters (Sa, Sq, Sz, Vvv, Vvc)	Physical
Surface Microhardness (Vickers, IIT)	Instrumented Indentation Test (IIT), Vickers hardness	Mechanical
Tensile Strength	Tensile test – maximum force supported	Mechanical
Cyclic Compression	Repeated compression test – thickness stability	Mechanical
Three-Point Bending	Three-point bending test – maximum force under deflection	Mechanical
Elastic Modulus (Young's Modulus)	Tensile dynamometer – stiffness and deformation	Mechanical
Dynamic Mechanical Analysis (DMA)	Storage modulus and temperature-dependent viscoelastic behavior	Mechanical
Shape Recovery Capacity	Recovery angle and percentage after thermal deformation	Mechanical
Stress Relaxation	Force decay under sustained strain over time	Mechanical

The thermoformed aligners included materials such as Zendura A, Zendura FLX, Duran, Erkodur, CA PRO+, and Erkoloc-Pro, while the 3D-printed aligners were made with resins like TC-85, NextDent, Dental LT, and Noxi, utilizing printing technologies such as Stereolithography (SLA), Digital Light Processing (DLP), and Selective Laser Sintering (SLS), with thickness variations ranging from 0.5 mm to 1 mm.

Physical properties

Geometric Properties and Thickness Variation

The thickness analysis revealed statistically significant differences between the fabrication methods ($p < 0.001$). Thermoformed aligners showed an average thickness reduction of −39.76% (SD = 14.09), with extreme values observed

in the Erkoloc-Pro material (−53.31%). In contrast, 3D-printed aligners showed an average increase of +11.02% (SD = 21.43), with the IZZI aligner standing out (+27.99%) (Koenig, Choi *et al.,* 2022). One study reported divergent data, showing an increase in thickness for 3D aligners (+8.20 mm; SD = 0.06) compared to thermoformed ones (7.88 mm; SD = 0.072), with no statistical significance ($p > 0.05$) (Jindal, Juneja *et al.,* 2019).

Regarding geometric accuracy, the 3D-printed aligners presented a lower mean absolute deviation (0.133 mm; SD = 0.043) compared to the thermoformed Zendura FLX (0.186 mm; SD = 0.124) and Essix ACE (0.299 mm; SD = 0.241), with a statistically significant difference ($p < 0.05$) (Koenig, Choi *et al.,* 2022). The evaluation of thickness in correlation with the gap between the aligner and the model revealed median values of 504.68 µm (IQR: 460.68–558.40) for thermoformed aligners and 614.24 µm (IQR: 559.27–687.53) for 3D aligners ($p < 0.001$). The gap width presented medians of 69.80 µm (IQR: 0–115.17) for thermoformed aligners and 69.80 µm (IQR: 34.90–131.75) for 3D aligners (Park, Choi *et al.,* 2023).

Souman *et al.,* (2023) identified a statistically significant difference ($p < 0.001$) in accuracy and fit: 3D-printed aligners showed an average distance of 1.10 mm (SD = 0.089) between the aligner and the model, while the thermoformed aligners showed 0.540 mm (SD = 0.122)(Souman 2023).

Thermal Properties

The thermal analysis by Differential Scanning Calorimetry (DSC) revealed that the TC-85 material, used in 3D aligners, exhibited the lowest glass transition temperature (Tg = 42.3°C), indicating higher thermal responsiveness. In contrast, thermoformed materials presented higher Tg values, such as Zendura A (92.2°C) and Zendura FLX (107.1°C), which are characterized by greater rigidity and lower thermal sensitivity (Atta, Bourauel *et al.,* 2024).

Color Change and Translucency

Orthodontic aligners are subject to color changes due to various extrinsic factors. One study used a spectrophotometer to analyze the translucency of thermoformed and 3D-printed aligners, utilizing the CIELab color system coordinates. The authors observed that the thermoformed aligners made of PETG presented median translucency values of 67.82 (IQR: 67.64–68.05) for single-layer models and

66.15 (IQR: 65.84–66.45) for multi-layer models. In contrast, the 3D-printed aligners made with TC-85 material showed a translucency value of 10.76 (IQR: 9.17–15.81) when cleaned only with 99.5% isopropyl alcohol. However, when subjected to cleaning in a centrifuge at 500 rpm for 6 minutes, the 3D-printed aligners reached a translucency of 66.19 (IQR: 65.44–66.36), comparable to the thermoformed aligners (Park, Choi *et al.,* 2023).

Another group of authors evaluated the color change in orthodontic aligners after exposure to different pigmented substances (coffee, black tea, cola, and Red Bull energy drink). Using a compact colorimeter, the researchers measured color changes based on the CIELab system, with ΔE* values converted to units of the National Bureau of Standards (NBS) to relate the magnitude of color change to its clinical relevance. The ΔE* value represents the total difference between two colors in the CIELab three-dimensional color space and is calculated based on the differences in the L* (lightness), a* (red-green axis), and b* (yellow-blue axis) components. The greater the ΔE*, the higher the visual perception of color change(Šimunović, Čekalović Agović *et al.,* 2024).

The results indicated an average ΔE* value of 5.208 for the thermoformed aligners, while the 3D-printed aligners showed an average of 11.376 ($p < 0.001$), indicating greater susceptibility to pigmentation in the 3D-printed models (Šimunović, Čekalović Agović *et al.,* 2024).

Surface Roughness and Finish

The surface roughness parameters were evaluated for both unused and used 3D-printed and thermoformed aligners. For the Sa parameter (average surface roughness), the average values were 1.72 ± 1.10 μm for unused 3D aligners and 3.78 ± 1.70 μm for used 3D aligners. For thermoformed aligners, the values were 6.79 ± 2.39 μm for unused and 2.68 ± 1.40 μm for used aligners. For the Sq parameter (root mean square deviation of surface height), the values were 2.35 ± 1.61 μm for unused 3D aligners, 4.87 ± 2.25 μm for used 3D aligners, 10.4 ± 4.89 μm for unused thermoformed aligners, and 3.37 ± 3.00 μm for used thermoformed aligners. For the Sp parameter (maximum peak height), the average values were 6.92 ± 6.81 μm for unused 3D aligners, 18.9 ± 12.8 μm for used 3D aligners, 44.4 ± 28.9 μm for unused thermoformed aligners, and 12.5 ± 11.3 μm for used thermoformed aligners. Regarding the Sz parameter (total height between the

highest peak and the deepest valley), the values were 16.5 ± 19.3 µm for unused 3D aligners, 42.1 ± 32.8 µm for used 3D aligners, 121.0 ± 92.4 µm for unused thermoformed aligners, and 24.5 ± 18.8 µm for used thermoformed aligners. Finally, for the Sv parameter (maximum valley depth), the values were 9.59 ± 13.3 µm for unused 3D aligners, 23.2 ± 23.6 µm for used 3D aligners, 76.4 ± 67.7 µm for unused thermoformed aligners, and 12.1 ± 9.64 µm for used thermoformed aligners(Eslami, Kopp *et al.,* 2024).

In the same study, the authors also evaluated porosity parameters. For the Vvv parameter (volume of voids in the valleys, mm^3/mm^2), the values were: 0.27 ± 0.29 (unused 3D), 0.54 ± 0.38 (used 3D), 1.54 ± 1.10 (unused thermoformed), and 0.37 ± 0.30 (used thermoformed). The Vvc parameter (volume of material on the peaks, mm^3/mm^2) was 2.40 ± 1.48 (unused 3D), 6.19 ± 3.05 (used 3D), 8.34 ± 2.69 (unused thermoformed), and 3.90 ± 2.08 (used thermoformed) (Eslami, Kopp *et al.,* 2024).

Another study conducted by Koletsi, Panayi *et al.,* (2023) used an optical profilometer to assess the surface roughness of different aligner groups. For the Sa parameter, the median values (IQR) were: 124 nm (106–143) for unused thermoformed, 131 nm (104–164) for used Invisalign, 54 nm (36–66) for unused 3D, and 295 nm (264–464) for used 3D. For the Sq parameter, the values were: 182 nm (161–200) for unused thermoformed, 203 nm (166–247) for used Invisalign, 138 nm (77–162) for unused 3D, and 499 nm (373–822) for used 3D (Koletsi, Panayi *et al.,* 2023).

The Sz parameter showed the following values: 3671 nm (2981–5260) for unused thermoformed, 9002 nm (3452–12,153) for used Invisalign, 5995 nm (4192–8414) for unused 3D, and 12,842 nm (10,656–20,836) for used 3D. For the Sc parameter (volume of valleys above the mean line, nm^3/nm^2), the median values were: 204 (174–247) for unused thermoformed, 219 (168–261) for used Invisalign, 66 (49–96) for unused 3D, and 425 (394–597) for used 3D. Finally, for the Sv parameter (volume of valleys below the mean line, nm^3/nm^2), the values were: 20 (17–22) for unused thermoformed, 22 (12–34) for used Invisalign, 13 (7–18) for unused 3D, and 62 (40–113) for used 3D (Koletsi, Panayi *et al.,* 2023).

Mechanical Properties

Surface Microhardness:

Instrumented indentation tests (IIT) showed that the materials CA Pro, Zendura A, and Zendura FLX presented initial Vickers hardness of 2.7 (SD = 0.1), 13.4 (SD = 0.3), and 10.3 (SD = 0.2), respectively. After thermoforming, the values were 2.7 (SD = 0.1), 12.0 (SD = 0.2), and 7.9 (SD = 0.3), with a statistically significant difference for most materials ($p < 0.001$), except for CA Pro ($p = 0.899$). The 3D aligners showed an average of 8.1 (SD = 0.9) (Atta, Bourauel *et al.,* 2024). Another study demonstrated that after clinical use, 3D-printed aligners showed significantly higher Vickers hardness compared to thermoformed aligners ($p < 0.001$), although no significant difference was found between the groups before intraoral exposure ($p = 0.636$) (Sayahpour, Zinelis *et al.,* 2024).

Tensile Strength:

In tensile strength tests, Shirey *et al.,* (2023) observed that the thermoformed materials EX3 and LD30 supported maximum forces of 64.41 MPa (SD = 7.25) and 40.04 MPa (SD = 5.00), respectively. In contrast, 3D aligners made with proprietary resins and the OD-Clear TF exhibited resistance of 28.11 MPa (SD = 3.75) and 9.34 MPa (SD = 1.96), respectively(Shirey, Mendonca *et al.,* 2023).

Kuntz *et al.,* (2024), when evaluating tensile strength in Newtons, reported that the aligners Accusmile, Angel, Invisalign, and Suresmile exhibited resistance of 386.4 N (SD = 56.58), 203.0 N (SD = 27.22), 170.0 N (SD = 82.74), and 259.5 N (SD = 26.46), respectively. The 3D-printed GRAPHY aligner showed resistance of 261.8 N (SD = 54.6)(Kuntz, Aranda *et al.,* 2024).

Cyclic Compression:

Cyclic compression analysis was addressed in only one study, aiming to assess the final thickness of the aligner after the application of repeated loads. The authors identified that the thermoformed aligner made with PETG maintained stable behavior under repeated compression, despite also showing thickness reduction. In contrast, the 3D aligner produced with TC-85 material demonstrated a progressively greater decline in resistance over time ($p < 0.01$) (Bae, Kim *et al.,* 2025).

Three-Point Bending:

The three-point bending test was utilized by several authors to evaluate the maximum load supported by the aligners under a specific deflection depth (Hertan, McCray *et al.,* 2022; Atta, Bourauel *et al.,* 2024; Sharifa, Bourauela *et al.,* 2024; Sarı, Camcı *et al.,* 2025). Atta *et al.,* (2024) investigated the maximum force supported by aligners at different temperatures. At 37°C and under a maximum deflection of 2 mm, the data showed that thermoformed aligners exhibited a maximum force of approximately 3.6 N (SD = 0.8), while 3D-printed aligners demonstrated a force of approximately 0.4 N (SD = 0.4) (Atta, Bourauel *et al.,* 2024).

Hertan, McCray *et al.,* (2022) assessed the maximum bending force at different deflection levels (0.1 mm; 0.2 mm; and 0.3 mm) and found that the thermoformed aligners exhibited average forces of 5.26 ± 0.51 N, 10.52 ± 0.69 N, and 16.16 ± 0.71 N, respectively. In comparison, 3D-printed aligners demonstrated values of 2.59 ± 0.62 N, 3.15 ± 0.65 N, and 3.49 ± 0.70 N, respectively (Hertan, McCray *et al.,* 2022).

Sarı, Camcı *et al.,* (2025) conducted the three-point bending test to simulate cyclic loads on different types of aligners immersed in various liquids (orange juice, soy sauce, red wine, and cola), comparing thermoformed aligners with 3D-printed ones. The results showed that, at a deflection of 1 mm, the maximum forces recorded were similar between the groups; however, statistical analysis revealed significant differences ($p < 0.05$) in all comparisons, favoring the 3D-printed aligners (Sarı, Camcı *et al.,* 2025).

Sharifa, Bourauel *et al.,* (2024) reported different values for the maximum force under a deflection of 2 mm, also considering the influence of temperature. At 37°C, the thermoformed Zendura FLX aligner exhibited a maximum force of 1.73 N, while the 3D aligner made with TC-85 material demonstrated a force of 0.87 N.(Sharifa, Bourauela *et al.,* 2024)

Elastic Modulus:

Kuntz *et al.,* (2024) conducted a study to evaluate the elastic modulus (Young's modulus) and compressive strength of 80 orthodontic aligners from five different brands, including thermoformed and 3D-printed types. Mechanical testing was performed using a Traction Dynamometer LRX, which applied a tensile force at a crosshead speed of 5 mm/min for up to 4 minutes or until specimen fracture. The authors reported an elastic modulus of up to 2.65 GPa and a compressive strength of

342 MPa for 3D-printed aligners, surpassing the values observed in thermoformed aligners. Although no statistically significant differences were found between thermoformed and 3D-printed groups overall, brand-specific differences were detected. At baseline (D0), Accusmile aligners (7.38 ± 1.83 GPa) exhibited a significantly higher modulus than Angel (3.40 ± 1.05 GPa) and Invisalign (3.81 ± 1.29 GPa). After 14 days (D14), Accusmile aligners (7.33 ± 1.93 GPa) maintained a significantly higher modulus compared to Angel (3.15 ± 0.39 GPa), Invisalign (4.60 ± 9.84 GPa), and Suresmile (4.63 ± 1.98 GPa), with P < 0,0001. Materials with a higher Young's modulus demonstrate greater stiffness and reduced deformation under applied loads, which may influence clinical performance (Kuntz, Aranda *et al.,* 2024).

Dynamic Mechanical Properties

A group of researchers conducted a set of Dynamic Mechanical Analysis (DMA) tests and analyses on 3D-printed and thermoformed aligners. The authors identified that the 3D aligners showed storage modulus values (in MPa) subject to significant variations according to the exposure temperature. At 20°C, values around 3000 MPa were observed, while at 45°C, these values decreased to approximately 1500 MPa. In contrast, the thermoformed aligners CA Pro, Zendura A, and Zendura FLX maintained their storage modulus values practically constant with temperature variations, with values of 1000 MPa, 1500 MPa, and 800 MPa, respectively (Atta, Bourauel *et al.,* 2024).

A second study also employed dynamic mechanical analysis to compare the shape memory capacity of the materials. In this research, the authors compared thermoformed aligners made with polyethylene terephthalate (PET) and 3D aligners produced with the TC-85 resin. The results showed that the thermoformed aligners exhibited a storage modulus of 1262 MPa, while the TC-85 aligners exhibited 710.60 MPa, indicating more flexible behavior in the 3D-printed aligners (Lee, Kim *et al.,* 2022).

Shape Recovery Capacity

The shape recovery capacity was significantly higher in the TC-85 material, used in 3D-printed aligners. The average recovery angle values observed were 15.2° (SD = 4.5), 98.8° (SD = 6.2), and 155° (SD = 5.7), at temperatures of 30°C, 37°C, and 45°C, respectively, with recovery percentages of 8.4%, 56.9%, and

86.1%, respectively. In contrast, the thermoformed aligners showed significantly inferior performance. The CA-Pro aligner exhibited, at 30°C, 37°C, and 45°C, shape recovery percentages of 1.8%, 2.2%, and 2.9%, with recovery angles of 3.2 ± 1.0°, 4.0 ± 0.9°, and 5.2 ± 1.9°, respectively. This trend was also observed in the Zendura A and Zendura FLX aligners. All comparisons between the different aligner fabrication methods regarding shape recovery capacity showed statistical significance ($p < 0.001$) (Atta, Bourauel *et al.,* 2024).

A study conducted in South Korea also investigated the shape recovery capacity of the aligners. Thermoformed aligners made of polyethylene terephthalate glycol (PETG) and 3D aligners produced with the TC-85 material were used. The results demonstrated that the thermoformed aligners showed a shape recovery rate of 0%, while the 3D aligners showed recovery rates of 50% after 1 minute, 90% after 10 minutes, and 96% after 60 minutes, all tested at 37°C (Lee, Kim *et al.,* 2022).

Stress Relaxation

In stress relaxation analyses, the 3D-printed aligners exhibited inferior performance compared to the thermoformed aligners. A study conducted in Italy evaluated the initial and final forces of the aligners subjected to continuous stress for 8 hours in two consecutive tests, calculating the percentage of force decay. The thermoformed aligners Zendura FLX and Duran exhibited a force decay of 47.4% and 62.0%, respectively, in the first test. In the second test, both recorded a decay of 29.0%. The Zendura FLX did not show a statistically significant difference between the tests ($p > 0.9$), while Duran presented $p = 0.026$ (Cremonini, Brucculeri *et al.,* 2024).

The study also evaluated the force decay of the 3D aligners Tera and Noxi, which showed a reduction of 90.0% and 32.0% in the first test, and 100.0% and 23.0% in the second test, respectively ($p = 0.020$ and $p = 0.010$) (Cremonini, Brucculeri *et al.,* 2024).

A second study, conducted by the same group of authors with an expanded sample and stress-relaxation evaluation in different regions of the aligners, revealed that in the first test, the thermoformed aligners AS and F22 presented an average force decay of 50.3% (SD = 1.3) and 46.8% (SD = 5.5), respectively ($p = 0.212$). In the subsequent test, the values were 39.0% (SD = 5.5) and 35.9% (SD = 1.1) ($p = 0.284$)(Cremonini, Cappelletti *et al.,* 2025).

The 3D aligners evaluated in this study were the Noxi models, divided into three groups with variations in gingival margins. In the first test, the groups showed stress relaxation of 44.7% (SD = 7.8), 40.7% (SD = 3.5), and 42.5% (SD = 3.5) (p = 0.212). In the second test, the values were 39.0% (SD = 2.6), 37.4% (SD = 6.2), and 45.4% (SD = 6.9) (p = 0.284) (Cremonini, Cappelletti *et al.,* 2025).

Shirey *et al.,* (2023) also evaluated this variable, though with a smaller sample of only three aligners per group. The authors applied a 2% strain on the aligners, maintained for 2 hours. The thermoformed EX30 and LD30 aligners exhibited final residual stress of 59.99% (SD = 3.02) and 52.57% (SD = 12.28), respectively. In comparison, the 3D aligners from brand "X" (name protected by patent) and OD-Clear TF exhibited residual stress of only 6.98% (SD = 2.64) and 4.39% (SD = 0.84), respectively (Shirey, Mendonca *et al.,* 2023).

Meta-analysis

After applying the eligibility criteria, four studies met the methodological requirements for inclusion in the quantitative meta-analyses. Among them, two studies (Koletsi, Panayi *et al.,* 2023; Eslami, Kopp *et al.,* 2024) provided data on surface roughness parameters, allowing the comparison between thermoformed and 3D-printed aligners before and after clinical use. Another two studies (Jindal, Juneja *et al.,* 2019; Bandić, Vodanović *et al.,* 2024) presented comparable data on dimensional variation between the planned thickness and the found thickness after aligner fabrication.

In the dataset obtained from the meta-analysis of roughness for unused aligners, a statistically significant difference was observed in the Sa parameter, the average absolute surface roughness, with considerably higher values for 3D-printed aligners. The standardized mean difference (SMD) was 2.73, with a 95% confidence interval ranging from 2.14 to 3.31 ($p < 0.00001$), with no evidence of heterogeneity between studies ($I^2 = 0\%$), indicating robustness in the findings. On the other hand, the Sq parameter, the root mean square height deviation, did not show a statistically significant difference between the groups (SMD = 0.37; 95% CI: –1.99 to 2.72; p = 0.76), and exhibited extremely high heterogeneity ($I^2 = 95\%$), limiting the reliability of the statistical synthesis. For the Sv parameter, the maximum valley depth, thermoformed aligners showed higher values compared to 3D-printed aligners, with an SMD of –1.19 (95% CI: –2.29 to –0.08; p = 0.04), and substantial heterogeneity

between studies (I^2 = 76%). The Sz parameter, the total height between the highest peaks and deepest valleys, did not show a statistically significant difference between groups (SMD = –0.47; 95% CI: –2.31 to 1.36; p = 0.61), and exhibited high heterogeneity (I^2 = 92%)(Koletsi, Panayi *et al.,* 2023; Eslami, Kopp *et al.,* 2024).

In the analysis of aligners already used clinically by patients, significant changes were also observed in the surface roughness parameters. The Sa parameter showed a statistically significant difference between groups, with lower values in thermoformed aligners after use, indicating greater surface smoothing. The SMD was –1.07, with a 95% confidence interval between –2.12 and –0.02 (p = 0.04), and considerable heterogeneity (I^2 = 75%). In contrast, the Sq parameter did not show a statistically significant difference between groups (SMD = 0.71; 95% CI: –1.14 to 0.29; p = 0.16), with zero heterogeneity (I^2 = 0%), indicating consistency between the included studies. The Sv parameter also showed no statistical difference (SMD = 0.27; 95% CI: –1.89 to 2.44; p = 0.80), but with very high heterogeneity (I^2 = 95%). On the other hand, the Sz parameter, measuring the total amplitude of the surface topography, showed a significant difference in favor of the 3D-printed aligners, which maintained higher values after clinical use. The SMD was 1.70, with a confidence interval between 0.67 and 2.74 (p = 0.001), and substantial heterogeneity (I^2 = 74%)(Koletsi, Panayi *et al.,* 2023; Eslami, Kopp *et al.,* 2024).

Finally, the meta-analysis of the variation between the expected and found thickness after fabrication was conducted based on the data from Bandic *et al.,* (2024) and Jindal *et al.,* (2019), involving 20 samples per group. The results showed no statistically significant difference between thermoformed and 3D-printed aligners, with an SMD of 1.48 (95% CI: –7.26 to 4.30; p = 0.62) and extremely high heterogeneity (I^2 = 97%)(Jindal, Juneja *et al.,* 2019; Bandić, Vodanović *et al.,* 2024).

The detailed data, as well as the respective forest plots for the meta-analyses of surface roughness and thickness variation of the aligners, are presented in Supplemental Materials 3 and 4, respectively.

Risk of Bias Among Studies

No risks were reported.

Additional Analyses

No additional analyses were conducted.

DISCUSSION

This systematic review included 23 in vitro studies comparing orthodontic aligners manufactured by thermoforming and 3D printing, with emphasis on physical, mechanical, thermal, geometric, structural, and optical properties. In general, thermoformed aligners, particularly those made of Zendura A, Zendura FLX, and Duran, demonstrated higher surface hardness, tensile strength, and flexural resistance (Atta, Bourauel *et al.,* 2024; Bandić, Vodanović *et al.,* 2024; Sarı, Camcı *et al.,* 2025; Wendl, Wendl *et al.,* 2025). However, they showed significant thickness reduction, greater surface roughness, and lower shape recovery capacity (Koenig, Choi *et al.,* 2022; Shirey, Mendonca *et al.,* 2023; Eslami, Kopp *et al.,* 2024). In contrast, 3D-printed aligners, especially those using TC-85, Dental LT, and Noxi resins, presented superior dimensional stability, higher geometric accuracy, improved shape memory behavior, and more favorable performance under thermal variations (Koletsi, Panayi *et al.,* 2023; Park, Choi *et al.,* 2023; Sharifa, Bourauela *et al.,* 2024; Šimunović, Čekalović Agović *et al.,* 2024; Cremonini, Cappelletti *et al.,* 2025). Despite their advantages in form recovery and adaptability, 3D-printed materials showed lower resistance to cyclic loading, higher susceptibility to pigmentation, and reduced mechanical strength in certain tests (Jindal, Juneja *et al.,* 2019; Lee, Kim *et al.,* 2022; Kuntz, Aranda *et al.,* 2024; Bae, Kim *et al.,* 2025). These findings suggest that the type and composition of the materials used in each manufacturing method directly influence the mechanical behavior and clinical performance of the aligners (Jindal, Worcester *et al.,* 2020; Hertan, McCray *et al.,* 2022; Souman 2023; Spangler, Ammoun *et al.,* 2023; Cremonini, Brucculeri *et al.,* 2024; Sayahpour, Zinelis *et al.,* 2024).

The ability to maintain planned thickness or to customize thickness distribution within the same aligner model represents a key advantage in improving the predictability of orthodontic movements. Thermoformed aligners exhibited fragility in geometric stability, particularly due to significant thickness loss during the thermal molding process. Several studies have demonstrated that aligner thickness directly affects the magnitude and direction of the forces delivered to the teeth, thereby influencing the efficacy and accuracy of dental movements (Grant, Foley *et al.,* 2023;

Alhasyimi, Ayub *et al.,* 2024; Bandić, Vodanović *et al.,* 2024). Bandić *et al.,* (2024) reported average thickness reductions greater than 30% in thermoformed aligners, with extreme cases,such as Erkoloc-Pro, presenting thinning of up to 53.3%, especially in incisal and occlusal regions, which are more susceptible to deformation during thermoforming. In contrast, 3D-printed aligners showed significantly better dimensional stability, with variations ranging from 4% to 23% above the virtual design and lower coefficients of variation compared to thermoformed counterparts. This superior stability not only ensures better control over the forces applied but also opens the possibility of designing aligners with region-specific thickness modulation. Such customization, either by preserving planned thickness or increasing it in specific areas, could enhance biomechanical precision and movement predictability. Furthermore, the digital workflow enables adaptive modeling for complex cases, where differentiated thicknesses can be used to reinforce specific zones or modulate force application according to the movement strategy. Some authors suggest that excessive thickness in printed models may be associated with the use of resins not originally developed for orthodontic purposes or with variations in printer calibration and resolution (Edelmann, English *et al.,* 2020; Lee, Kim *et al.,* 2022; Bandić, Vodanović *et al.,* 2024).

Koenig *et al.,* (2022) confirmed this superiority by reporting lower thickness variation and greater fidelity to digital modeling in printed aligners, with a mean dimensional deviation of less than 0.15 mm, while thermoformed aligners exhibited greater deviations and irregularities that could compromise clinical efficacy (Koenig, Choi *et al.,* 2022). Park *et al.,* (2023) corroborated these findings, noting that thermoformed aligners exhibited greater thickness reduction after fabrication (Park, Choi *et al.,* 2023). Regarding geometric accuracy, the printed aligners exhibited lower mean absolute deviations relative to reference models (0.11 mm vs. 0.13 mm), lower RMS (0.147 mm vs. 0.174 mm), and lower standard deviation (0.015 mm vs. 0.021 mm), with statistical significance ($p < 0.001$) (Bandić, Vodanović *et al.,* 2024). This precision was most evident in complex anatomical models, as demonstrated by Spangler *et al.,* (2023), who evaluated arches with varying degrees of crowding. Jindal *et al.,* (2020) and Koenig *et al.,* (2022) presented comparable data. Jindal *et al.,* (2020) observed that the thermoformed aligners had average measurements of 7.88 mm (SD = 0.072), while the printed aligners showed 8.20 mm (SD = 0.069), suggesting results distinct from those reported by Bandic *et al.,* (2024). Nevertheless,

Koenig *et al.,* (2022) compared two thermoformed models from different brands and one printed model, concluding that the thermoformed aligners exhibited greater accuracy deviation. The dimensional fidelity of the printed aligners may favor the predictability of dental movements, especially those requiring greater control, such as rotations and torque, although further studies are needed to confirm this advantage (Jindal, Worcester *et al.,* 2020; Koenig, Choi *et al.,* 2022; Park, Choi *et al.,* 2023; Spangler, Ammoun *et al.,* 2023; Bandić, Vodanović *et al.,* 2024).

Shape memory capacity represents a significant biomechanical advantage in orthodontic treatment, as it enables the aligner to recover its original configuration after being deformed intraorally. This property enhances the continuity and consistency of the force applied to teeth, potentially improving the efficiency and predictability of dental movements. In thermal analyses, the thermoformed aligners exhibited glass transition temperatures (Tg) above 90°C, such as Zendura FLX (107.1°C), indicating high thermal stability but lower elastic adaptive response capacity. In contrast, the TC-85 printed aligner exhibited a Tg of 42.3°C (Atta, Bourauel *et al.,* 2024), allowing shape memory activation at intraoral temperature. It is noteworthy that Tg refers to the midpoint of the DSC curve, although the onset of the memory effect occurs from 30.4°C, a temperature lower than the average intraoral temperature. Lee *et al.,* (2022), using dynamic mechanical analysis, identified a Tg of 68.85°C for TC-85, highlighting that different evaluation methods influence the observed values(Gracia-Fernandez, Gomez-Barreiro *et al.,* 2010). The growing trend of using shape memory polymers is corroborated by studies aiming to improve their properties (Elshazly, Keilig *et al.,* 2021; Elshazly, Keilig *et al.,* 2022; Lee, Kim *et al.,* 2022). Angular recovery tests showed that printed aligners reached angles of up to 155° at 45°C, with recovery rates exceeding 85%, whereas thermoformed aligners did not exceed 6° and 3%, respectively (Atta, Bourauel *et al.,* 2024). Lee *et al.,* (2022) warned that full recovery may take more than one hour. Wang *et al.,* (2017) demonstrated that thermoformed aligners based on polyurethane also exhibit, albeit slightly, a memory effect due to the alternated structure of rigid and flexible segments. DMA analyses revealed that although the printed aligners exhibit greater thermal sensitivity, with a reduction in the storage modulus from 3000 to 1500 MPa, the combination of dimensional stability and shape recovery ensures satisfactory clinical performance (Atta, Bourauel *et al.,* 2024). Sayahpour *et al.,* (2024) also pointed out that the printed aligners have greater resistance to thermal

deformations due to their viscoelastic properties (Wang, Liu *et al.,* 2017; Lee, Kim *et al.,* 2022; Sayahpour, Zinelis *et al.,* 2024; Wang, Zhou *et al.,* 2024).

It is essential to emphasize that the comparison between different types of aligners must consider the multiple variables involved in the manufacturing processes. In the case of thermoformed aligners, the molding technique, whether by pressure or vacuum, can directly affect the final material's physico-mechanical properties, altering aspects such as thickness, stiffness, and dimensional stability, which hinders comparison across studies. Similarly, aligners produced by direct three-dimensional printing (DPA) also exhibit variability in their properties, influenced by factors such as the type of printer used, the printing orientation, and especially the time and temperature of the post-curing UV process (Jindal, Juneja *et al.,* 2019). Even when the same resin is used, these technical parameters can lead to significant differences in mechanical strength, elasticity, and even cytotoxicity. Therefore, the lack of standardization in manufacturing methods, both for thermoformed and printed aligners, epresents a major challenge for comparative analysis among current scientific studies (Bichu, Alwafi *et al.,* 2023).

Regarding mechanical properties, the thermoformed aligners demonstrated greater point resistance in flexural tests, with forces up to 3.6 N, attributed to their hardness and rigidity (Atta, Bourauel *et al.,* 2024). Lombardo *et al.,* (2016) emphasized that single-layer thermoformed aligners are more resistant to bending than multi-layer ones. In contrast, the printed aligners exhibited constant and controlled force over time, which contributes to greater predictability in treatment and a potential reduction in the number of trays. Under simulated clinical use conditions, the printed aligners also outperformed the thermoformed ones. TC-85 resisted over 480 N after 500 compression cycles, while the thermoformed PETG only withstood 115 N (Bae, Kim *et al.,* 2025). In traction tests, the NOVA aligner reached forces up to 30 N, compared to 19 to 27 N in the thermoformed aligners (Cremonini, Cappelletti *et al.,* 2025). Jindal *et al.,* (2020) observed greater mechanical resistance and lower roughness in the printed aligners, indicating greater durability and comfort. Stress relaxation behavior revealed that TC-85 lost 100% of its force after 8 hours, while the thermoformed Zendura FLX and Duran maintained between 38% and 71% of the initial force (Cremonini, Brucculeri *et al.,* 2024). While this represents an apparent advantage for the thermoformed aligners, the recovery capacity of the printed aligners compensates for this loss. It is noted, however, that Cremonini *et al.,* (2024)

used only one sample per group, justifying the decision based on evidence that increasing the sample size does not significantly alter the results (Lombardo, Arreghini *et al.,* 2017; Al-Nadawi, Kravitz *et al.,* 2021). Cremonini *et al.,* (2025a) also tested aligners with customized thickness gradients, which showed lower relaxation in critical areas such as molars, reinforcing the importance of digital customization(Cremonini, Cappelletti *et al.,* 2025).

Color stability and pigmentation changes in aligners have been frequently evaluated in laboratory studies. However, the clinical relevance of these findings remains debatable, considering that aligners are typically replaced every 10 to 15 days. Within such a short usage period, color changes tend to have minimal aesthetic impact in practice, and therefore, associating discoloration with compromised long-term aesthetics may not be appropriate (Bichu, Alwafi *et al.,* 2023). On the other hand, it is important to highlight that 3D-printed aligners have demonstrated lower surface microhardness compared to thermoformed ones, a factor that could have clinical implications. Surface microhardness is associated not only with color changes and surface roughness but also with the potential for fractures and loss of retention during use (Kohda, Iijima *et al.,* 2013; Maleki, Bagherifard *et al.,* 2023). While thermoformed aligners such as Zendura A showed higher microhardness values (13.4 VHN) compared to printed aligners (ranging from 8.1 VHN for TC-85 to 2.7 VHN for CA Pro) (Atta, Bourauel *et al.,* 2024), this advantage may be counterbalanced by their increased susceptibility to chemical degradation under acidic conditions (Sharifa, Bourauela *et al.,* 2024). Conversely, printed aligners demonstrated greater structural stability after simulated use (Eslami, Kopp *et al.,* 2024) and lower bacterial adhesion (Souman 2023), which are desirable features for periodontal health. Although thermoformed aligners may initially exhibit superior translucency, Park *et al.,* (2023) reported a reduction in this property following UV aging, further supporting the notion that material performance over time should be interpreted in light of clinical usage duration and manufacturing limitations (Park, Choi *et al.,* 2023)(Park, Choi *et al.,* 2023).Surface roughness assessment revealed significant differences between the manufacturing methods. Roughness and porosity are critical parameters, as more irregular surfaces favor biofilm accumulation and increased bacterial adhesion, creating niches conducive to microbial proliferation (Suter, Zinelis *et al.,* 2020). Meta-analyses demonstrated that printed aligners had significantly higher average roughness (Sa) compared to thermoformed ones in

unused samples (SMD = 2.73; p < 0.00001), with no heterogeneity (I^2 = 0%), providing robustness to the results. This increased roughness is attributed to the 3D printing process, which uses successive deposition of photopolymer layers, resulting in surfaces with greater texture and microaltitudes. This can affect both the interaction of the aligner with the soft tissues and its hygiene. In contrast, roughness in thermoformed aligners may be linked to the undulations and imperfections of the 3D model used in the molding process (Low, Lee *et al.,* 2011).

After clinical use, the thermoformed aligners exhibited lower average roughness, possibly due to surface abrasion from intraoral contact (Papadopoulou, Cantele *et al.,* 2019; Eslami, Kopp *et al.,* 2024). Koletsi *et al.,* (2022), however, reported an increase in roughness after clinical use, which may be explained by the larger number of samples and the expanded area of evaluation. Both studies demonstrated an increase in roughness in the printed aligners after clinical use, a discrepancy that may be related to differences in resin curing protocols. Regarding the Sz parameter (total amplitude between peaks and valleys), no statistically significant difference was found between the groups (SMD = –0.47; 95% CI: –2.31 to 1.36; p = 0.61), although heterogeneity was high (I^2 = 92%), which limits the generalization of the findings and highlights the need for methodological standardization in laboratory studies(Koletsi, Panayi *et al.,* 2023).

Roughness analysis after clinical use revealed a partial inversion of patterns. The Sa parameter showed significantly lower values in the thermoformed aligners (SMD = –1.07; 95% CI: –2.12 to –0.02; p = 0.04; I^2 = 75%), a result attributed to abrasion caused by masticatory forces, contact with soft tissues, and the action of saliva. This progressive smoothing may compromise mechanical and aesthetic characteristics over time. In contrast, the Sz parameter was significantly higher in the printed aligners after use (SMD = 1.70; 95% CI: 0.67 to 2.74; p = 0.001; I^2 = 74%), suggesting greater resistance to topographic degradation and loss of roughness, possibly due to the photopolymerizable polymer's crosslinking density and the precision of additive manufacturing. Other parameters, such as Sq and Sv, showed no significant differences between the groups, with high heterogeneity indices ($I^2 \geq 74\%$)(Koletsi, Panayi *et al.,* 2023).

The meta-analysis of thickness variation between nominal and actual values, based on the studies of Bandic *et al.,* (2024) and Jindal *et al.,* (2019), did not demonstrate statistical significance (SMD = 1.48; 95% CI: –7.26 to 4.30; p = 0.62),

with extremely high heterogeneity (I^2 = 97%). While Bandic *et al.,* (2024) reported greater discrepancies in the printed aligners, Jindal *et al.,* (2019) observed higher dimensional accuracy in the same models. Discrepancies may be related to different printing equipment, resin types, measurement calibration methods, or variations in the thermoforming process. Despite the small number of studies addressing this variable, dimensional fidelity is a critical factor for the efficacy of orthodontic movements and clinical predictability(Jindal, Juneja *et al.,* 2019; Bandić, Vodanović *et al.,* 2024).

CONCLUSION

The analysis of the in vitro studies revealed that thermoformed aligners have higher surface hardness and flexural resistance but suffer significant thickness loss and lower geometric precision, which may compromise more complex dental movements. Additionally, they have lower shape recovery capacity and less control over force distribution. In contrast, 3D printed aligners stand out for their superior dimensional stability, morphological precision, elastic recovery, and tensile strength. Although they exhibit higher surface roughness before use, they maintain their topographic characteristics better after clinical use, indicating greater resistance to wear. Thermoformed aligners, on the other hand, tend to smooth the surface during use, which may enhance comfort but compromise the stability of the movement over time. Despite still facing challenges, such as maintaining force over time and surface wear, 3D printed aligners present themselves as a promising technology with great potential to redefine biomechanical and functional standards in orthodontics. However, more clinical studies are needed to consolidate these findings and support more precise and personalized therapeutic decisions.

Table 7 - Comparison of Physical and Mechanical Properties of Thermoformed and 3D-Printed Orthodontic Aligners

Characteristic	Type	Thermoformed Aligners	3D-Printed Aligners
Thickness and geometric accuracy	Physical	Significant thickness loss and lower geometric accuracy	Greater dimensional stability and morphological precision
Surface topography during clinical use	Physical	Surface tends to smooth during use, increasing comfort but compromising	Initially rougher surface, but maintains topography after use, showing higher

		movement stability	wear resistance
Surface hardness	Mechanical	Higher	Lower
Flexural strength	Mechanical	Higher	Lower
Shape recovery (elasticity)	Mechanical	Lower elastic recovery capacity	Better elasticity and higher tensile strength
Force control	Mechanical	Less control over force distribution	Better force control and stability
Biomechanical and functional potential	Mechanical	Limited for complex tooth movements	Promising technology with potential to redefine biomechanical and functional standards
Need for clinical evidence	-	More established data but with known biomechanical limitations	Requires further clinical studies for full validation

Data Availability Statements

The data underlying this article will be shared on reasonable request to the corresponding author.

Conflict of interest: The authors have no conflict of interest.

Fundings: personal funding.

REFERENCES

Abreu, L. G. (2018). "Orthodontics in Children and Impact of Malocclusion on Adolescents' Quality of Life." Pediatr Clin North Am **65**(5): 995-1006.

Al-Nadawi, M., N. D. Kravitz, *et al.,* (2021). "Effect of clear aligner wear protocol on the efficacy of tooth movement." Angle Orthod **91**(2): 157-163.

Albertini, P., M. Colombo, *et al.,* (2022). "Advances in orthodontic aligner materials: A critical review of property testing methodologies." Materials Science and Engineering: C **134**: 112683.

Alexandropoulos, A., Y. S. Al Jabbari, *et al.,* (2015). "Chemical and mechanical characteristics of contemporary thermoplastic orthodontic materials." Aust Orthod J **31**(2): 165-170.

Alhasyimi, A. A., A. Ayub, *et al.,* (2024). "Effectiveness of the Attachment Design and Thickness of Clear Aligners during Orthodontic Anterior Retraction: Finite Element Analysis." Eur J Dent **18**(1): 174-181.

Allison, P. J., D. Locker, *et al.,* (1997). "Quality of life: a dynamic construct." Soc Sci Med **45**(2): 221-230.

Arslan Avan, B., O. C. Bodur, *et al.,* (2025). "An in-vitro assessment of bisphenol a release from thermoplastic orthodontic appliances exposed to various beverages." BMC Oral Health **25**(1): 750.

Atta, I., C. Bourauel, *et al.,* (2024). "Physiochemical and mechanical characterisation of orthodontic 3D printed aligner material made of shape memory polymers (4D aligner material)." J Mech Behav Biomed Mater **150**: 106337.

Bae, B. G., Y. H. Kim, *et al.,* (2025). "A study on the compressive strength of three-dimensional direct printing aligner material for specific designing of clear aligners." Sci Rep **15**(1): 2489.

Bandić, R., K. Vodanović, *et al.,* (2024). "Thickness Variations of Thermoformed and 3D-Printed Clear Aligners." Acta Stomatol Croat **58**(2): 145-155.

Bichu, Y. M., A. Alwafi, *et al.,* (2023). "Advances in orthodontic clear aligner materials." Bioact Mater **22**: 384-403.

Blundell, H. L., T. Weir, *et al.,* (2022). "Predictability of overbite control with the Invisalign appliance comparing SmartTrack with precision bite ramps to EX30." Am J Orthod Dentofacial Orthop **162**(2): e71-e81.

Borda, A. F., J. S. Garfinkle, *et al.,* (2020). "Outcome assessment of orthodontic clear aligner vs fixed appliance treatment in a teenage population with mild malocclusions." Angle Orthod **90**(4): 485-490.

Boyd, R. L. (2008). "Esthetic orthodontic treatment using the invisalign appliance for moderate to complex malocclusions." J Dent Educ **72**(8): 948-967.

Bräscher, A. K., D. Zuran, *et al.,* (2016). "Patient survey on Invisalign(®) treatment comparing [corrected] the SmartTrack(®) material to the previously used [corrected] aligner material." J Orofac Orthop **77**(6): 432-438.

Can, E., N. Panayi, *et al.,* (2022). "In-house 3D-printed aligners: effect of in vivo ageing on mechanical properties." Eur J Orthod **44**(1): 51-55.

Condò, R., G. Mampieri, *et al.,* (2021). "SEM characterization and ageing analysis on two generation of invisible aligners." BMC Oral Health **21**(1): 316.

Condo, R., L. Pazzini, *et al.,* (2018). "Mechanical properties of "two generations" of teeth aligners: Change analysis during oral permanence." Dent Mater J **37**(5): 835-842.

Cremonini, F., L. Brucculeri, *et al.,* (2024) "Comparison of stress relaxation properties between 3-dimensional printed and thermoformed orthodontic aligners: A pilot study of in vitro simulation of two consecutive 8-hours force application." APOS Trends Orthod **14**, 225-234 DOI: doi: 10.25259/APOS_201_2023.

Cremonini, F., M. Cappelletti, *et al.,* (2025) "Force Expressed by 3D-Printed Aligners with Different Thickness and Design Compared to Thermoformed Aligners: An in Vitro Study." Applied Sciences **15**, 2911 DOI: https://doi.org/10.3390/app15062911.

Cremonini, F., M. Cappelletti, *et al.,* (2025). "An In Vitro Comparison Study Regarding Retention Force Expressed by Thermoformed Aligners and 3D-Printed Aligners with Different Thickness and Design." Appl. Sci. **15**: 1345.

Dalaie, K., H. Behnia, *et al.,* (2021). "The effects of thermoforming and artificial aging on the mechanical properties of PET-G aligners: A three-point bending and Vickers hardness study." Journal of the Mechanical Behavior of Biomedical Materials **116**: 104329.

Dasy, H., A. Dasy, *et al.,* (2015). "Effects of variable attachment shapes and aligner material on aligner retention." Angle Orthod **85**(6): 934-940.

Di Spirito, F., F. D'Ambrosio, *et al.,* (2023). "Impact of Clear Aligners versus Fixed Appliances on Periodontal Status of Patients Undergoing Orthodontic Treatment: A Systematic Review of Systematic Reviews." Healthcare (Basel) **11**(9).

Dos Reis-Prado, A. H., L. G. Abreu, *et al.,* (2023). "Influence of sodium hypochlorite on cyclic fatigue resistance of nickel-titanium instruments: A systematic review and meta-analysis of in vitro studies." Clin Oral Investig **27**(11): 6291-6319.

Dos Reis-Prado, A. H., L. G. Abreu, *et al.,* (2021). "Comparison between immediate and delayed post space preparations: a systematic review and meta-analysis." Clin Oral Investig **25**(2): 417-440.

Edelmann, A., J. D. English, *et al.,* (2020). "Analysis of the thickness of 3-dimensional-printed orthodontic aligners." Am J Orthod Dentofacial Orthop **158**(5): e91-e98.

Eliades, T. and C. Bourauel (2005). Intraoral aging of orthodontic materials: the picture we miss and its clinical relevance. Am J Orthod Dentofacial Orthop. United States. **127:** 403-412.

ElNaghy, R. and M. Hasanin (2023). "Impact of malocclusions on oral health-related quality of life among adolescents." Evid Based Dent **24**(3): 140-141.

Elshazly, T. M., L. Keilig, *et al.,* (2021). "Primary Evaluation of Shape Recovery of Orthodontic Aligners Fabricated from Shape Memory Polymer (A Typodont Study)." Dent J (Basel) **9**(3).

Elshazly, T. M., L. Keilig, *et al.,* (2022) "Potential application of 4D technology in fabrication of orthodontic aligners." Front. Mater **8**, 794536.

Eslami, S., S. Kopp, *et al.,* (2024). "Alterations in the surface roughness and porosity parameters of directly printed and Invisalign aligners after 1 week of intraoral usage: An in vivo prospective investigation." Am J Orthod Dentofacial Orthop **165**(1): 73-79.

Fang, D., F. Li, *et al.,* (2020). "Changes in mechanical properties, surface morphology, structure, and composition of Invisalign material in the oral environment." Am J Orthod Dentofacial Orthop **157**(6): 745-753.

FayyazAhamed, S., S. M. Kumar, *et al.,* (2020). Cytotoxic evaluation of directly 3D printed aligners and Invisalign.

Flores-Mir, C., J. Brandelli, *et al.,* (2018). "Patient satisfaction and quality of life status after 2 treatment modalities: Invisalign and conventional fixed appliances." Am J Orthod Dentofacial Orthop **154**(5): 639-644.

Ganta, G. K., K. Cheruvu, *et al.,* (2021). "Clear aligners, the aesthetic solution: a review." International Journal of Dental Materials **3**(3): 90-95.

Gao, M., X. Yan, *et al.,* (2022). "Comparison of pain perception, anxiety, and impacts on oral health-related quality of life between patients receiving clear aligners and fixed appliances during the initial stage of orthodontic treatment." (1460-2210 (Electronic)).

Göranson, E., M. Sonesson, *et al.,* (2023). "Malocclusions and quality of life among adolescents: a systematic review and meta-analysis." Eur J Orthod **45**(3): 295-307.

Gracia-Fernandez, C. A., S. Gomez-Barreiro, *et al.,* (2010) "Comparative study of the dynamic glass transition temperature by DMA and TMDSC." Polym. Test **29**, 1002 – 1006.

Grant, J., P. Foley, *et al.,* (2023). "Forces and moments generated by 3D direct printed clear aligners of varying labial and lingual thicknesses during lingual movement of maxillary central incisor: an in vitro study." Prog Orthod **24**(1): 23.

Hahn, W., B. Engelke, *et al.,* (2010). "Initial forces and moments delivered by removable thermoplastic appliances during rotation of an upper central incisor." Angle Orthod **80**(2): 239-246.

Haouili, N., N. D. Kravitz, *et al.,* (2020). "Has Invisalign improved? A prospective follow-up study on the efficacy of tooth movement with Invisalign." Am J Orthod Dentofacial Orthop **158**(3): 420-425.

Hennessy, J. and E. A. Al-Awadhi (2016). "Clear aligners generations and orthodontic tooth movement." J Orthod **43**(1): 68-76.

Hertan, E., J. McCray, *et al.,* (2022). "Force profile assessment of direct-printed aligners versus thermoformed aligners and the effects of non-engaged surface patterns." Prog Orthod **23**(1): 49.

Iliadi, A., D. Koletsi, *et al.,* (2020). "Safety Considerations for Thermoplastic-Type Appliances Used as Orthodontic Aligners or Retainers. A Systematic Review and Meta-Analysis of Clinical and In-Vitro Research." Materials (Basel) **13**(8).

Jindal, P., M. Juneja, *et al.,* (2019). "Mechanical and geometric properties of thermoformed and 3D printed clear dental aligners." Am J Orthod Dentofacial Orthop **156**(5): 694-701.

Jindal, P., F. Worcester, *et al.,* (2020). "Mechanical behaviour of 3D printed vs thermoformed clear dental aligner materials under non-linear compressive loading using FEM." J Mech Behav Biomed Mater **112**: 104045.

Joffe, L. (2003). "Invisalign: early experiences." J Orthod **30**(4): 348-352.

Kesling, H. D. (1945). "The philosophy of the tooth positioning appliance." American Journal of Orthodontics and Oral Surgery **31**(6): 297-304.

Kiyak, H. A. (2008). "Does orthodontic treatment affect patients' quality of life?" J Dent Educ **72**(8): 886-894.

Ko, J., R. D. Bloomstein, *et al.,* (2021). "Effect of build angle and layer height on the accuracy of 3-dimensional printed dental models." Am J Orthod Dentofacial Orthop **160**(3): 451-458 e452.

Koenig, N., J. Y. Choi, *et al.,* (2022). "Comparison of dimensional accuracy between direct-printed and thermoformed aligners." Korean J Orthod **52**(4): 249-257.

Kohda, N., M. Iijima, *et al.,* (2013) "Effects of mechanical properties of thermoplastic materials on the initial force of thermoplastic appliances." Angle Orthod **83**, 476 – 483.

Koletsi, D., N. Panayi, *et al.,* (2023). "In vivo aging-induced surface roughness alterations of Invisalign(®) and 3D-printed aligners." J Orthod **50**(4): 352-360.

Kumar, S. M. (2019). Cytotoxicity of 3D Printed Materials: An In Vitro study.

Kuntz, L., L. Aranda, *et al.,* (2024). "Effects of aging on the tensile strength and surface condition of orthodontic aligners: a comparative study of five models." Eur J Orthod **46**(6).

Landis, J. R. and G. G. Koch (1977). "The measurement of observer agreement for categorical data." Biometrics **33**(1): 159-174.

Lee, S. Y., H. Kim, *et al.,* (2022). "Thermo-mechanical properties of 3D printed photocurable shape memory resin for clear aligners." Sci Rep **12**(1): 6246.

Levrini, L., A. Mangano, *et al.,* (2015). "Periodontal health status in patients treated with the Invisalign(®) system and fixed orthodontic appliances: A 3 months clinical and microbiological evaluation." Eur J Dent **9**(3): 404-410.

Linjawi, A. I. and A. M. Abushal (2022). "Adaptational changes in clear aligner fit with time." Angle Orthod **92**(2): 220-225.

Lombardo, L., A. Arreghini, *et al.,* (2017). "Predictability of orthodontic movement with orthodontic aligners: a retrospective study." Prog Orthod **18**(1): 35.

Low, B., W. Lee, *et al.,* (2011). "Ultrastructure and morphology of biofilms on thermoplastic orthodontic appliances in 'fast' and 'slow' plaque formers." Eur J Orthod **33**(5): 577-583.

Maleki, E., Bagherifard, *et al.,* (2023) "Correlation of residual stress, hardness and surface roughness with crack initiation and fatigue strength of surface treated additive manufactured AlSi10Mg: experimental and machine learning approaches." J. Mater. Res. Technol **24**, 3265 – 3283.

Maspero, C. and G. M. Tartaglia (2020). 3D Printing of Clear Orthodontic Aligners: Where We Are and Where We Are Going. Materials (Basel). Switzerland. **13**.

Milovanović, A., A. Sedmak, *et al.,* (2021). "The effect of time on mechanical properties of biocompatible photopolymer resins used for fabrication of clear dental aligners." J Mech Behav Biomed Mater **119**: 104494.

Moher, D., A. Liberati, *et al.,* (2009). "Preferred reporting items for systematic reviews and meta-analyses: the PRISMA statement." PLoS Med **6**(7): e1000097.

Monisha, J. and E. Peter (2024). "Efficacy of clear aligner wear protocols in orthodontic tooth movement-a systematic review." Eur J Orthod **46**(3).

Moshiri, M., N. Kravitz, *et al.,* (2021). "Invisalign eighth-generation features for deep-bite correction and posterior arch expansion." Seminars in Orthodontics **27**.

Nakornnoi, T., W. Srirodjanakul, *et al.,* (2024). "The biomechanical effects of clear aligner trimline designs and extensions on orthodontic tooth movement: a systematic review." BMC Oral Health **24**(1): 1523.

Papadopoulou, A. K., A. Cantele, *et al.,* (2019). "Changes in Roughness and Mechanical Properties of Invisalign(®) Appliances after One- and Two-Weeks Use." Materials (Basel) **12**(15).

Papadopoulou, A. K. P., Moschos A. Zafiriadis, Lekkas (2015). "Clinical effectiveness of clear aligner therapy: A systematic review. ." Progress in Orthodontics **16**(1): 1-11.

Papadopoulou, A. K. P., Moschos A. Zafiriadis, Lekkas (2019). "Evaluation of orthodontic treatment outcome with clear aligners using the Peer Assessment Rating Index." Journal of Orofacial Orthopedics **80**(2): 61–67.

Park, S. Y., S. H. Choi, *et al.,* (2023). "Comparison of translucency, thickness, and gap width of thermoformed and 3D-printed clear aligners using micro-CT and spectrophotometer." Sci Rep **13**(1): 10921.

Phan, X. and P. H. Ling (2007). "Clinical limitations of Invisalign." J Can Dent Assoc **73**(3): 263-266.

Raszewski, Z., K. Chojnacka, *et al.,* (2022). "Mechanical Properties and Biocompatibility of 3D Printing Acrylic Material with Bioactive Components." J Funct Biomater **14**(1).

Ribeiro, L. G., L. S. Antunes, *et al.,* (2023). "Impact of malocclusion treatments on Oral Health-Related Quality of Life: an overview of systematic reviews." Clin Oral Investig **27**(3): 907-932.

Rossini, G., S. Parrini, *et al.,* (2015). "Efficacy of clear aligners in controlling orthodontic tooth movement: a systematic review." Angle Orthod **85**(5): 881-889.

Ryu, J. H., J. S. Kwon, *et al.,* (2018). "Effects of thermoforming on the physical and mechanical properties of thermoplastic materials for transparent orthodontic aligners." Korean J Orthod **48**(5): 316-325.

Safavi, M., A. Bordbar-Khiabani, *et al.,* (2022). "Additive Manufacturing: An Opportunity for the Fabrication of Near-Net-Shape NiTi Implants." Journal of Manufacturing and Materials Processing **6**: 65.

Sarı, T., H. Camcı, *et al.,* (2025) "Evaluation of mechanical changes to clear aligners caused by exposure to different liquids." Australasian Orthodontic Journal **40**, 75-86 DOI: DOI: 10.2478/aoj-2024-0022.

Sayahpour, B., S. Zinelis, *et al.,* (2024). "Effects of intraoral aging on mechanical properties of directly printed aligners vs. thermoformed aligners: an in vivo prospective investigation." Eur J Orthod **46**(1).

Schünemann HB, J., Guyatt G, Oxman A (2013). "GRADE handbook for grading quality of evidence and strength of recommendations." GRADE Working Group.

Sharifa, M., C. Bourauela, *et al.,* (2024) "Force system of 3D-printed orthodontic aligners made of shape memory polymers: an in vitro study." VIRTUAL AND PHYSICAL PROTOTYPING **19**, e2361857 DOI: https://doi.org/10.1080/17452759.2024.2361857.

Shirey, N., G. Mendonca, *et al.,* (2023). "Comparison of mechanical properties of 3-dimensional printed and thermoformed orthodontic aligners." Am J Orthod Dentofacial Orthop **163**(5): 720-728.

Šimunović, L., S. Čekalović Agović, *et al.,* (2024). "Color and Chemical Stability of 3D-Printed and Thermoformed Polyurethane-Based Aligners." Polymers (Basel) **16**(8).

Souman, O. (2023) "Comparison of Thickness Between Thermoformed and Printed Orthodontic Aligners." Loma Linda University Electronic Theses, Dissertations & Projects, 2665.

Spangler, T., R. Ammoun, *et al.,* (2023). "The effect of crowding on the accuracy of 3-dimensional printing." Am J Orthod Dentofacial Orthop **164**(6): 879-888.

Srivastava, R., B. Jyoti, *et al.,* (2017). "Sequential Removal Orthodontics: An Alternative Approach." International Journal of Contemporary Medicine Surgery and Radiology **22**: 32-36.

Suter, F., S. Zinelis, *et al.,* (2020). "Roughness and wettability of aligner materials." J Orthod **47**(3): 223-231.

Wajekar, N., S. Pathak, *et al.,* (2022). "Rise & review of invisalign clear aligner system." IP Indian Journal of Orthodontics and Dentofacial Research **8**: 7-11.

Wang, Y., S. Zhou, *et al.,* (2024). "Comparison of treatment effects between clear aligners and fixed appliances in patients treated with miniscrew-assisted molar distalization." Eur J Orthod **46**(3).

Wang, Z., J. Liu, *et al.,* (2017). "The Study of Thermal, Mechanical and Shape Memory Properties of Chopped Carbon Fiber-Reinforced TPI Shape Memory Polymer Composites." Polymers (Basel) **9**(11).

Weir, T. (2017). "Clear aligners in orthodontic treatment." Aust Dent J **62 Suppl 1**: 58-62.

Wendl, T., B. Wendl, *et al.,* (2025). "An analysis of initial force and moment delivery of different aligner materials." Biomed Tech (Berl) **70**(3): 259-267.

Zheng, M., R. Liu, *et al.,* (2017). "Efficiency, effectiveness and treatment stability of clear aligners: A systematic review and meta-analysis." Orthod Craniofac Res **20**(3): 127-133.

Zinelis, S., N. Panayi, *et al.,* (2022). "Comparative analysis of mechanical properties of orthodontic aligners produced by different contemporary 3D printers." Orthod Craniofac Res **25**(3): 336-341.

.

Legend of Figures

Figure 1. Systematic review flowchart

Legend of Tables

Table 1 - Search strategies employed in databases

Table 2 - Classification and Utilization Frequency of Orthodontic Aligners in Clinical Studies

Table 3 - Different tests used to study clear aligners

Table 4 - Data extraction

Table 5 – Bias analysis

Table 6 - Test Classification by Physical and Mechanical Properties

Table 7 - Comparison of Physical and Mechanical Properties of Thermoformed and 3D-Printed Orthodontic Aligners

Legend of Supplemental Material

Supplemental Material 1. Articles Excluded After Full Text Review

Supplemental Material 2. Bias Relationship by Analyzed Category

Supplemental Material 3. Data extracted from the meta-analysis of roughness

Supplemental Material 4. Data extracted from the meta-analysis of the dimensional variation. Expected and found thickness in thermoformed and 3D-printed aligners

Figure 1 - Systematic review flowchart

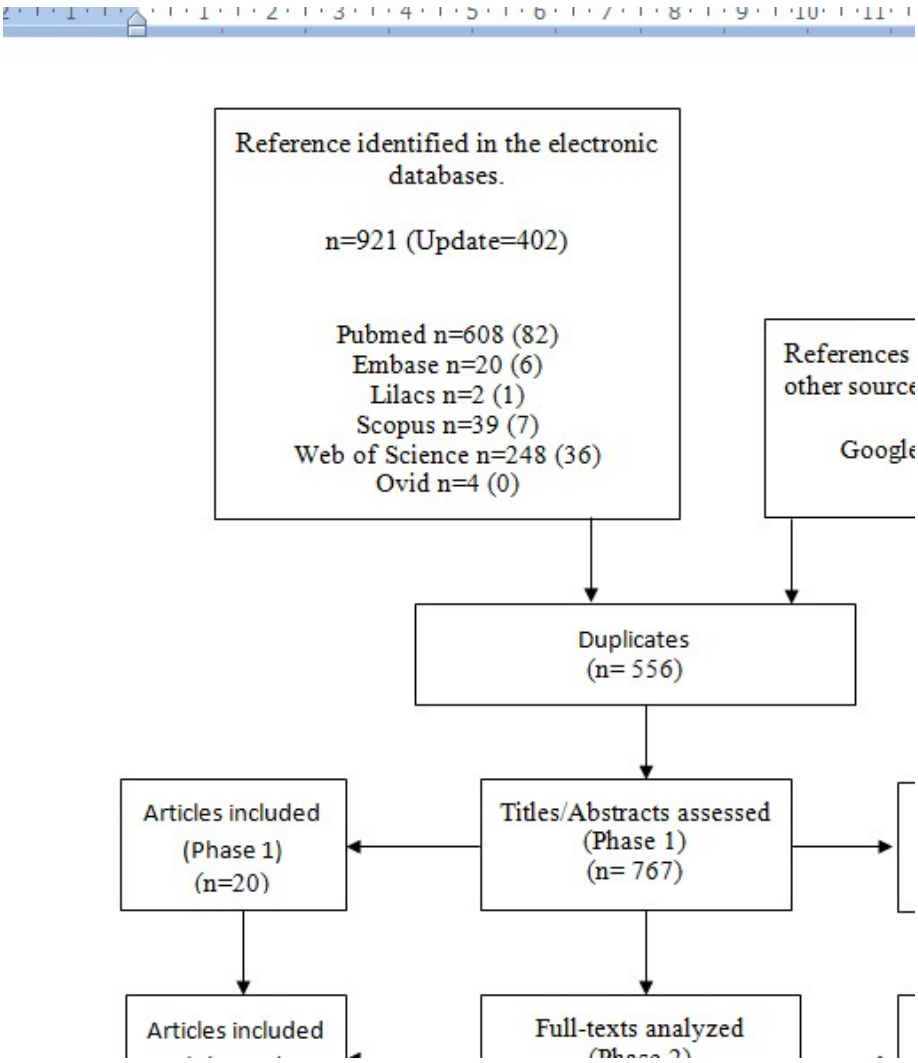

Corresponding author: Jader Oliva Jorge. Department of Restorative Dentistry, School of Dentistry, Universidade Federal de Minas Gerais. Avenida Presidente Antônio Carlos, 6627, Belo Horizonte, Minas Gerais, Brazil. CEP: 31270-901. E-mail:Jader.oj@gmail.com

Funding sources: This research did not receive any specific grant from funding agencies in the public, commercial, or not-for-profit sectors.

Conflicts of interest: The authors declare that they have no conflict of interest.

Author contribution: **Jader Oliva Jorge:** investigation, data curation, methodology, conceptualization and writing – original draft, visualization; **Beatriz Rezende Bergo:** Writing – review and editing, data curation; **Carina Cristina Montalvany-Antonucci**[1]**:** Writing – review and editing, **Lucas Guimarães Abreu:** , formal analysis, methodology, conceptualization, writing – review and edit; **Soraia Macari:** Supervision, Project administration, formal analysis, methodology, conceptualization, writing – review and edit .

Supplementary Files for Comparison between the physical, mechanical properties and accuracy of orthodontic aligners manufactured by thermoforming and by direct three-dimensional printing: a systematic review and meta-analysis

Contents

Articles Excluded After Full Text Review

1. **BICHU, Y. M. *et al.,*** *Advances in orthodontic clear aligner materials*. Bioactive Materials, v. 22, p. 384-403, 2022. DOI: 10.1016/j.bioactmat.2022.10.006. **Reason for exclusion**: This article does not compare the physical, mechanical properties, and accuracy of orthodontic aligners made by thermoforming and direct 3D printing. This article is a narrative review, which does not present comparative groups and does not meet the inclusion criteria of a systematic review.

2. **ZINELIS, S. *et al.,*** *Comparative analysis of mechanical properties of orthodontic aligners produced by different contemporary 3D printers*. Orthodontics & Craniofacial Research, v. 25, n. 3, p. 336-341, 2022. DOI: 10.1111/ocr.12537. **Reason for exclusion**: This article does not compare the physical, mechanical properties, and accuracy of orthodontic aligners made by thermoforming and direct 3D printing. This article does not include a comparative group with thermoformed orthodontic aligners.

3. **CAN, E. *et al.,*** *In-house 3D-printed aligners: effect of in vivo ageing on mechanical properties*. European Journal of Orthodontics, v. 44, n. 1, p. 51-55, 2022. DOI: 10.1093/ejo/cjab022. **Reason for exclusion**: This article does not compare the physical, mechanical properties, and accuracy of orthodontic aligners made by thermoforming and direct 3D printing. This article does not present a comparative group with thermoformed orthodontic aligners.

4. **DALAIE, K. *et al.,*** *Dynamic mechanical and thermal properties of clear aligners after thermoforming and aging*. Progress in Orthodontics, v. 22, n. 1, p. 15, 2021. DOI: 10.1186/s40510-021-00362-8. **Reason for exclusion**: This article does not compare the physical, mechanical properties, and accuracy of orthodontic aligners made by thermoforming and direct 3D printing. This article does not present a comparative group with 3D printed orthodontic aligners.

5. **EDELMANN, A. *et al.,*** *Analysis of the thickness of 3-dimensional-printed orthodontic aligners*. American Journal of Orthodontics and Dentofacial Orthopedics, v. 158, n. 5, p. e91-e98, 2020. DOI: 10.1016/j.ajodo.2020.07.029. **Reason for exclusion**: This article does not compare the physical, mechanical properties, and accuracy of orthodontic aligners made by thermoforming and direct 3D printing. This article does not present a comparative group with thermoformed orthodontic aligners.

6. **FERLIAS, N. *et al.,*** *In Vitro Comparison of Different Invisalign and 3Shape Attachment Shapes to Control Premolar Rotation*. Frontiers in Bioengineering and Biotechnology, v. 10, p. 840622, 2022. DOI: 10.3389/fbioe.2022.840622. **Reason for exclusion**: This article does not compare the physical, mechanical properties, and accuracy of orthodontic aligners made by thermoforming and direct 3D printing. This article addresses the position and shape of attachments used to correct malocclusion with different aligners, and therefore does not meet the inclusion criteria for this systematic review.

7. **CIAVARELLA, D. *et al.,*** *Occlusal Plane Modification in Clear Aligners Treatment: Three Dimensional Retrospective Longitudinal Study*. Dentistry Journal, v. 11, n. 1, p. 8, 2022. DOI: 10.3390/dj11010008. **Reason for exclusion**: This article does not compare the physical, mechanical properties, and accuracy of orthodontic aligners made by thermoforming and direct 3D printing. This article is a retrospective longitudinal study assessing occlusal modifications in patients using orthodontic aligners, thus it does not meet the inclusion criteria for this systematic review.

8. **GUO, R. *et al.,*** *Biomechanical analysis of miniscrew-assisted molar distalization with clear aligners: a three-dimensional finite element study*. European Journal of Orthodontics, v. 46, n. 1, p. cjad077, 2024. DOI: 10.1093/ejo/cjad077. **Reason for exclusion**: This article does not compare the physical, mechanical properties, and accuracy of orthodontic aligners made by thermoforming and direct 3D printing. This article assesses occlusal modifications in patients using orthodontic aligners, and thus it does not meet the inclusion criteria for this systematic review.

9. **WANG, Y. *et al.,*** *Comparison of treatment effects between clear aligners and fixed appliances in patients treated with miniscrew-assisted molar distalization*. European Journal of Orthodontics, v. 46, n. 3, p. cjae021, 2024. DOI: 10.1093/ejo/cjae021.

   Reason for exclusion: This article does not compare the physical, mechanical properties, and accuracy of orthodontic aligners made by thermoforming and direct 3D printing. This article assesses occlusal modifications in patients using orthodontic aligners and includes a control group of patients using fixed orthodontic appliances, thus it does not meet the inclusion criteria for this systematic review.

10. **YAN, X. *et al.,*** *Effectiveness of clear aligners in achieving proclination and intrusion of incisors among Class II division 2 patients: a multivariate analysis*. Progress in Orthodontics, v. 24, n. 1, p. 12, 2023. DOI: 10.1186/s40510-023-00463-6.

    Reason for exclusion: This article does not compare the physical, mechanical properties, and accuracy of orthodontic aligners made by thermoforming and direct 3D printing. This article assesses occlusal modifications in patients using orthodontic aligners, thus it does not meet the inclusion criteria for this systematic review.

11. **ALJUMAILY, E.; AL-KHATIB, A.** *Hardness and elastic modulus assessment for two aligner materials before and after thermocycling: a comparative study*. Georgian Medical News, n. 339, p. 77-82, 2023.

    Reason for exclusion: This article does not compare the physical, mechanical properties, and accuracy of orthodontic aligners made by thermoforming and direct 3D printing. This article does not present a comparative group with 3D printed orthodontic aligners.

12. **LIU, J. Q. *et al.,*** *Different biomechanical effects of clear aligners in closing maxillary and mandibular extraction spaces: Finite element analysis*. American Journal of Orthodontics and Dentofacial Orthopedics, v. 163, n. 6, p. 811-824, 2023. DOI: 10.1016/j.ajodo.2022.07.021.

    Reason for exclusion: This article does not compare the physical, mechanical properties, and accuracy of orthodontic aligners made by thermoforming and direct 3D printing. This article assesses occlusal modifications in patients using orthodontic

aligners and includes a control group of patients using fixed orthodontic appliances, thus it does not meet the inclusion criteria for this systematic review.

13. **KIONG, M. *et al.,*** *Effect of attachment flash on clear aligner force delivery: an in vitro study*. BMC Oral Health, v. 24, n. 1, p. 538, 2024. DOI: 10.1186/s12903-024-04284-9.
Reason for exclusion: This article does not compare the physical, mechanical properties, and accuracy of orthodontic aligners made by thermoforming and direct 3D printing. This article addresses the position and shape of attachments used to correct malocclusion with different aligners, and therefore does not meet the inclusion criteria for this systematic review.
14. **ELKHOLY, F. *et al.,*** *Forces and moments delivered by PET-G aligners to an upper central incisor for labial and palatal translation*. Journal of Orofacial Orthopedics, v. 76, n. 6, p. 460-475, 2015. DOI: 10.1007/s00056-015-0307-3.
Reason for exclusion: This article does not compare the physical, mechanical properties, and accuracy of orthodontic aligners made by thermoforming and direct 3D printing. This article assesses occlusal modifications in patients using orthodontic aligners, and thus does not meet the inclusion criteria for this systematic review.

15. **LI, Y. *et al.,*** *Stress and movement trend of lower incisors with different IMPA intruded by clear aligner: a three-dimensional finite element analysis*. Progress in Orthodontics, v. 24, n. 1, p. 5, 2023. DOI: 10.1186/s40510-023-00454-7.
Reason for exclusion: This article does not compare the physical, mechanical properties, and accuracy of orthodontic aligners made by thermoforming and direct 3D printing. This article assesses occlusal modifications in patients using orthodontic aligners, thus it does not meet the inclusion criteria for this systematic review.

16. **BENNETT, G. W.; DIGIOVANNI, T.** *Effect of wall thickness of 3D-printed models on resisting deformation from thermal forming in-office aligners*. Clinical and Experimental Dental Research, v. 10, n. 1, p. e827, 2024. DOI: 10.1002/cre2.827.
Reason for exclusion: This article does not compare the physical, mechanical properties, and accuracy of orthodontic aligners made by thermoforming and direct 3D printing. This article evaluates the effect of thermoformed orthodontic aligners on

3D printed models, and thus does not meet the inclusion criteria for this systematic review.

17. **SIM, M.; PARK, S.** *Orthodontic treatment using directly 3D-printed clear aligners*. Journal of Clinical Orthodontics, v. 57, n. 10, p. 606-613, 2023. **Reason for exclusion**: This article does not compare the physical, mechanical properties, and accuracy of orthodontic aligners made by thermoforming and direct 3D printing. This article does not present a comparative group with thermoformed orthodontic aligners.

18. **ZHANG, Y. *et al.,*** *Effects of upper arch expansion using clear aligners on different stride and torque: a three-dimensional finite element analysis*. BMC Oral Health, v. 23, n. 1, p. 891, 2023. DOI: 10.1186/s12903-023-03655-y. **Reason for exclusion**: This article does not compare the physical, mechanical properties, and accuracy of orthodontic aligners made by thermoforming and direct 3D printing. This article assesses occlusal modifications in patients using orthodontic aligners, and thus does not meet the inclusion criteria for this systematic review.

19. **BEHYAR, M. *et al.,*** *Modular 3D printable orthodontic measuring apparatus for force and torque measurements of thermoplastic/removable appliances*. Biomedical Engineering/Biomedizinische Technik, v. 66, n. 6, p. 593-601, 2021. DOI: 10.1515/bmt-2020-0294.
Reason for exclusion: This article does not compare the physical, mechanical properties, and accuracy of orthodontic aligners made by thermoforming and direct 3D printing. This article does not present a comparative group with 3D printed orthodontic aligners.

20. **GHORABA, O. *et al.,*** *Effect of the Height of a 3D-Printed Model on the Force Transmission and Thickness of Thermoformed Orthodontic Aligners*. Materials, v. 17, n. 12, p. 3019, 2024. DOI: 10.3390/ma17123019. **Reason for exclusion**: This article does not compare the physical, mechanical properties, and accuracy of orthodontic aligners made by thermoforming and direct 3D printing. This article does not present a comparative group with 3D printed orthodontic aligners.

21. **FAN, Y.; ZHANG, X.** *In vitro study examines posterior torque impact on 3D mechanics of anterior teeth in clear aligner treatment*. BMC Oral Health, v. 24, n. 1, p. 486, 2024. DOI: 10.1186/s12903-024-04240-7.
Reason for exclusion: This article does not compare the physical, mechanical properties, and accuracy of orthodontic aligners made by thermoforming and direct 3D printing. This article assesses occlusal modifications in patients using orthodontic aligners, and thus does not meet the inclusion criteria for this systematic review.

22. **LASANCE, S. J. *et al.,*** *Degree of cure of orthodontic composite attachments underneath aligners*. European Journal of Oral Sciences, v. 132, n. 1, p. e12963, 2024. DOI: 10.1111/eos.12963.
Reason for exclusion: This article does not compare the physical, mechanical properties, and accuracy of orthodontic aligners made by thermoforming and direct 3D printing. This article addresses the position and shape of attachments used to correct malocclusion with different aligners, and therefore does not meet the inclusion criteria for this systematic review.

23. **JIANG, T. *et al.,*** *Clear aligners for maxillary anterior en masse retraction: a 3D finite element study*. Scientific Reports, v. 10, n. 1, p. 10156, 2020. DOI: 10.1038/s41598-020-67273-2.
Reason for exclusion: This article does not compare the physical, mechanical properties, and accuracy of orthodontic aligners made by thermoforming and direct 3D printing. This article assesses occlusal modifications in patients using orthodontic aligners and does not have comparative groups, thus does not meet the inclusion criteria for this systematic review.

24. **KIM, K. B.; GRAF, S.** *Direct printing of clear aligners*. Journal of Clinical Orthodontics, v. 57, n. 8, p. 450-458, 2023.
Reason for exclusion: This article does not compare the physical, mechanical properties, and accuracy of orthodontic aligners made by thermoforming and direct 3D printing. This article does not present a comparative group with thermoformed orthodontic aligners.

Table 1 - Search strategies employed in databases

Databases	Key Words	Results of the 1st search*	Results of the 2nd search**
PubMed	1 - Invisalign OR clear aligner OR vacuum thermoforming aligner OR thermoformed aligners OR in office aligner OR in house aligner OR TFA 2 – Graphy Aligner OR 3D Aligner OR Three dimensional impression Aligner OR 3D-printed clear aligners OR 3 dimensional printed aligners OR direct printed aligners OR DPA 3- 1 AND 2	608	82
Embase	1 - Invisalign OR “clear aligner” OR “vacuum thermoforming aligner” OR “thermoformed aligners” OR “in office aligner” OR “in house aligner” OR TFA 2 - “Graphy Aligner” OR “3D Aligner” OR “Three dimensional impression Aligner” OR “3D-printed clear aligners” OR “3 dimensional printed aligners” OR “direct printed aligners” OR DPA 3- 1 AND 2	20	6
Lilacs	1 - Vacuum thermoforming aligner OR thermoformed aligners 2 - 3D Aligner OR Three dimensional impression Aligner 3 – 1 AND 2	2	1

Web of Science	Same as PubMed	248	36
Ovid	Same as PubMed	4	0
Scoopus	Same as PubMed	39	77
Gray Literature	Same as PubMed	0	200

*From the beginning of the database until December 2024,** *From December 2024 to May 2025.*

Table 4 - Data extraction

<table>
<tr>
<td>Atta et al.,, 2024 Germany (English)</td>
<td>Group 1 (G1): Thermoformed aligner CA® Pro (CP), manufactured by Scheu-Dental (Iserlohn, Germany). Average thickness: 0.75 mm. The thermoforming process involved heating for 25 seconds at 220°C, followed by a pressure application of 4.8 bar and cooling for 60 seconds. The aligner consists of a three-layer sheet, with a soft thermoplastic elastomeric layer between two rigid copolymer layers.

Group 2 (G2): Thermoformed aligner Zendura A (ZA), manufactured by Bay Materials (Fremont, USA). Average thickness: 0.75 mm. The thermoforming process involved heating for 50 seconds at 220°C, followed by a pressure application of 4.8 bar and cooling for 60 seconds. The aligner is composed of a single-layer sheet made of thermoplastic polyurethane (TPU).

Group 3 (G3): Thermoformed aligner Zendura FLX (ZF), manufactured by Bay Materials (Fremont, USA). Average thickness: 0.75 mm. The thermoforming process involved heating for 50 seconds at 220°C, followed by a pressure application of 4.8 bar and cooling for 60 seconds. The aligner consists of a three-layer sheet with a soft intermediate</td>
<td>Differential Scanning Calorimetry (DSC)
Thermal analyses were conducted using a differential scanning calorimeter (STARe SW Mettler Toledo V16.10; Greifensee, Switzerland). Each specimen underwent two heating cycles up to 240 °C and one cooling cycle down to 40 °C, with a heating/cooling rate of 10 °C/min. The analyses were performed under a nitrogen atmosphere. The glass transition temperature (Tg) was determined by identifying the midpoint during the second heating cycle. Two specimens (n = 2) were tested per material, and the average Tg value was subsequently calculated.

Dynamic Mechanical Analysis (DMA)
Three specimens per material (n = 3) were prepared for DMA testing. The test was performed using a dynamic mechanical analyzer (DMA Q800; TA Instruments, New Castle, USA), with frequencies ranging from 0 to 100 Hz and a strain rate of 0.1%, in stress relaxation mode,</td>
<td>
Glass Transition Temperature (Tg) Measured by Differential Scanning Calorimetry (DSC) for Different Orthodontic Aligner Materials
<table>
<tr><td>Material</td><td>CA Pro</td><td>Zendura A</td><td>Zendura FLX</td><td>TC 85</td></tr>
<tr><td>Tg (°C)</td><td>79.9</td><td>92.2</td><td>107.1</td><td>42.3</td></tr>
</table>
Dynamic Mechanical Analysis (DMA) at Different Temperatures for Different Materials: Tera Harz
<table>
<tr><th>Temperature (°C)</th><th>Frequency(Hz)</th><th>Storage Modulus (MPa)</th><th>Observations</th></tr>
<tr><td>20</td><td>0.01–100</td><td>100–3000</td><td>Modulus increases with frequency.</td></tr>
<tr><td>25</td><td>0.01–100</td><td>~150–2800</td><td>Similar increase observed at 20°C.</td></tr>
<tr><td>30</td><td>0.01–100</td><td>~200–2500</td><td>General decreasing trend in modulus at higher temperatures.</td></tr>
<tr><td>35</td><td>0.01–100</td><td>~300–2000</td><td>Progressive reduction in modulus with increasing temperature.</td></tr>
<tr><td>45</td><td>0.01–100</td><td>~500–1500</td><td>Significantly lower storage modulus.</td></tr>
</table>
Dynamic Mechanical Analysis (DMA) at Different Temperatures for Different Materials: CA Pro (CP)
<table>
<tr><th>Temperature (°C)</th><th>Frequency(Hz)</th><th>Storage Modulus (MPa)</th><th>Observations</th></tr>
<tr><td>20–45</td><td>0.01–100</td><td>~1000</td><td>Little variation with temperature or frequency.</td></tr>
</table>
Dynamic Mechanical Analysis (DMA) at Different Temperatures for Different Materials: Zendura (ZA)
<table>
<tr><th>Temperature (°C)</th><th>Frequency(Hz)</th><th>Storage Modulus (MPa)</th><th>Observations</th></tr>
<tr><td>20–45</td><td>0.01–100</td><td>~1500</td><td>Little variation with temperature or frequency.</td></tr>
</table>
Dynamic Mechanical Analysis (DMA) at Different Temperatures for Different Materials: Zendura FLX (ZF)
<table>
<tr><th>Temperature (°C)</th><th>Frequency(Hz)</th><th>Storage Modulus (MPa)</th><th>Observations</th></tr>
<tr><td>20–45</td><td>0.01–100</td><td>~800</td><td>Little variation with temperature or frequency.</td></tr>
</table>
</td>
</tr>
</table>

layer of thermoplastic elastomeric TPU.

Group 4 (G4): Direct 3D printed aligner Graphy Tera Harz TC-85 (TC-85), manufactured by Graphy (Seoul, South Korea). Average thickness: 0.6 mm. The 3D printing was performed using a DLP-type 3D printer (Uniz NBEE; Uniz, CA, USA) with a 100 µm layer thickness, followed by UV light photopolymerization (wavelength: 405 nm) under nitrogen for 25 minutes using a specialized post-curing device (Tera Harz Cure; Graphy, South Korea). The aligner is composed of urethane acrylate oligomers and acrylic monomers.

Note:

The thermoplastic sheets of the three materials (CP, ZA, ZF) were thermoformed using a Biostar device (Scheu-Dental GmbH, Iserlohn, Germany), according to the manufacturer's guidelines. This process resulted in sheet thinning from 0.75 mm to approximately 0.6 mm, as measured with a digital caliper (Fisher Scientific International Inc., Hampton, NH, USA). The resulting specimens were cut into rectangular strips measuring 50 × 10 × 0.6 mm using scissors, and the edges were polished with a polishing machine. In contrast, the TC-85 specimens were directly 3D printed into rectangular strip shapes of 50 × 10 × 0.6 mm.

at temperatures of 20, 25, 30, 35, 40, and 45 °C.

Shape Recovery Test

Shape recovery evaluation was performed at three different temperatures: 30 °C, 37 °C, and 45 °C. A total of 18 specimens were prepared for each material, with 6 specimens designated for each recovery temperature (n = 6). The specimens underwent a standardized process: first softened by immersion in boiling water at 100 °C, then bent to 180°, and quickly cooled in cold water for 1 minute to harden while retaining the deformed shape. Specimens were then stored at 4 °C for 1 hour to preserve their temporary shape until testing. To assess shape recovery under conditions similar to the oral environment, each specimen was immersed in a water bath at 30 °C, 37 °C, or 45 °C for 10 minutes.

The ImageJ software (National Institutes of Health, Maryland, USA) was used to measure both the initial bending angle (θ_initial) and the final recovery angle (θ_final).

Three-Point Bending Test (3PB)

Intergroup Comparison of Shape Recovery Angle and Recovery Percentage at Different Temperatures for Different Materials

Temperature (°C)	Property	CA Pro	Zendura A	Zendura FLX	TC-85	p-valuep
30 °C	Recovery Angle (°)	3.2 ± 1.0^{B}	3.0 ± 0.9^{B}	2.7 ± 1.2^{B}	15.2 ± 4.5^{B}	<0.001*
	Recovery (%)	1.8 %	1.7 %	1.5 %	8.4 %	
37 °C	Recovery Angle (°)	4.0 ± 0.9^{B}	3.5 ± 0.8^{B}	3.3 ± 1.0^{B}	98.8 ± 6.2^{A}	<0.001*
	Recovery (%)	2.2 %	1.9 %	1.9 %	54.9 %	
45 °C	Recovery Angle (°)	5.2 ± 1.9^{B}	4.0 ± 1.4^{B}	3.7 ± 1.6^{B}	155.0 ± 5.7^{A}	<0.001*
	Recovery (%)	2.9 %	2.2 %	2.0 %	86.1 %	

*Capital and lowercase letters denote statistically significant differences within the same horizontal row and vertical column, respectively; significant ($p < 0.05$)

Maximum Bending Force at a 2 mm Deflection for Different Aligners at Different Temperatures

Material	Temperature (°C)		
	30°C	37°C	45°C
CA Pro	≈ 2.7 ± 0.8 N	≈ 2,7 N ± 0.2 N	≈ 2.6 ±1.1 N
Zendura A	≈ 3.2 ± 1.8 N	≈ 3.6 ± 0.8 N	≈ 2.2 ± 0.8 N
Zendura FLX	≈ 2.9 ± 0.6N	≈ 2.4 ± 0.4 N	≈ 2.3 ± 0.6 N
TC-85	≈ 0.7 ± 0.6N	≈ 0.4 ± 0.4N	≈ 0.1 ± 0.2N

Vickers Microhardness Values for Different Orthodontic Aligner Materials at Room Temperature

Stage	CA Pro	Zendura A	Zendura FLX	TC-85	p-valuep
As Received	$2,7 \pm 0,1^{Ca}$	$13,4 \pm 0,3^{Aa}$	$10,3 \pm 0,2^{Ba}$	NA	<0,001*
Thermoformed/3D Printed	$2,7 \pm 0,1^{Ca}$	$12,0 \pm 0,2^{Ab}$	$7,9 \pm 0,3^{Bb}$	$8,1 \pm 0,9^{B}$	<0,001*
p-value	0,899	<0,001*	<0,001*	NA	

*Capital and lowercase letters indicate statistically significant differences in the same horizontal row and vertical column, respectively. significant ($p < 0.05$).

		A customized mechanical setup (orthodontic measurement simulation system, OMSS; Oral Technology, University Hospital Bonn, Bonn, Germany) (Bourauel *et al.,*, 1992) was used to measure the maximum force when each specimen was deflected by 2 mm in a three-point bending configuration with a span length of 24 mm. The setup included a temperature-controlled chamber, allowing tests to be conducted at various temperatures: 30 °C, 37 °C, and 45 °C. A total of 18 specimens per material were prepared, with 6 specimens assigned to each test temperature (n = 6). **Surface Microhardness** Surface microhardness was measured using a Vickers microhardness tester (Qness 60 M Evo; QATM, Mammelzen, Germany) at room temperature. A load of 1.96 N (200 g-force) was applied for 10 seconds (HV 0.2) to create indentations. Five indentations were made on each sample, with a minimum spacing of 50 µm between them. The mean Vickers hardness number (VHN) was calculated for each	

<table>
<tr>
<td></td>
<td></td>
<td>sample. For thermoformable sheets (CP, ZA, ZF), hardness testing was conducted both on the received material and after thermoforming, with a total of 12 samples per material (6 specimens for each stage). For TC-85, the hardness test was conducted only after post-curing (n = 6).</td>
<td></td>
</tr>
<tr>
<td>Bae et al.,, 2025 South Korea (English)</td>
<td>Group 1 (G1): Direct 3D printed aligner Graphy Tera Harz TC-85 (TC-85), manufactured by Graphy (Seoul, South Korea). The manufacturing process employed TC-85 DAC printed with an LCD-type 3D printer (Slash2 4K, Uniz Inc., China) to produce the experimental specimens directly. Post-curing was performed using THC (Graphy Inc., South Korea) under nitrogen for 20 minutes, with a total energy exposure of 480 J at a UV wavelength of 405 nm. Simulating a condition in which compressive force is applied to specific dental regions, the aligners were fabricated with a rectangular protruding area termed RPA, measuring 1 mm in thickness. The raised areas were filled. N = 17 samples.

Group 2 (G2): Thermoformed aligner 3A GS030, made from polyethylene terephthalate glycol (PETG), with a thickness of 0.75 mm, manufactured by 3A MEDES Co. The thermoforming process</td>
<td>Compression Cycle Tests
A compression cycle experiment was conducted using an LTM 3h electrodynamic testing machine (Zwick Roell, Germany). The crosshead speed of the cyclic testing device was set to 1 mm/s. Compression depths were defined at 100, 300, 500, and 700 µm, respectively. For the PETG group (control group 1), five specimens were used for the 100 µm compression depth, and five specimens each for 300, 500, and 700 µm, totaling 20 specimens for the experiment.
For the blank TC-85 group (control group 2), three specimens were used for the 100 µm depth, four specimens for 300 µm, and five specimens each for 500 and 700 µm, totaling 17 specimens.
For the complete TC-85 group (experimental</td>
<td>Changes in Force Magnitude by Compression Depth (µm)

Material — Compression Depth (Mean ± SD)
<table>
<tr><th></th><th>100 µm</th><th>300 µm</th><th>500 µm</th><th>700 µm</th><th>Significance</th></tr>
<tr><td>PETG</td><td>-15.9 ± 0.34</td><td>- 47.69 ± 0.90</td><td>-82.09 ± 2.01</td><td>-115.51 ± 2.66</td><td>** a,b,c,d</td></tr>
<tr><td>TC-85 - Filled</td><td>-20.07 ± 1.31</td><td>-228.61 ± 21.94</td><td>-339.64 ± 27.72</td><td>-360.46 ± 33.63</td><td>** a,b,c,d</td></tr>
<tr><td>TC-85 - Empty</td><td>-27.74 ± 1.46</td><td>-256.22 ± 18.23</td><td>-414.22 ± 25.74</td><td>-485.07 ± 31.18</td><td>** a,b,c,d</td></tr>
</table>
The Kruskal-Wallis test was performed, followed by post-hoc Bonferroni analysis. Letters a, b, c, d indicate 100 µm, 300 µm, 500 µm, and 700 µm, respectively. *p < 0.05, *p < 0.01

Changes in Force Magnitude According to Each Sample Cycle Based on Compression Depth
<table>
<tr><th>Compression Depth (µm)</th><th>PETG (N)</th><th>TC-85 Blank (N)</th><th>TC-85 Full (N)</th></tr>
<tr><td>100</td><td>≈ 15 (stable across cycles)</td><td>< 25 → < 20 (declined over cycles)</td><td>≈ 30 (declined over cycles)</td></tr>
<tr><td>300</td><td>≈ 50 (stable across cycles)</td><td>> 300 → ≈ 200 (declined over cycles)</td><td>> 300 → < 250 (declined over cycles)</td></tr>
<tr><td>500</td><td>< 100 (stable across cycles)</td><td>~400 → ≈ 310 (declined over cycles)</td><td>400–500 (declined over cycles)</td></tr>
<tr><td>700</td><td>> 100 (stable across cycles)</td><td>< 500 → > 300 (declined over cycles)</td><td>> 600 → > 450 (declined over cycles)</td></tr>
</table>
</td>
</tr>
</table>

	involved placing a PETG sheet in the MINISTAR S device (SCHEU-DENTAL, Iserlohn, Germany) and heating it for 30 seconds, ensuring the PETG sheet surface temperature remained below 60 °C. A vacuum pressure of 3.7 bar was applied to the prepared model, followed by 1-minute cooling. After trimming the model edges, the specimens were cut to appropriate sizes for each sample. The aligners featured rectangular protruding areas (RPAs) with 1 mm thickness. *N = 20 samples.* **Group 3 (G3):** Direct 3D printed aligner Graphy Tera Harz TC-85 (TC-85), manufactured by Graphy (Seoul, South Korea). The same TC-85 DAC and LCD Slash2 4K printer were used to produce the experimental specimens directly. Post-curing was performed under nitrogen for 20 minutes with 480 J of energy at 405 nm UV light. Simulating localized compressive force distribution, this group used TC-85 aligners fabricated with a rectangular protrusion (RPA) of 1 mm thickness. However, in this group, the raised areas were *not* filled. *N = 19 samples.* **Note:** The models with RPA were 3D printed. Then, PETG sheets were thermoformed over these models and trimmed into rectangular specimens of 7 × 8 mm for cyclic compression tests. The TC-85 material enabled direct printing of	group), five specimens were used for the 100 µm depth, four specimens for 300 µm, and five specimens each for 500 and 700 µm, totaling 19 specimens. A total of 500 compression cycles were performed for each measurement. To evaluate specimen thickness consistency, measurements were taken for each sample using a digital caliper (GAU-178.00, Eurotool, Inc., USA).	

<table>
<tr><td></td><td>aligners with inclined surfaces, allowing selective pressure application in targeted areas.</td><td></td><td></td></tr>
<tr><td>Bandic et al.,, 2024 Croatia (English)</td><td>Group 1 (G1): Thermoformed aligner Duran+, 0.5 mm thickness, manufactured by SCHEU-DENTAL GmbH. N = 3 pairs.

Group 2 (G2): Thermoformed aligner Duran+, 0.625 mm thickness, manufactured by SCHEU-DENTAL GmbH. N = 3 pairs.

Group 3 (G3): Thermoformed aligner Duran+, 0.75 mm thickness, manufactured by SCHEU-DENTAL GmbH. N = 3 pairs.

Group 4 (G4): Thermoformed aligner Erkodur, 0.5 mm thickness, manufactured by Erich Kopp GmbH, Pfalzgrafenweiler, Germany. N = 3 pairs.

Group 5 (G5): Thermoformed aligner Erkodur, 0.6 mm thickness, manufactured by</td><td>Thickness Variation Analysis
The left sides of the upper and lower aligners were used for analysis. All samples were measured using an electronic micrometer (UNIVERSAL ELECTRONIC MICROMETER, Schut Geometrical Metrology, Groningen, Netherlands; precision: 0.001 mm) at a total of 20 points per aligner. Measurements were conducted independently by three researchers.
Aligner thickness was measured at the following locations:

● Central incisor: buccal surface, incisal edge, cingulum, and palatal/lingual surface;
● Canine: buccal surface, cusp tip, cingulum, and</td><td>Percentage of Deviations in Thickness for Different Manufacturing Processes
<table><tr><th>Manufacturing Processes</th><th>N</th><th>Mean (%)</th><th>SD</th><th>EP</th><th>Coefficient of Variation</th></tr><tr><td>Thermoforming</td><td>3960</td><td>-39,764</td><td>14,096</td><td>0,224</td><td>-0,354</td></tr><tr><td>3D Printing</td><td>2160</td><td>11,020</td><td>21,434</td><td>0,461</td><td>1,945</td></tr></table>The difference between thermoformed and 3D printed groups was statistically significant (Kruskal-Wallis test, $p < 0.001$).

Average Percentage Deviation in Thickness for Different Thermoformed Aligners
<table><tr><th>Material</th><th>Mean Percentage (%)</th></tr><tr><td>Zendura A</td><td>-32,408</td></tr><tr><td>Zendura FLX</td><td>-35,455</td></tr><tr><td>Duran</td><td>-35,993</td></tr><tr><td>Erkodur</td><td>-37,446</td></tr><tr><td>CA PRO+</td><td>-42,604</td></tr><tr><td>Erkoloc-Pro</td><td>-53,310</td></tr></table>Significant differences between thermoformed materials were identified (Kruskal-Wallis test, $p < 0.001$).

Post Hoc Dunn Comparisons with Bonferroni Correction for Thermoformed Materials
Comparison z Wi Wj p p (Bonferroni)</td></tr>
</table>

	Erich Kopp GmbH, Pfalzgrafenweiler, Germany. *N = 3 pairs.* **Group 6 (G6):** Thermoformed aligner Erkodur, 0.8 mm thickness, manufactured by Erich Kopp GmbH, Pfalzgrafenweiler, Germany. *N = 3 pairs.* **Group 7 (G7):** Thermoformed aligner Zendura A, 0.76 mm thickness, manufactured by Bay Materials LLC, Fremont, California, USA. *N = 3 pairs.* **Group 8 (G8):** Thermoformed aligner Erkoloc-Pro, 1.00 mm thickness, manufactured by Erkodent Erich Kopp GmbH. *N = 3 pairs.* **Group 9 (G9):** Thermoformed aligner Erkoloc-Pro, 1.30 mm thickness, manufactured by Erkodent Erich Kopp GmbH. *N = 3 pairs.* **Group 10 (G10):** Thermoformed aligner Zendura FLX, 0.76 mm thickness, manufactured by FLX, Bay Materials LLC. *N = 3 pairs.* **Group 11 (G11):** Thermoformed aligner CA PRO, 0.75 mm thickness, manufactured by SCHEU-DENTAL GmbH. *N = 3 pairs.* **Group 12 (G12):** 3D printed aligner NextDent (NextDent B.V., Soesterberg, Netherlands), manufactured according to the manufacturer's instructions, 0.5 mm thickness. *N = 3 pairs.*	palatal/lingual surface; ● **First premolar:** buccal surface, buccal cusp tip, central fissure, palatal/lingual cusp tip (measured twice); ● **First molar:** buccal surface, mesiobuccal cusp tip, distobuccal cusp tip, central fissure, mesiopalatal/mesiolingual cusp tip, distopalatal/distolingual cusp tip, and palatal/lingual surface.	CA PRO+ - Duran -7,309 1.773,688 2.282,246 < 0,001*** < 0,001*** CA PRO+ - Erkodur -5,413 1.773,688 2.150,341 < 0,001*** < 0,001*** CA PRO+ - Erkoloc-Pro 11,738 1.773,688 907,401 < 0,001*** < 0,001*** CA PRO+ - Zendura A -9,330 1.773,688 2.568,778 < 0,001*** < 0,001*** CA PRO+ - Zendura FLX -6,534 1.773,688 2.330,469 < 0,001*** < 0,001*** Duran - Erkodur 2,681 2.282,246 2.150,341 0,007** 0,110 Duran - Erkoloc-Pro 24,994 2.282,246 907,401 < 0,001*** < 0,001*** Duran - Zendura A -4,118 2.282,246 2.568,778 < 0,001*** < 0,001*** Duran - Zendura FLX -0,693 2.282,246 2.330,469 0,488 1,000 Erkodur - Erkoloc-Pro 22,596 2.150,341 907,401 < 0,001*** < 0,001*** Erkodur - Zendura A -6,014 2.150,341 2.568,778 < 0,001*** < 0,001*** Erkodur - Zendura FLX -2,589 2.150,341 2.330,469 0,010** 0,144 Erkoloc-Pro - Zendura A -22,512 907,401 2.568,778 < 0,001*** < 0,001*** Erkoloc-Pro - Zendura FLX -19,283 907,401 2.330,469 < 0,001*** < 0,001*** Zendura A - Zendura FLX 2,797 2.568,778 2.330,469 0,005** 0,077 z: z-statistic. Wi and Wj: reference values. p: significance value. p (Bonferroni): adjusted significance value. Statistically significant (** p < 0.001; ** p < 0.01).* **Average Percentage Deviation in Thickness for 3D Printed Aligners** **Material** **Mean Percentage (%)** NextDent +4,04 NextDent A +5,883 IZZI +23,137 **Post Hoc Dunn Comparisons with Bonferroni Correction for 3D Printed Materials** **Comparison** **z** **Wi** **Wj** **p** **p (Bonferroni)** IZZI – NextDent 17,288 1.445,626 877,349 < 0,001*** < 0,001*** IZZI – NextDent A 16,035 1.445,626 918,525 < 0,001*** < 0,001*** NextDent – NextDent A -1,253 877,349 918,525 0,210 0,631 z: z-statistic. Wi and Wj: reference values. p: significance value. p (Bonferroni): adjusted significance value. Statistically significant (** p < 0.001; ** p < 0.01).* **Maxilla vs. Mandible** The thickness of thermoformed aligners deviated more in the maxilla with statistically significant differences (Kruskal-Wallis test, p < 0.001). The thickness of thermoformed aligners deviated more in the mandible with statistically significant differences (Kruskal-Wallis test, p < 0.001). **Same Material with Different Initial Thicknesses** **Percentage of Deviations in Thickness for Materials with Different Initial Thicknesses – Descriptive Statistics**

Group 13 (G13): 3D printed aligner NextDent (NextDent B.V., Soesterberg, Netherlands), manufactured according to the manufacturer's instructions, 0.6 mm thickness. *N = 3 pairs.*

Group 14 (G14): 3D printed aligner NextDent (NextDent B.V., Soesterberg, Netherlands), manufactured according to the manufacturer's instructions, 0.7 mm thickness. *N = 3 pairs.*

Group 15 (G15): 3D printed aligner NextDent A (NextDent B.V., Soesterberg, Netherlands), produced using a modified post-printing protocol without residual resin drainage, 0.5 mm thickness. *N = 3 pairs.*

Group 16 (G16): 3D printed aligner NextDent A (NextDent B.V., Soesterberg, Netherlands), produced using a modified post-printing protocol without residual resin drainage, 0.6 mm thickness. *N = 3 pairs.*

Group 17 (G17): 3D printed aligner NextDent A (NextDent B.V., Soesterberg, Netherlands), produced using a modified post-printing protocol without residual resin drainage, 0.7 mm thickness. *N = 3 pairs.*

Note:

An intraoral scan of a normocclusion patient was obtained using the Trios scanner (3Shape, Copenhagen, Denmark), and the STL file was generated using Maestro 3D Ortho Studio software, version

Material	Initial Thickness (mm)	N	Mean (%)	SD	EP	Coefficient of Variation
Duran	0,5	360	-36,584	12,928	0,681	-0,353
	0,625	360	-34,246	13,022	0,686	-0,380
	0,75	360	-37,149	13,168	0,694	-0,354
Erkodur	0,5	360	-37,297	11,807	0,622	-0,317
	0,6	360	-37,897	11,859	0,625	-0,313
	0,8	360	-37,145	12,353	0,651	-0,333
Erkoloc-Pro	1	360	-58,331	7,459	0,393	-0,128
	1,3	360	-48,289	9,414	0,496	-0,195
IZZI	0,5	240	27,997	18,413	1,189	0,658
	0,6	240	25,427	15,235	0,983	0,599
	0,7	240	15,988	13,237	0,854	0,828
Nextdent	0,5	240	0,354	19,077	1,231	53,865
	0,6	240	5,954	22,906	1,479	3,847
	0,7	240	5,813	20,962	1,353	3,606
Nextdent A	0,5	240	8,532	24,823	1,602	2,910
	0,6	240	10,337	18,461	1,192	1,786
	0,7	240	-1,220	16,483	1,064	-13,511

Analysis of Thickness Deviations for Different Initial Thicknesses:

● Duran material: Significant difference between 0.625 mm and 0.75 mm (Kruskal-Wallis test, $p = 0.007$; Post Hoc Dunn, $p = 0.008$).

● Erkodur material: No significant difference in thickness deviations among different initial thicknesses (Kruskal-Wallis test, $p = 0.565$).

● Erkoloc-Pro material: Significant difference in thickness deviations between the two initial thicknesses (Kruskal-Wallis test, $p < 0.001$).

● IZZI material: Significant difference in thickness deviations between 0.7 mm, 0.5 mm, and 0.6 mm thicknesses (Kruskal-Wallis test, $p < 0.001$; Post Hoc Dunn, $p < 0.001$).

● NextDent material: Significant difference between 0.5 mm and 0.6 mm, and 0.7 mm thicknesses (Kruskal-Wallis test, $p = 0.003$; Post Hoc Dunn, $p = 0.011$, $p = 0.006$).

● NextDent A material: Significant differences in thickness deviations between 0.7 mm and the other two groups (0.5 mm and 0.6 mm) (Kruskal-Wallis test, $p < 0.001$; Post Hoc Dunn, $p < 0.001$).

Variations Due to Measurement Point Position

Measurement points were grouped into three categories: 1 - protrusive shapes (cusps, incisal edge, and cingulum); 2 - all aligner edges (buccal, palatal, lingual); and 3 - all fissures in the first premolars and first molars.

Percentage Deviation of Declared Thickness for Different Measurement Points on the Tooth for Thermoformed

<table>
<tr>
<td></td>
<td>5 (AGE Solutions®, Pontedera, Italy). 3D models of the patient's dentition were printed from the STL file using the IZZI Ortho printer (3Dtech, Zagreb, Croatia).
Thermoplastic sheets were thermoformed on the printed models using the Biostar® device (SCHEU-DENTAL GmbH, Iserlohn, Germany).
The 3D printed aligners were produced directly from the STL file using the IZZI Direct printer (3Dtech, Zagreb, Croatia).</td>
<td></td>
<td>
Aligners – Descriptive Statistics
<table>
<tr><th>Measurement Point</th><th>N</th><th>Média (%)</th><th>DP</th><th>EP</th><th>Coeficiente de Variação</th></tr>
<tr><td>1</td><td>1998</td><td>-39,649</td><td>13,511</td><td>0,302</td><td>-0,341</td></tr>
<tr><td>2</td><td>1566</td><td>-42,147</td><td>14,407</td><td>0,364</td><td>-0,342</td></tr>
<tr><td>3</td><td>396</td><td>-30,922</td><td>12,055</td><td>0,606</td><td>-0,390</td></tr>
</table>
● As diferenças entre os três grupos morfológicos para alinhadores termoformados foram significativas (teste de Kruskal-Wallis, p < 0,001; Post Hoc de Dunn, p < 0,001)

Percentage Deviation of Declared Thickness for Different Measurement Points on the Tooth for 3D Printed Aligners – Descriptive Statistics
<table>
<tr><th>Measurement Point</th><th>N</th><th>Mean (%)</th><th>SD</th><th>EP</th><th>Coefficient of Variation</th></tr>
<tr><td>1</td><td>1080</td><td>11,002</td><td>21,394</td><td>0,651</td><td>1,944</td></tr>
<tr><td>2</td><td>864</td><td>6,906</td><td>19,285</td><td>0,656</td><td>2,793</td></tr>
<tr><td>3</td><td>216</td><td>27,567</td><td>21,917</td><td>1,491</td><td>0,795</td></tr>
</table>
Statistical Differences Between the Three Morphological Groups for Thermoformed and 3D Printed Aligners
Statistically significant differences were observed for both thermoformed (Kruskal-Wallis test, p < 0.001; Post Hoc Dunn, p < 0.001) and 3D printed aligners (Kruskal-Wallis test, p < 0.001; Post Hoc Dunn, p < 0.001).
</td>
</tr>
<tr>
<td>Cremonine et al.,, 2024
Italy
(English)</td>
<td>Group 1 (G1): Zendura FLX aligner, manufactured by Bay Materials LLC, Fremont, California, USA. Fabricated from single-layer discs (0.76 mm thickness) made of thermoplastic polyurethane (TPU). N = 1 sample.

Group 2 (G2): Duran aligner, manufactured by SCHEU, Iserlohn, Germany. Fabricated from single-layer discs (0.76 mm thickness) made of modified PET-G. N = 1 sample.

Group 3 (G3): Tera aligner, manufactured by Graphy Inc., Seoul, South Korea. The aligner was directly 3D printed using the SprintRay Pro S printer (SprintRay Inc., Los Angeles, CA, USA), DLP Refined technology, and TeraHarz TC-85 resin. Post-curing was performed using the Tera Harz Cure device (Graphy</td>
<td>Stress-Relaxation Test
The stress-relaxation test was performed using a motorized vertical test stand TVO-S (AstraLab, Mariano Comense, Italy), which applied a controlled vertical compression at a specific point, under a predefined constant load. The 3D-printed stereolithography model was fixed to a horizontal support using superglue to ensure that the force was applied consistently at the same point and perpendicularly to the model's plane. Each aligner sample was properly positioned prior to testing.
The upper right central incisor (tooth 1.1) was removed from the</td>
<td>
Initial Stress, Final Stress, and Stress Decay for Each Tested Aligner
<table>
<tr><th>Material</th><th colspan="3">Test 01</th><th colspan="3">Test 02</th></tr>
<tr><td></td><td>Initial Force (N)</td><td>Final Force (N)</td><td>Stress Decay (%)</td><td>Initial Force (N)</td><td>Final Force (N)</td><td>Stress Decay (%)</td></tr>
<tr><td>Zendura FLX</td><td>9.5</td><td>5</td><td>47.4</td><td>3.5</td><td>2.5</td><td>29</td></tr>
<tr><td>Duran</td><td>6.5</td><td>2.5</td><td>62</td><td>7</td><td>5</td><td>29</td></tr>
<tr><td>Tera</td><td>14.5</td><td>0</td><td>90</td><td>13.5</td><td>0</td><td>100</td></tr>
<tr><td>Noxi</td><td>20.5</td><td>14</td><td>32</td><td>17.5</td><td>13.5</td><td>23</td></tr>
</table>
Paired Sample t-Test for Comparison of Significant Differences Between Test 1 and Test 2 for Each Material
<table>
<tr><th>Time</th><th>Material</th><th>Mean Test 01 (n)</th><th>Mean Test 02 (n)</th><th>Test Statistic</th><th>df</th><th>p-value</th></tr>
<tr><td rowspan="4">1 h</td><td>Zendura FLX</td><td>6.9</td><td>2.6</td><td>765.2</td><td>3537.0</td><td><0.001</td></tr>
<tr><td>Duran</td><td>4.8</td><td>5.4</td><td>−232.7</td><td>3537.0</td><td><0.001</td></tr>
<tr><td>Tera</td><td>2.0</td><td>−0.6</td><td>140.1</td><td>3537.0</td><td><0.001</td></tr>
<tr><td>Noxi</td><td>15.2</td><td>14.1</td><td>80.1</td><td>3537.0</td><td><0.001</td></tr>
<tr><td>2 h</td><td>Zendura FLX</td><td>6.5</td><td>2.4</td><td>1013.5</td><td>7105.0</td><td><0.001</td></tr>
</table>
</td>
</tr>
</table>

	Inc., Seoul, South Korea). Design and 0.75 mm thickness were defined using CAD software. *N = 1 sample.* **Group 4 (G4):** Noxi aligner, manufactured by Noxi, Sweden & Martina, Due Carrare, Padova, Italy. The aligner was directly 3D printed using plastic SLS technology with a 3D EOS printer (EOS GmbH, Krailling, Germany), using polyamide. Design and 0.75 mm thickness were defined using CAD software. *N = 1 sample.* **Note:** Prior to testing, the thickness of all aligners was measured and confirmed using a digital external gauge (Kroeplin K110, Kroeplin GmbH, Gartenstraße 50, 36381 Schlüchtern, Germany). The same maxillary model from a previously treated orthodontic patient was used to thermoform the first two clear aligners and to digitally design and 3D print the other two aligners in the study.	model near the location where the force would subsequently be applied to the aligner, without performing any additional cuts. The horizontal support was then placed into a bath measuring 20 cm × 20 cm × 10 cm, filled with distilled water at 37 °C. This bath was positioned beneath the load cell. To maintain the water temperature at a constant 37 °C, a Julabo Labortechnik GmbH immersion heater (Seelbach, Germany) was placed in a separate bath, also filled with distilled water. Both water baths were connected via inlet and outlet tubing to ensure continuous circulation. The test for each sample was conducted over a continuous period of 8 hours. Once the aligner was properly positioned on the model, a crosshead speed of 1 mm/min was set, reaching a deformation of 0.5 mm within the first 30 seconds of testing. Due to the removal of the upper right central incisor, the magnitude of aligner deflection was measured at that location, as there was no contact with the model. The load corresponding to the 0.5 mm deflection was	

8 h	Duran	4.5	5.0	−274.3	7105.0	<0.001
	Tera	1.9	−0.3	203.4	7105.0	<0.001
	Noxi	14.8	13.8	139.7	7105.0	<0.001
	Zendura FLX	5.6	2.1	1237.5	28589.0	<0.001
	Duran	3.7	3.6	41.0	28589.0	<0.001
	Tera	1.3	−0.1	292.1	28589.0	<0.001
	Noxi	14.3	13.0	451.0	28589.0	<0.001

*df: Degrees of freedom. *p < 0.05 is statistically significant.

Median Stress Relaxation (%) for Each Aligner After 8 Hours

Material	**Test 1 Median Stress Relaxation (%)**	**Test 2 Median Stress Relaxation (%)**	***p-value***
Zendura FLX	47.4	29	>0.9
Duran	62	29	0.026
Tera	90	100	0.020
Noxi	32	23	0.010

**p < 0.05 is statistically significant.*

Brown-Forsythe Test Performed

Time	**Material**	**Mean Test 1**	**Test Statistic**	**df1**	**df2**	**p-value**
1h	Zendura FLX	6.9	76175.0	3.0	6774.6	<0.001
	Duran	4.8				
	Tera	2				
	Noxi	15.2				
2h	Zendura FLX	6.5	245428.7	3.0	17045.7	<0.001
	Duran	4.5				
	Tera	1.9				
	Noxi	14.8				
3h	Zendura FLX	5.6	1793146.3	3.0	95984.1	<0.001
	Duran	3.7				
	Tera	1.3				
	Noxi	14.3				

*df1 and df2: Degrees of freedom. *p < 0.05 is statistically significant.

		maintained constant throughout the observation period. Stress-relaxation data were collected every second to generate a precise curve for each material tested. Additionally, two equivalent tests were conducted sequentially, with an 8-hour interval between them, in order to simulate the intermittency of deflection force. These tests enabled the determination and comparison of the initial and final average stresses for each material.	
Cremonine *et al.*,, 2025a Italy (English)	**Group 1 (NHVH):** Direct 3D printed Noxi aligner, made of polyamide, with vertical and horizontal thickness gradient (vertical: 0.65 mm at the incisal margin, gradually increasing to 0.95 mm at the gingival margin; horizontal: 0.65 mm in the incisors, increasing to 0.95 mm in the molars). The gingival margin was trimmed 2 mm above the gingival contour. *N = 9 samples.* **Group 2 (NHH):** Direct 3D printed Noxi aligner, made of polyamide, with horizontal thickness gradient (0.65 mm in the incisors, increasing to 0.95 mm in the molars) and gingival margin trimmed 2 mm above the gingival contour. *N = 9 samples.* **Group 3 (NHZ):** Direct 3D printed Noxi aligner, made of	**Stress-Relaxation Test** Two test models were created based on the digital scan used to fabricate the aligners. The first model was generated by importing the file into Rhinoceros 8 software (Robert McNeel & Associates, Seattle, CA, USA), where the model was segmented to remove element 1.1 up to 1 mm from the gingival margin near the location where the force would be applied. The same process was applied to the second model, removing element 2.6. The test models were printed using a high-speed 3D printer (Nexa 3D Xip) with Xdent201 resin (Nexa3D, Ventura,	**Correlation Matrix Between Items** Correlation Matrix Between Items: Gingival Incisor Correlation Matrix Between Items: Medium Incisor Correlation Matrix Between Items: Incisivo incisal Correlation Matrix Between Items: Gingival molar Correlation Matrix Between Items: Medium molar Correlation Matrix Between Items: Ocluso molar 1.00 0.90 0.96 0.90 1.00 0.92 0.96 0.92 1.00 1.00 0.94 0.94 0.94 1.00 0.93 0.94 0.93 1.00 1.00 0.94 0.96 0.94 1.00 0.92 0.96 0.92 1.00 1.00 0.97 0.92 0.97 1.00 0.93 0.92 0.93 1.00 1.00 0.91 0.91 0.91 1.00 0.92 0.91 0.92 1.00 1.00 0.96 0.96 0.96 1.00 0.96 0.96 0.96 1.00 **Force Comparison at Each Point Between Aligners in 1.1** **Point Aligner n Mean F (df1, df2) p-value Eta-squared**

polyamide, with horizontal thickness gradient (0.65 mm in the incisors, increasing to 0.95 mm in the molars) and gingival margin trimmed at the zenith of the tooth. *N = 9 samples.*

Group 4 (F22): Thermoformed F22 aligner with a straight gingival margin (trimmed at the zenith), made of EvoFlex (Bay Materials LLC, Fremont, CA, USA), with 0.76 mm thickness. *N = 9 samples.*

Group 5 (AS): Thermoformed F22 aligner with a scalloped gingival margin, made of EvoFlex (Bay Materials LLC, Fremont, CA, USA), with 0.76 mm thickness. *N = 9 samples.*

Note:

A maxillary arch scan from a previously treated orthodontic patient was acquired using an intraoral scanner (Trios, 3Shape, Copenhagen, Denmark) and selected for the study (Figure 1). The same upper arch model was used for the design and production of all aligners. The test model for thermoforming was printed using the high-speed Nexa 3D Xip printer (Nexa3D, Ventura, CA, USA) with XDent201 Grey resin (Nexa3D, Ventura, CA, USA). Printing was performed with a 100 µm layer thickness and a total print time of approximately 30 minutes.

CA, USA), and positioned vertically to ensure stability and adequate space for material testing. A motorized vertical test stand, TVO-S (AstraLab, Mariano Comense, Italy), was used to apply a single-point vertical compression with a constant and predefined load. The models were placed inside a container (24 cm × 12 cm × 14 cm) serving as a horizontal support to ensure that the force was applied consistently at the same location and remained perpendicular to the model plane. This container was filled with distilled water maintained at a constant temperature of 37 °C and positioned beneath the load cell. A 100W immersion heater (Isw-100W, INKBIRD, Shenzhen, China) was used to maintain the water temperature at 37 °C (Figure 4).

Each sample underwent a 3-hour stress-relaxation test. After properly positioning the aligner on the model, a crosshead speed of 1 mm/min was set, reaching the desired deflection within one minute of testing. A constant deflection force of 1 N was maintained, with data collected every second to generate an accurate stress-relaxation

			(SD)			
	AS	10,752	1.4 (0.2)			
	F22	10,752	3.2 (0.4)			
Gingival	NHH	10,752	3.2 (0.4)	297,934.011 (4, 37,236.278)	<0.001 *	0.957
	NHVH	10,752	7.2 (0.6)			
	NHZ	10,752	2.8 (0.3)			
	AS	10,752	4.3 (0.5)			
	F22	10,752	5.3 (0.7)			
Medium	NHH	10,752	5.9 (0.4)	98,293.072 (4, 43,204.643)	<0.001 *	0.878
	NHVH	10,752	8.7 (0.6)			
	NHZ	10,752	5.5 (0.4)			
	AS	10,752	6.3 (0.8)			
	F22	10,752	7.8 (0.7)			
Incisal	NHH	10,752	10.1 (0.8)	53,640.504 (4, 49,636.352)	<0.001 *	0.797
	NHVH	10,752	9.8 (0.6)			
	NHZ	10,752	8.0 (0.6)			

*NHVH (NOXI Horizontal Vertical High); NHH (NOXI Horizontal High); NHZ (NOXI Horizontal Zenith); F22 (straight gingival margin — cut at zenith); AS (cut gingival margin); n, sample size; SD, standard deviation; F (df1, df2), F distribution; *p < 0.05 (statistically significant).

Initial Stress, Final Stress, Stress Decay, and Comparison of Stress Decay Between Aligner Types Tested in Element 1.1

Material	**Point**	**Initial Force (N)**	**Final Force (N)**	**Stress Relaxation (%)**	**Mean**	**Median**	**SD**	**25th Percentile**	**75th Percentile**	**p-value**
AS	Gingival	2.0	1.0	50.0						
	Medium	6.6	3.5	51.7	50.3	50.0	1.3	49.2	51.7	
	Incisal	10.8	5.5	49.2						
F22	Gingival	5.2	2.0	51.9						
	Medium	6.6	3.5	47.6	46.8	47.6	5.5	41.0	51.9	
	Incisal	5.5	8	41.0						
NHH	Gingival	6.0	2.8	53.3						
	Medium	9.2	5.6	38.0	44.7	42.9	7.8	38.0	53.3	0.212
	Incisal	16.3	9.5	42.9						
NHVH	Gingival	11.7	6.5	44.4						
	Medium	13.7	8.7	40.1	40.7	40.1	3.5	37.4	44.4	
	Incisal	14.7	9.7	37.4						
NHZ	Gingival	4.3	2.5	46.5						
	Medium	8.8	5.2	40.9	42.5	40.9	3.5	40.0	46.5	
	Incisal	12.5	7.5	40.0						

NHVH (NOXI Horizontal Vertical High); NHH (NOXI Horizontal High); NHZ (NOXI Horizontal Zenith); F22 (straight gingival margin — cut at zenith); AS (cut gingival margin); SD, standard deviation

curve for each material. An external force gauge mount (Sauter TVO-A01) was connected to a computer equipped with the Sauter AFH Fast data acquisition software (AstraLab, Mariano Comense, Italy), which provided a relaxation curve (force [N] vs. time [s]) for each observation period.
Each type of aligner was tested at three distinct points (gingival, middle, and incisal/occlusal) on elements 1.1 and 2.6. Three equivalent tests were conducted for each point using different aligners for each repetition.

Force Comparison at Each Point Between Aligners in 2.6

Point	Aligner	n	Mean (SD)	F (df1, df2)	p-value	Eta-squared
Gingival	AS	10,752	2.2 (0.2)	209,619.977 (4, 39,266.816)	<0.001 *	0.940
	F22	10,752	5.7 (0.4))			
	NHH	10,752	7.4 (0.6)			
	NHVH	10,752	6.8 (0.7)			
	NHZ	10,752	4.0 (0.4)			
Medium	AS	10,752	5.2 (0.3)	140,950.949 (4, 45,639.097)	<0.001 *	0.913
	F22	10,752	7.4 (0.5)			
	NHH	10,752	9.8 (0.6)			
	NHVH	10,752	8.3 (0.4)			
	NHZ	10,752	6.1 (0.6)			
Incisal	AS	10,752	6.1 (0.6)	127,554.367 (4, 46,685.640)	<0.001 *	0.905
	F22	10,752	8.4 (0.7)			
	NHH	10,752	12.0 (0.8)			
	NHVH	10,752	9.3 (0.4)			
	NHZ	10,752	8.4 (0.6)			

NHVH (High Horizontal Vertical NOXI); NHH (High Horizontal NOXI), NHZ (Zenith Horizontal NOXI), F22 (straight gingival margin — zenith cut); AS (scalloped gingival margin); N, sample size; SD, standard deviation; F (df1, df2), F distribution; * p-value < 0.05 (statistically significant).

Initial Stress, Final Stress, Stress Relaxation, and Comparison of Stress Decay Between Aligners Tested in Element 2.6

Material	Point	Initial Force (N)	Final Force (N)	Stress Relaxation (%)	Mean	Median	SD	25th Percentile	75th Percentile	p-value
AS	Gingival	3.3	2.0	39.4						
	Medium	7.2	4.8	33.3	39.0	39.4	5.5	33.3	44.2	
	Incisal	9.5	5.3	44.2						
F22	Gingival	8.2	5.3	34.6						
	Medium	11.0	7.0	36.4	35.9	36.4	1.1	34.6	36.6	
	Incisal	12.3	7.8	36.6						
NHH	Gingival	11.2	6.2	44.6						
	Medium	11.8	7.8	34.4	39.0	38.5	2.6	36.7	41.9	0.284
	Incisal	13.2	8.8	33.3						
NHVH	Gingival	11.7	6.8	41.9						
	Medium	14.7	9.2	36.7	37.4	34.4	6.2	33.3	44.6	
	Incisal	18.2	11.3	38.5						
NHZ	Gingival	7.2	3.5	51.4						
	Medium	10.0	5.3	47.0	45.4	47.0	6.9	37.9	51.4	
	Incisal	13.2	8.2	37.9						

NHVH (NOXI Horizontal Vertical High); NHH (NOXI Horizontal High); NHZ (NOXI Horizontal Zenith); F22 (straight gingival margin — cut at zenith); AS (cut gingival margin); SD, standard deviation.

<table>
<tr><td></td><td></td><td></td><td></td></tr>
<tr>
<td>Cremonine et al.,, 2025b
Italy
(English)</td>
<td>Group 1 (AA): Adult maxillary model with aligned dentition (ideal upper arch, exhibiting all fully erupted permanent teeth correctly aligned with appropriate axial inclinations). N = 2 samples.

Group 2 (AF): Adult maxillary model with permanent dentition exhibiting moderate crowding. N = 2 samples.

Group 3 (AD): Adult maxillary model with permanent dentition presenting microdontia and diastemata. N = 2 samples.

Group 4 (DM): Early mixed dentition model. N = 2 samples.

Group 5 (AA_A2G): Adult maxillary model with aligned dentition (ideal upper arch with fully erupted and aligned permanent teeth), with the addition of two round pressure</td>
<td>Tensile Test for Model Displacement
The Sauter TVO-A01 device was used for tensile testing, applying vertical displacement forces to the aligners. For convenient data acquisition, an external force gauge mount (Sauter TVO-A01) was connected to a computer running the Sauter AFH Fast 2.0 software (AstraLab, Mariano Comense, Italy). The machine generated a force (N) vs. time (s) curve, capturing the process until the aligner was completely dislodged from the model.
To simulate vertical displacement forces, three metal chains with equal-length mechanical connector</td>
<td>Maximum Force Between Aligners in Aligned Adult Model (AA), Aligned Adult Model with Two Round Attachments (AA_2GP), and Aligned Adult Model with Four Round Attachments (AA_4GP)
<table>
<tr><th>Group</th><th>Subgroup</th><th>Maximum Force (N)</th><th>Approx. Standard Deviation</th></tr>
<tr><td>AA</td><td>NOVA</td><td>12.0</td><td>±2.5</td></tr>
<tr><td>AA</td><td>F22</td><td>10.7</td><td>±2.0</td></tr>
<tr><td>AA</td><td>NUA</td><td>7.2</td><td>±1.5</td></tr>
<tr><td>AA</td><td>NOVZ</td><td>7.0</td><td>±1.2</td></tr>
<tr><td>AA</td><td>AS</td><td>5.2</td><td>±1.0</td></tr>
<tr><td>AA</td><td>NUZ</td><td>3.3</td><td>±0.8</td></tr>
<tr><td>AA_2GP</td><td>NOVA</td><td>22.8</td><td>±3.0</td></tr>
<tr><td>AA_2GP</td><td>F22</td><td>18.7</td><td>±2.5</td></tr>
<tr><td>AA_2GP</td><td>NUA</td><td>14.0</td><td>±2.2</td></tr>
<tr><td>AA_2GP</td><td>NUZ</td><td>12.3</td><td>±2.0</td></tr>
<tr><td>AA_2GP</td><td>NOVZ</td><td>12.0</td><td>±1.8</td></tr>
<tr><td>AA_2GP</td><td>AS</td><td>9.3</td><td>±1.5</td></tr>
<tr><td>AA_4GP</td><td>F22</td><td>36.5</td><td>±3.5</td></tr>
<tr><td>AA_4GP</td><td>NUA</td><td>32.0</td><td>±3.0</td></tr>
<tr><td>AA_4GP</td><td>NOVA</td><td>30.0</td><td>±3.0</td></tr>
<tr><td>AA_4GP</td><td>NOVZ</td><td>29.0</td><td>±3.0</td></tr>
<tr><td>AA_4GP</td><td>NUZ</td><td>26.2</td><td>±2.8</td></tr>
<tr><td>AA_4GP</td><td>AS</td><td>19.0</td><td>±2.0</td></tr>
</table>
Maximum Force Between Aligners in Aligned Adult Model (AA), Adult Model with Dental Crowding (AF), Adult Model with Small Teeth and Diastema (AD), and Early Mixed Dentition Model (DM)
<table>
<tr><th>Group</th><th>Subgroup</th><th>Maximum Force (N)</th><th>Approx. Standard Deviation</th></tr>
<tr><td>AA</td><td>NOVA</td><td>12.0</td><td>±2.5</td></tr>
</table>
</td>
</tr>
</table>

	points ("pegadas"). *N = 2 samples.* **Group 6 (AA_A4G):** Adult maxillary model with aligned dentition (ideal upper arch with fully erupted and aligned permanent teeth), with the addition of four round pressure points ("pegadas"). *N = 2 samples.* **Grupo de alinhadores** **Group 1 (NUZ):** 3D printed Noxi aligners (Sweden & Martina, Due Carrare, Italy) with zenith-trimmed margin and uniform thickness gradient (aligners with evenly distributed thickness and a gingival margin positioned at 0 mm). **Group 2 (NUA):** 3D printed Noxi aligners (Sweden & Martina, Due Carrare, Italy) with high-trimmed margin and uniform thickness gradient (aligners with uniform 0.65 mm thickness and a gingival margin positioned at 2 mm). **Group 3 (NOVZ):** 3D printed Noxi aligners (Sweden & Martina, Due Carrare, Italy) with zenith-trimmed margin and both horizontal and vertical thickness gradients (aligners with differential thickness gradients vertically—from gingival to occlusal—and horizontally—from posterior to anterior; with thickness values of 0.95 mm at the gingival zone, 0.65 mm in the anterior occlusal region, and 0.95 mm in the	rings were used. One end of each chain was attached to a steel plate customized to align with the standardized hook positions on the model for each occlusal type, while the other end was connected to the hook of the aligner. The traction speed was set at 5 mm/min, ensuring standardized displacement conditions. Each combination of material, margin design, and gradient was tested on each occlusal model type, and every test was performed in triplicate. Comparative tests were conducted to evaluate the maximum displacement force among the aligners and to compare the maximum force between aligner pairs for each model.	AA F22 10.7 ±2.0 AA NUA 7.2 ±1.5 AA NOVZ 7.0 ±1.2 AA AS 5.2 ±1.0 AA NUZ 3.3 ±0.8 AF NOVA 28.7 ±4.0 AF F22 27.2 ±3.5 AF NOVZ 17.3 ±2.8 AF NUA 15.3 ±2.5 AF AS 12.8 ±2.2 AF NUZ 12.5 ±2.0 AD F22 10.8 ±1.8 AD NUZ 6.2 ±1.5 AD NOVZ 4.5 ±1.2 AD NOVA 3.0 ±1.0 AD AS 2.2 ±0.8 AD NUA 1.7 ±0.7 DM NOVZ 5.2 ±1.5 DM NOVA 2.7 ±1.0 DM F22 2.7 ±0.8 DM NUA 1.7 ±0.6 DM NUZ 0.7 ±0.5 DM AS 0.5 ±0.3 **Pairwise Comparisons of Maximum Force Between Aligners** **Sample 1 / Sample 2** — **Median** — **25th Percentile** — **75th Percentile** — **Statistical Test** — **Standard Error** — **Standardized Statistical Test** — **p** AS / NUZ — 7,3 / 9,3 — 2 / 3,5 — 13 / 14,5 — 6,5 — 10,435 — 0,623 — 0,533 AS / NUA — 7.3 / 10 — 2 / 2 — 13 / 16.5 — 9.944 — 10.435 — 0.953 — 0.341 AS / NOVZ — 7.3 / 9.3 — 2 / 6 — 13 / 16.5 — 15.278 — 10.435 — 1.464 — 0.143 AS / NOVA — 7.3 / 18 — 2 / 3.5 — 13 / 26.5 — 22.722 — 10.435 — 2.177 — 0.029 ** AS / F22 — 7.3 / 14.5 — 2 / 10.5 — 13 / 27 — 27.889 — 10.435 — 2.673 — 0.008 * NUZ / NUA — 9.3 / 10 — 3.5 / 2 — 14.5 / 16.5 — 3.444 — 10.435 — 0.33 — 0.741 NUZ / NOVZ — 9.3 / 9.3 — 3.5 / 6 — 14.5 / 16.5 — 8.778 — 10.435 — 0.841 — 0.4 NUZ / NOVA — 9.3 / 18 — 3.5 / 3.5 — 14.5 / 26.5 — 16.222 — 10.435 — 1.555 — 0.12

	posterior occlusal region; gingival margin positioned at 0 mm). **Group 4 (NOVA):** 3D printed Noxi aligners (Sweden & Martina, Due Carrare, Italy) with high-trimmed margin and both horizontal and vertical thickness gradients (aligners with 0.95 mm thickness in the gingival area, 0.65 mm in the anterior occlusal region, and 0.95 mm in the posterior occlusal region; gingival margin positioned at 2 mm). **Group 5 (F22):** Thermoformed aligners made from Zendura FLX (Bay Materials, Fremont, CA, USA), with a straight gingival margin. **Group 6 (AS):** Thermoformed aligners made from Zendura FLX (Bay Materials, Fremont, CA, USA), with a scalloped gingival margin. **Note:** All models were created using 3D printing technology with the Nexa3D Xip printer (Nexa3D, Ventura, CA, USA). The material used was Xdent 20 resin (Xdent Lab, Ho Chi Minh City, Vietnam). Test models were designed using Rhinoceros 8 software (Robert McNeel and Associates, Seattle, CA, USA) for CAD modeling. A central hole (0.5 cm in diameter and 0.5 cm in depth) was designed in the plaster model for stabilization on the Sauter TVO-A01 machine		

NUZ F22	9.3 14.5	3.5 10.5	14.5 27	21.389	10.435	2.05	0.04 **
NUA NOVZ	10 9.3	2 6	16.5 16.5	5.333	10.435	0.511	0.609
NUA NOVA	10 18	2 3.5	16.5 26.5	12.778	10.435	1.224	0.221
NUA F22	10 14.5	2 10.5	16.5 27	17.944	10.435	1.72	0.086 *
NOVZ NOVA	9.3 18	6 3.5	16.5 26.5	7.444	10.435	0.713	0.476
NOVZ F22	9.3 14.5	6 10.5	16.5 27	12.611	10.435	1.209	0.227
NOVA F22	18 14.5	3.5 10.5	26.5 27	5.167	10.435	0.495	0.621

Pairwise comparison of maximum force between aligners for each model

Model	Sample 1 Sample 2	Median	25th Percentile	75th Percentile
AA	NUZ	3.5	2.5	4
	F22	10.5	10.5	11
	NUZ	3.5	2.5	4
	NOVA	11	9.5	15.5
	AS	5	5	5.5
	F22	10.5	10.5	11
	AS	5	5	5.5
	NOVA	11	9.5	15.5
AA_2GP	AS	9.5	9	9.5
	F22	19	17.5	19.5
	AS	9.5	9	9.5
	NOVA	22	20.5	26
	NOVZ	12	10	14
	NOVA	22	20.5	26
	NUZ	11.5	11	14.5
	NOVA	22	20.5	26
AA_4GP	NUZ	25.5	23.5	29.5

	(AstraLab, Mariano Comense, Italy) using a 0.5 cm × 0.7 cm screw during tensile testing. Each model was duplicated and equipped with three hooks: two on the first molars and one in the incisal region. Hooks were designed with uniform dimensions for all models. Based on their coordinates, steel plates were created to ensure perpendicular traction of the aligners during testing. Additionally, hooks included a drilling guide for post-thermoforming perforation, identical to the hole designed for nylon aligners. The same drill bit was used for all holes, performed by a single operator. The Noxi aligners (Sweden & Martina, Due Carrare, Italy) were printed with hooks directly included. STL files were modified to digitally integrate the hooks using Rhinoceros 8, considering aligner thickness during thermoforming to ensure perfect alignment between the 3D-printed and thermoformed aligner hooks—avoiding external variables that could affect test accuracy.			F22	36.5	35.5	37.5
				AS	18.5	18	20.5
				NUA	31.5	29.5	35
				AS	18.5	18	20.5
				NOVA	31.5	29.5	35
				AS	18.5	18	20.5
				F22	36.5	35.5	37.5
				NOVZ	27.5	25.5	34
				F22	36.5	35.5	37.5
			4F	NUZ	12	11	14.5
				NOVA	26.5	24.5	35
				NUZ	12	11	14.5
			F22		27	26	28.5
				AS	13	12	13.5
				NOVA	26.5	24.5	35
				AS	13	12	13.5
				F22	27	26	28.5
			AD	AS	2	2	2.5
				F22	10.5	10.5	11.5
				NUA	2	1	2
				F22	10.5	10.5	11.5
				NOVA	2.5	2	4.5
				F22	10.5	10.5	11.5
				AS	2	2	2.5
				NUZ	5.5	5.5	7.5
				NUA	2	1	2
				NUZ	5.5	5.5	7.5
			DM	NUZ	0.5	0.5	1
				NOVZ	4	3.5	8
				NUZ	0.5	0.5	1
				NOVA	2.5	2	3.5

				NUZ	0.5	0.5	1		
				F22	2.5	2.5	3		
				AS	0.5	0.5	0.5		
				NOVZ	4	3.5	8		
				AS	0.5	0.5	0.5		
				NOVA	2.5	2	3.5		
				AS	0.5	0.5	0.5		
				F22	2.5	2.5	3		
				NUA	1.5	1.5	2		
				NOVZ	4	3.5	8		
			Pairwise comparison of maximum force between aligners for each model.						
			Model	**Sample 1 Sample 2**	**Statistical Test**	**or**	**Std.Err**	**Standard Error**	**p.**	**p.**	**Adj.**
			AA	NUZ	13.167		4.35	3.027	0.002**	0.037	0.022
				F22							
				NUZ	13.833		4.35	3.18	0.001**	0.291	0.191
				NOVA							
				AS	−10.167		4.35	−2.337	0.019**		
				F22							
				AS	−10.833		4.35	−2.49	0.013**		
				NOVA							
			AA_2GP	AS	−12		4.354	−2.756	0.006**	0.088	
				F22							

				AS NOVA	−15	4.354	−3.445	<0.001**	0.009	0.00
				NOVZ NOVA	9.833	4.354	2.258	0.024**	0.359	0.35
				NUZ NOVA	9.667	4.354	2.22	0.026**	0.396	0.39
				NUZ F22	10.333	4.352	2.374	0.018**	0.264	0.26
				AS NUA	10.333	4.352	2.374	0.018**	0.264	0.26
			AA_4GP	**AS** NOVA	8.167	4.352	1.876	0.061*	0.909	0.90
				AS F22	15	4.352	3.447	<0.001**	0.009	0.00
				NOVZ F22	8.167	4.352	1.876	0.061*	0.909	0.90
				NUZ NOVA	11.833	4.354	2.718	0.007**	0.099	0.09
			4F	NUZ F22	12.167	4.354	2.794	0.005**	0.078	0.07

				AS	11.5	4.354	2.641	0.008**	4	0.12
				NOVA						
				AS	11.833	4.354	2.718	0.007**	9	0.09
				F22						
				AS	11.667	4.298	2.715	0.007**		0.1
				F22						
				NUA	14	4.298	3.258	0.001**	7	0.01
				F22						
			AD	NOVA	9.5	4.298	2.21	0.027**	6	0.40
				F22						
				AS	8	4.298	1.861	0.063*		0.94
				NUZ						
				NUA	−10.33	4.298	−2.404	0.016**	3	0.24
				NUZ	3					
				NUZ	12.833	4.298	2.986	0.003**	2	0.04
				NOVZ						
				NUZ	8.333	4.298	1.939	0.053*	8	0.78
			DM	NOVA						
				NUZ	8.667	4.298	2.017	0.044**	6	0.65
				F22						
				AS	13.833	4.298	3.219	0.001**	9	0.01

			NOVZ AS 9.333 4.298 2.172 0.03** 0.448 NOVA AS 9.667 4.298 2.249 0.024** 0.367 F22 NUA 8.667 4.298 2.017 0.044** 0.656 NOVZ
Eslami *et al.*, 2024 Germany (English)	**Group 1 (DP-Clin):** 3D printed aligners made with Tera Harz TC-85 DAC resin, manufactured by Graphy, Seoul, South Korea. Retrieved after 1 week of intraoral use. *N = 34 samples.]* **Group 2 (INV-Clin):** Invisalign® aligners, manufactured by Align Technology, San Jose, CA, USA, made of SmartTrack material. Retrieved after 1 week of intraoral use. *N = 34 samples.* **Group 3 (DP-Ctr):** 3D printed aligners made with Tera Harz TC-85 DAC resin, manufactured by Graphy, Seoul, South Korea. Not used. *N = 34 samples.* **Group 4 (INV-Ctr):** Invisalign® aligners, manufactured by Align Technology, San Jose, CA, USA, made of SmartTrack material. Not used. *N = 34 samples.* **Note:** The 3D printed aligners were fabricated using the Sprintray Pro 55 3D printer (Sprintray, Los Angeles, CA, USA) and Tera Harz TC85A	**Surface Roughness and Porosity Test** The buccal surface of the upper right central incisor of the aligners was selected for sample preparation, as this area has a relatively flat geometry that allows for more accurate evaluations. The internal surface of the aligners was analyzed using confocal laser scanning microscopy (CLSM) with a Keyence VK-X100 microscope (Keyence, Osaka, Japan). The acquisition area of 1000.0 × 1419.9 µm was measured using a nominal 10x objective lens. The software's specialist module was used for image acquisition, and the VK-Analyzer software (Keyence, Osaka, Japan) was employed to measure surface roughness and porosity parameters. Automatic tilt correction was applied	**Descriptive Statistics of Surface Roughness and Porosity Parameters in the DP-Ctr, DP-Clin, INV-Ctr, and INV-Clin Groups** **Surface Roughness and Porosity Parameter** / **DP-Ctr** / **DP-Clin** / **INV-Ctr** / **INV-Clin** Sa (mm) 1,72 ± 1,10 3,78 ± 1,70 6,79 ± 2,39 2,68 ± 1,40 Sq (mm) 2,35 ± 1,61 4,87 ± 2,25 10,4 ± 4,89 3,37 ± 3,00 Sp (mm) 6,92 ± 6,81 18,9 ± 12,8 44,4 ± 28,9 12,5 ± 11,3 Sz (mm) 16,5 ± 19,3 42,1 ± 32,8 121,0 ± 92,4 24,5 ± 18,8 Sv (mm) 9,59 ± 13,3 23,2 ± 23,6 76,4 ± 67,7 12,1 ± 9,64 Vvv (mm³/mm²) 0,27 ± 0,29 0,54 ± 0,38 1,54 ± 1,10 0,37 ± 0,30 Vvc (mm³/mm²) 2,40 ± 1,48 6,19 ± 3,05 8,34 ± 2,69 3,90 ± 2,08 The values presented represent the mean ± standard deviation **Median Regressions (Quantiles) for Surface Roughness Parameters with Predictor Variables Type of Material (DP/INV) and Intraoral Use (Ctr/Clin)** **Parameter (Unit)** / **Reference Category** / **Predictor Category** / **Coefficient+** / **p-value** Sa (mm) INV-Ctr INV-Clin -4,468 < 0,001* INV-Ctr DP-Ctr -5,145 < 0,001* INV-Ctr DP-Clin -3,053 < 0,001* DP-Ctr DP-Clin 2,09 < 0,001* Sq (mm) INV-Ctr INV-Clin -6,444 < 0,001* INV-Ctr DP-Ctr -7,400 < 0,001* INV-Ctr DP-Clin -4,943 < 0,001* DP-Ctr DP-Clin 2,457 < 0,001* Sp (mm) INV-Ctr INV-Clin -29,744 < 0,001* INV-Ctr DP-Ctr -33,508 < 0,001* INV-Ctr DP-Clin -24,27 < 0,001* DP-Ctr DP-Clin 9,418 < 0,001* Sv (mm) INV-Ctr INV-Clin -46,297 < 0,001* INV-Ctr DP-Ctr -50,454 < 0,001* INV-Ctr DP-Clin -41,592 < 0,001*

	aligner resin (Graphy, Seoul, South Korea). Aligners were oriented vertically with minimal supports and printed in successive 100 µm layers. Excess resin was removed via centrifugation for 6 minutes at 600 rpm. The aligners were then cured for 20 minutes at level 2 under nitrogen using the Graphy Tera Harz Cure THC 2 UV curing system (Graphy, Seoul, South Korea). Recovered aligners underwent gentle cleaning, with no chemical or abrasive agents, including rinsing with water and plaque removal using a soft toothbrush.	using the secondary curved surface function to compensate for surface curvature. A Gaussian regression filter and short/long wavelength cutoff filters were applied in accordance with ISO 25178 standards to suppress image noise and separate surface texture from form. After measuring the surface roughness and porosity parameters for each sample, height-related measurements were recorded: arithmetic mean height (Sa), root mean square height (Sq), maximum peak height (Sp), maximum valley depth (Sv), and maximum height difference between the highest peak and the deepest valley (Sz). Functional volumetric parameters were also recorded to assess surface porosity: void volume (Vvv) and void count (Vvc).		DP-Ctr	DP-Clin	8,862	< 0,001*
			Sz (mm)	INV-Ctr	INV-Clin	-81,149	< 0,001*
				INV-Ctr	DP-Ctr	-86,449	< 0,001*
				INV-Ctr	DP-Clin	-58,666	< 0,001*
				DP-Ctr	DP-Clin	27,783	< 0,001*
			Vvv (mm^3/mm^2)	INV-Ctr	INV-Clin	-0,805	< 0,001*
				INV-Ctr	DP-Ctr	-0,946	< 0,001*
				INV-Ctr	DP-Clin	-0,629	< 0,001*
				DP-Ctr	DP-Clin	0,317	< 0,001*
			Vvc (mm^3/mm^2)	INV-Ctr	INV-Clin	-5,760	< 0,001*
				INV-Ctr	DP-Ctr	-6,846	< 0,001*
				INV-Ctr	DP-Clin	-3,494	< 0,001*
				DP-Ctr	DP-Clin	3,352	< 0,001*
			ositive values indicate higher surface roughness compared to the reference, while negative values indicate lower surface roughness				

Hertan *et al.*,, 2022 United States of America (English)	**Group 1 (G1):** Thermoformed aligners without attachments, fabricated from 125 mm round sheets with a thickness of 0.030 inches (ATMOS; American Orthodontics, Sheboygan, WI, USA). The aligners were produced using master models and thermoformed with a pressurized Biostar machine (Scheu-Dental GmbH, Iserlohn, Germany). *N = 10 samples.* **Group 2 (G2):** Thermoformed aligners with attachments, using the same material (125 mm ATMOS sheets, 0.030 inches thick). The manufacturing process was identical to G1, employing master models and pressure thermoforming with the Biostar device. *N = 10 samples.* **Group 3 (G3):** Direct 3D printed aligners without attachments, manufactured from Graphy Tera Harz TC-85DAC resin. The aligners were printed with a thickness of 0.50 mm and included a spacing of 0.05 mm between the aligner and the dental model. *N = 10 samples.* **Group 4 (G4):** Direct 3D printed aligners with attachments, also made from Graphy Tera Harz TC-85DAC resin, with a thickness of 0.50 mm and 0.05 mm spacing from the model. *N = 10 samples.* **Note:** A maxillary arch from a single patient was scanned using the Trios scanner (3Shape,	**Test to Evaluate and Compare Force Over Time** For this study, a test model was created from the master digital file, without attachments, and exported to MeshMixer software (Autodesk, San Rafael, CA, USA). The model was segmented to remove the upper right central incisor and modified to provide the vertical support and structural resistance required for subsequent testing. The model was printed using a Uniz Slash-C LCD 3D printer (Uniz, San Diego, CA, USA) with AnyCubic Clear 3D resin (AnyCubic, Shenzhen, China). The test was performed using a manual force testing stand operated by a handwheel and equipped with a high-resolution digital caliper (0.01 mm), paired with a ZP-50 digital force gauge (Baoshishan, Shenzhen, China), with an accuracy of 0.01 N. The calibration of the ZP-50 dynamometer was verified using a Correx portable dynamometer (Haag-Streit Diagnostics, Köniz, Switzerland). The ZP-50 force gauge was mounted to the testing stand in compression mode, and the test model was	**Comparison of Thermoformed Aligners without Attachments and Thermoformed Aligners with Attachments** **Displacement** | **Unit (N)** | **Thermoformed Aligners without Attachments** | **Thermoformed Aligners with Attachments** | **p-value** **Mean ± SD** | **Median** | **Mean ± SD** | **Median** 0,10 mm | Peak Force | 5,26±0,51 | 5.11 | 5,13±0,89 | 5.34 | 0,94 Stabilized Force | 4,73±0,50 | 4,60 | 4,6±0,84 | 4,74 | 0,97 0,20 mm | Peak Force | 10,52±0,69 | 10.52 | 10,37±1,21 | 10.39 | 0,82 Stabilized Force | 9,77±0,76 | 9,68 | 9,60±1,18 | 9,75 | 0,94 0,30 mm | Peak Force | 16,16±0,71 | 16.10 | 15,85±1,36 | 16.26 | 0,94 Stabilized Force | 15,04±0,8 | 14,89 | 14,84±1,48 | 15h30 | 0,55 **Comparison of 3D Aligners without Attachments and 3D Aligners with Attachments** **Displacement** | **Unit (N)** | **3D Aligners without Attachments** | **3D Aligners with Attachments** | **p-valueP** **Mean ± SD** | **Median** | **Mean ± SD** | **Median** 0,10 mm | Peak Force | 2,59±0,62 | 2,44 | 2,77±0,60 | 2,65 | 0,45 Stabilized Force | 0,76±0,18 0,79 | 0,73 | 0,81±0,21 | 0,79 | 0,65 0,20 mm | Peak Force | 3,15±0,65 3,52 | 3.18 | 3,58±0,51 | 3,52 | 0,14 Stabilized Force | 1,18±0,27 | 1.19 | 1,33±0,23 | 1.26 | 0,15 0,30 mm | Peak Force | 3,49±0,71 | 3,48 | 4,04±0,67 | 3,87 | 0,08 Stabilized Force | 1,57±0,37 | 1,52 | 1,78±0,39 | 1,69 | 0,24 **Comparison of 3D Aligners and Thermoformed Aligners** **Displacement** | **Unit (N)** | **3D Aligners** | **Thermoformed Aligners** | **p-valueP** **lower quartile** | **upper quartile** | **lower quartile** | **upper quartile** 0,10 mm | Peak Force | 2.25 | 3.12 | 5.11 | 4.88 | <.0001 Stabilized Force | 0.67 | 0.88 | 4.60 | 4.30 | <.0001 0,20 mm | Peak Force | 3.01 | 3.82 | 10.52 | 9.91 | <.0001 Stabilized Force | 1.10 | 1.35 | 9.68 | 9.14 | <.0001 0,30 mm | Peak Force | 3.29 | 4.18 | 16.10 | 15.64 | <.0001 Stabilized Force | 1.42 | 1.9 | 14.89 | 14.41 | <.0001

	Copenhagen, Denmark), and the file was processed in the uDesign 6.0 software (uLab Systems Inc., San Mateo, CA, USA). Two digital master models were created: one with no attachments, and another with horizontal rectangular attachments. The attachments measured 2.7 mm in depth, 4.2 mm in height, and 4.0 mm in width and were placed on all maxillary teeth with a gingivally beveled design. Four master models (two with and two without attachments) were printed using the SprintRay Pro DLP printer (SprintRay, Los Angeles, CA, USA). Thermoformed aligners were cured using the SprintRay Pro Cure, following manufacturer recommendations. The 3D printed aligners were fabricated on the SprintRay Pro 95 printer and centrifuged for 3 minutes to remove residual resin. The printed plates were then cured for 35 minutes in a Cure M device (Graphy Inc., Seoul, South Korea) under nitrogen, followed by an additional 35-minute post-curing stage submerged in glycerin, without nitrogen gas.	positioned on the base using a standard mini C-clamp. Due to the temperature-sensitive properties of 3D-printed aligners, which exhibit shape-memory behavior, it was necessary to simulate intraoral conditions. Aligners were heated to body temperature (approximately 37.5 °C) for at least 5 minutes by being individually submerged in a bag containing 30–60 ml of warm water maintained in a water bath heated by a ceramic positive temperature coefficient heater. The force gauge was lowered gradually until a force reading was detected by the digital gauge upon placing the aligner on the test model. The gauge was then raised until the force reading returned to zero. This process was repeated three times per sample. After zeroing the digital caliper, the aligner was vertically compressed on the external incisal edge of the missing upper right central incisor. Compression was applied until a displacement of 0.10 mm in the gingival direction was achieved, at which point the peak force (in N) was recorded. A	

<table>
<tr>
<td></td>
<td></td>
<td>stopwatch was started, and after 20 seconds, the force was recorded again. Compression was then continued to a displacement of 0.20 mm, followed by a new peak force reading and another measurement after 20 seconds of stabilization. This procedure was repeated until a displacement of 0.30 mm was reached.</td>
<td></td>
</tr>
<tr>
<td>Jindal et al.,, 2019
India
(English)</td>
<td>Group 1 (G1): Thermoformed orthodontic aligners fabricated from 3D printed dental models, using transparent Duran sheets with 1 mm thickness. The material properties included an elastic modulus of 2.2 GPa, Poisson’s ratio of 0.37, density of 1270 kg/m³, compressive strength of 92.9 MPa, and tensile strength of 2.65 MPa. N = 5 samples.

Group 2 (G2): Thermoformed orthodontic aligners fabricated from 3D printed dental models, using transparent DuranSoft sheets with 1 mm thickness. The material presented an elastic modulus of 1.9 GPa, Poisson’s ratio of 0.49, density of 1200 kg/m³, compressive strength of 69 MPa, and tensile strength of 63 MPa. N = 5 samples.

Group 3 (G3): Direct 3D printed aligners fabricated using</td>
<td>Compression Test
The compression test was performed using a universal testing machine, Instron 3367 (Instron Corp., Wilmington, DE), aiming to apply a maximum compressive force of 1000 N to all aligners evaluated. The aligners were compressed between two flat plates, with the lower plate remaining stationary and the upper plate moving at a rate of 50 N/min. The test was conducted under a 1000 N load cell. The deformation behavior of the aligners in response to the applied load was recorded and analyzed using compatible data acquisition software.
Accuracy Test
The accuracy of the aligners was</td>
<td>Compression Test
<table><tr><th></th><th>Maximum Load</th><th>Displacement</th></tr><tr><td>3D Aligners Not Cured</td><td>380 N</td><td>6,1 mm</td></tr><tr><td>3D Aligners Cured at 80°C for 20 Minutes</td><td>662 N</td><td>≈ 2.93 mm before Fracture</td></tr><tr><td>3D Aligners Cured at 80°C for 15 Minutes</td><td>531 N</td><td>≈ 2.93 mm before Fracture</td></tr><tr><td>Thermoformed Aligners</td><td>584 N</td><td>8,6 mm</td></tr></table>
Accuracy: Geometric Comparison Between STL Files and 3D Printed Aligners
<table><tr><th></th><th>STL File</th><th>3D Printed Aligners</th><th></th><th></th></tr><tr><th>Element</th><th>Tooth Height (mm)</th><th>Mean Tooth Height (mm)</th><th>Standard Deviation (mm)</th><th>Absolute Difference (mm)</th><th>Relative Difference (%)</th></tr><tr><td>1</td><td>6.14</td><td>6.10</td><td>0.06</td><td>0.04</td><td>0.65</td></tr><tr><td>2</td><td>7.50</td><td>7.69</td><td>0.03</td><td>0.19</td><td>2.53</td></tr><tr><td>3</td><td>7.80</td><td>7.82</td><td>0.05</td><td>0.02</td><td>0.26</td></tr><tr><td>4</td><td>8.91</td><td>9.20</td><td>0.08</td><td>0.29</td><td>3.25</td></tr><tr><td>5</td><td>9.53</td><td>9.59</td><td>0.08</td><td>0.06</td><td>0.63</td></tr><tr><td>6</td><td>8.00</td><td>8.15</td><td>0.07</td><td>0.15</td><td>1.88</td></tr><tr><td>7</td><td>8.20</td><td>8.27</td><td>0.06</td><td>0.07</td><td>0.90</td></tr><tr><td>8</td><td>8.55</td><td>8.07</td><td>0.08</td><td>0.48</td><td>5.61</td></tr><tr><td>9</td><td>8.31</td><td>9.17</td><td>0.07</td><td>0.86</td><td>10.35</td></tr><tr><td>10</td><td>9.08</td><td>9.32</td><td>0.05</td><td>0.24</td><td>2.64</td></tr><tr><td>11</td><td>9.70</td><td>9.78</td><td>0.09</td><td>0.08</td><td>0.82</td></tr><tr><td>12</td><td>7.67</td><td>7.94</td><td>0.06</td><td>0.27</td><td>3.52</td></tr></table></td>
</tr>
</table>

	biocompatible Dental LT resin. The aligners were printed using the Formlabs Form 2 printer (Somerville, MA, USA) with a thickness of 1 mm. Mechanical properties included an elastic modulus of 2.06 GPa, Poisson's ratio of 0.35, density of 1200 kg/m³, compressive strength of 342 MPa, and tensile strength of 211 MPa. *N = 5 samples.* **Note:** To fabricate the dental aligners, mandibular dentition scans were obtained from a real patient using a 3Shape E1 laboratory scanner equipped with a blue LED multiline system, with a scanning precision of 10–12 µm. The STL file generated was processed using the Maestro Studio CAD/CAM software. Additional steps included the marking of missing teeth, individual tooth measurements, identification of ideal arch length, interproximal reduction planning, and subsequent point-to-point plotting for aligner design.	assessed by measuring the height of each tooth on the fabricated aligners and the corresponding original dental models. Measurements were performed by five different observers. The crown height of each tooth was determined by measuring the distance between the intersection point of the midline of the buccal surface and the gingival margin, and the incisal edge. Tooth nomenclature was established as follows: Lower Right Second Molar Lower Right First Molar Lower Right Second Premolar Lower Right First Premolar Lower Right Canine Lower Right Lateral Incisor Lower Right Central Incisor Lower Left Central Incisor Lower Left Lateral Incisor Lower Left Canine Lower Left First Premolar Lower Left Second Premolar Lower Left First Molar Lower Left	13 6.10 6.16 0.09 0.06 0.98 14 7.46 7.58 0.07 0.12 1.61 **Accuracy: Geometric Comparison Between STL Files and Thermoformed Aligners** **Element** / **STL File Tooth Height (mm)** / **Thermoformed Aligners Mean Tooth Height (mm)** / **Standard Deviation (mm)** / **Absolute Difference (mm)** / **Relative Difference (%)** 1 6.14 6.13 0.08 0.01 0.16 2 7.50 6.96 0.07 0.81 10.80 3 7.80 7.59 0.09 0.21 2.69 4 8.91 9.14 0.07 0.23 2.58 5 9.53 8.65 0.05 0.88 9.23 6 8.00 8.66 0.08 0.66 8.25 7 8.20 8.72 0.08 0.52 6.39 8 8.55 8.12 0.08 0.17 1.99 9 8.31 9.08 0.07 0.19 2.29 10 9.08 9.07 0.06 0.00 0.00 11 9.70 7.43 0.07 0.63 6.49 12 7.67 7.67 0.07 0.24 3.13 13 6.10 6.07 0.08 0.03 0.49 14 7.46 6.93 0.06 0.53 7.10

<table>
<tr>
<td></td>
<td></td>
<td>Second Molar

These measurements were used to assess the precision of the tooth heights on the aligners by comparing them with the original dental models.</td>
<td></td>
</tr>
<tr>
<td>Jindal et al., 2020 India (English)</td>
<td>Group 1 (G1): Thermoformed orthodontic aligners fabricated from 3D-printed dental models using transparent Duran sheets with a thickness of 1 mm. The material exhibited a modulus of elasticity of 2.2 GPa, Poisson’s ratio of 0.37, density of 1270 kg/m³, compressive strength of 92.9 MPa, and tensile strength of 2.65 MPa.

Group 2 (G2): Thermoformed orthodontic aligners fabricated from 3D-printed dental models using transparent DuranSoft sheets with a thickness of 1 mm. The material presented a modulus of elasticity of 1.9 GPa, Poisson’s ratio of 0.49, density of 1200 kg/m³, compressive strength of 69 MPa, and tensile strength of 63 MPa.

Group 3 (G3): Directly 3D-printed orthodontic aligners manufactured using biocompatible Dental LT resin. The aligners were printed with 1 mm thickness using the Formlabs Form 2 printer (Somerville, MA, USA). The material exhibited a modulus of elasticity of 2.06 GPa, Poisson’s ratio of 0.35, density of 1200 kg/m³, compressive strength of</td>
<td>Finite Element Modeling (FEM) Process
After generating the CAD file of the dental aligner, the model was imported for further analysis into SolidWorks 2018 software, provided by Dassault Systèmes. To overcome the limitations of SolidWorks, a second software, GeoMagic Design X 2018 (3D Systems Inc., 2019), developed by 3D Systems, was used. Upon importing the model into SolidWorks, it was successfully meshed. The mesh generated was solid and of high quality, using 10-node tetrahedral elements. The final model consisted of a total of 91,107 degrees of freedom, 16,545 elements, and 33,161 nodes.
Using the p-adaptive meshing technique, only three simulations were required to achieve a result with less than 1% variation in maximum Von Mises</td>
<td>
<table>
<tr><th>Aspect</th><th>Duran (Convencional)</th><th>Durasoft (Convencional)</th><th>Dental LT (Resina)</th></tr>
<tr><td>Von Mises Maximum Stress (MPa)</td><td>8,98 MPa a 15,13 MPa</td><td>8,98 MPa a 15,13 MPa</td><td>8,94 MPa a 14,88 MPa</td></tr>
<tr><td>Simulated Bite Force</td><td>600 N</td><td>600 N</td><td>600 N</td></tr>
<tr><td>Stress Reduction</td><td>-</td><td>-</td><td>0.2%–7.7% compared to Duran and Durasoft</td></tr>
<tr><td>Stress Distribution</td><td>Similar in molars, canines, and incisors</td><td>Similar in molars, canines, and incisors</td><td>Slight reduction compared to Duran and Durasoft</td></tr>
</table>
Von Mises Maximum Stress (MPa)
<table>
<tr><th>Tooth Element</th><th>Dental LT</th><th>Duran</th><th>Durasoft</th></tr>
<tr><td>Left First Molar</td><td>≈ 11,47</td><td>11,55</td><td>11,88</td></tr>
<tr><td>Left Second Molar</td><td>8,94</td><td>8,98</td><td>8,98</td></tr>
<tr><td>Right First Molar</td><td>9,72</td><td>9,80</td><td>10,28</td></tr>
<tr><td>Right Second Molar</td><td>14,88</td><td>15,13</td><td>15,13</td></tr>
<tr><td>Left Canine</td><td>1,86</td><td>1,86</td><td>2,16</td></tr>
<tr><td>Left Incisors</td><td>1,15</td><td>1,15</td><td>1,22</td></tr>
<tr><td>Right Canine</td><td>1,71</td><td>1,71</td><td>1,71</td></tr>
<tr><td>Right Incisors</td><td>2,57</td><td>2,53</td><td>2,42</td></tr>
</table>
</td>
</tr>
</table>

<table>
<tr>
<td></td>
<td>342 MPa, and tensile strength of 211 MPa.

Note:
To create the dental aligners, mandibular scans of a patient’s dentition were obtained using a 3Shape E1 laboratory scanner equipped with a blue multiline LED, achieving a precision of 10–12 µm based on the patient’s actual teeth. The resulting STL file was processed in Maestro Studio CAD/CAM software to generate the initial CAD model. Additional steps included marking missing teeth, measuring individual teeth, identifying the ideal arch length, and verifying the need for interproximal reduction, followed by detailed point-to-point plotting for aligner design.</td>
<td>stress compared to previous results.
The relevant material properties for nonlinear analysis were then defined for each respective material. A static nonlinear analysis was performed, simulating a bite force pattern applied over a 30-second period on the 3D models of Duran, DuraSoft, and Dental LT aligners, distributed across 8 different sections that broadly covered the entire mandible.</td>
<td></td>
</tr>
<tr>
<td>Koenig et al.,, 2022 United States of America (English)</td>
<td>Group 1 (G1): Thermoformed orthodontic aligners fabricated from polyurethane Zendura FLX™ sheets (Zendura Dental, Fremont, CA, USA), with a thickness of 0.75 mm. The aligners were molded using the Biostar® thermoforming machine (Scheu-Dental GmbH, Iserlohn, Germany), following the manufacturer's recommendations. N = 12 samples.

Group 2 (G2): Thermoformed orthodontic aligners fabricated from polyethylene terephthalate copolyester Essix ACE™ sheets (Dentsply Sirona, Sarasota, FL, USA), with a thickness of 0.75 mm. The</td>
<td>Alignment and Precision Measurement Process
The STL file of the maxillary dental arch was imported into the metrology software Geomagic® Control X™ (3D Systems, Morrisville, NC, USA) and selected as the reference model. Subsequently, the STL files obtained from intraoral scans of the aligners were individually imported and superimposed onto the STL files of the maxillary dental arch. For this procedure, the best-fit alignment algorithm was used, which adjusts the</td>
<td>Average Absolute Discrepancies (in mm) Between the Master STL Mesh and the Aligner Type at Specific Reference Points and General Discrepancies (RMS)
<table><tr><th>Reference Point</th><th></th><th>Zendura FLX
Mean ± SD</th><th>95% CI</th></tr><tr><td rowspan="3">Incisal/Occlusal</td><td>MI</td><td>0.165 ± 0.136</td><td>0.104–0.247</td></tr><tr><td>PG</td><td>0.260 ± 0.089</td><td>0.217–0.316</td></tr><tr><td>ML</td><td>0.199 ± 0.103</td><td>0.147–0.254</td></tr><tr><td rowspan="3">Crown Center</td><td>FACC</td><td>0.211 ± 0.113</td><td>0.155–0.273</td></tr><tr><td>MP</td><td>0.126 ± 0.138</td><td>0.064–0.213</td></tr><tr><td>BP</td><td>0.250 ± 0.167</td><td>0.164–0.356</td></tr><tr><td rowspan="4">Gingival</td><td>GZ</td><td>0.076 ± 0.057</td><td>0.047–0.107</td></tr><tr><td>HP</td><td>0.117 ± 0.142</td><td>0.055–0.203</td></tr><tr><td>MC</td><td>0.224 ± 0.222</td><td>0.119–0.357</td></tr><tr><td>RMS</td><td>0.188 ± 0.074</td><td>0.151–0.229</td></tr></table>Average Absolute Discrepancies (in mm) Between the Master STL Mesh and the Aligner Type at Specific Reference Points and General Discrepancies (RMS)</td>
</tr>
</table>

aligners were molded using the Biostar® thermoforming machine (Scheu-Dental GmbH, Iserlohn, Germany), according to the manufacturer's instructions. *N = 12 samples.*

Group 3 (G3): Passive aligners manufactured from UV-curable Tera Harz TC-85DAP resin, digitally designed with a thickness of 0.5 mm, printed using the SprintRay Pro 3D printer, and post-cured with the Cure-M unit (Graphy Inc., Seoul, South Korea), according to the manufacturer's recommendations. *N = 12 samples.*

Note:

The STL file was based on a maxillary arch presenting a 3 mm discrepancy between tooth size and arch length. For Groups 1 and 2, the STL file was adapted using MeshMixer software (Autodesk, San Rafael, CA, USA) in a horseshoe format, and models were horizontally printed using the SprintRay Pro printer (DLP technology, SprintRay, Los Angeles, CA, USA) with photo-initiated methacrylate resin (SprintRay Die and Model Gray; flexural modulus: 1.8 GPa; flexural strength: 70.1 MPa). Layer thickness was set to 50 µm. Post-processing included two baths of 99.5% isopropyl alcohol for five minutes each, followed by post-curing in the Procure® unit (SprintRay). For Groups 1 and 2, after fabrication, aligners were

meshes to minimize the distance between data points.

Linear distances between the aligner scan meshes and the STL meshes of the maxillary arch were measured at three bilateral landmarks located on the incisal/occlusal portions of the teeth. The analyzed points were as follows:

Incisal/Occlusal Points:

MI**:** Midpoint of the incisal edge of the lateral incisors.

PG**:** Midpoint in the central groove of the second premolars.

ML**:** Tips of the mesiolingual cusps of the first molars.

Intermediate Points:

BP**:** Midpoint on the palatal surfaces of the first premolars.

MC**:** Central point at the gingival margin of the first molars.

Gingival Points:

GZ**:** Zenith point located at the gingival margins of the central incisors.

HP**:** Highest point on the palatal-gingival margin of the first premolars.

BP**:** Buccal fossae of the second molars.

These points were used to measure the accuracy of mesh

Reference Point		Essix ACE Mean ± SD	95% CI
Incisal/Occlusal	MI	0.206 ± 0.153	0.130–0.300
	PG	0.384 ± 0.206	0.285–0.511
	ML	0.433 ± 0.367	0.250–0.648
Crown Center	FACC	0.207 ± 0.087	0.162–0.252
	MP	0.255 ± 0.265	0.128–0.400
	BP	0.457 ± 0.350	0.124–0.323
Gingival	GZ	0.188 ± 0.271	0.088–0.352
	HP	0.213 ± 0.199	0.250–0.655
	MC	0.436 ± 0.422	0.220–0.676
	RMS	0.209 ± 0.094	0.167–0.263

Average Absolute Discrepancies (in mm) Between the Master STL Mesh and the Aligner Type at Specific Reference Points and General Discrepancies (RMS)

Reference Point		3D Printed Mean ± SD	95% CI
Incisal/Occlusal	MI	0.144 ± 0.043	0.091–0.136
	PG	0.072 ± 0.035	0.054–0.091
	ML	0.113 ± 0.033	0.096–0.131
Crown Center	FACC	0.162 ± 0.055	0.131–0.192
	MP	0.190 ± 0.043	0.167–0.214
	BP	0.102 ± 0.047	0.077–0.127
Gingival	GZ	0.079 ± 0.054	0.051–0.110
	HP	0.224 ± 0.041	0.201–0.246
	MC	0.107 ± 0.055	0.080–0.139
	RMS	0.140 ± 0.020	0.130–0.151

Statistical Significance Levels of Permutation t-tests Comparing the Fit of Aligners at Specific Anatomical Landmarks and General Discrepancies (RMS)

Reference Point		Zendura FLX	Essix ACE	3D Printed
Incisal/Occlusal	MI	0.2424	0.0436*	0.5000
	PG	0.0040*	0.0004*	0.0620
	ML	0.0096*	0.0008*	0.0420*
Crown Center	FACC	0.8916	0.0820	0.0752
	MP	0.1492	0.1488	0.4676
	BP	0.0052	0.0004*	0.0716
Gingival	GZ	0.0704	0.0096*	0.1464
	HP	0.0096*	0.0008*	0.0420*

	removed from the models, trimmed approximately 1 mm beyond the gingival margins, and sprayed with CAD/CAM spray (Yeti Dental, GmbH, Engen, Germany). A Trios 3 intraoral scanner (3Shape, Copenhagen, Denmark) was used to scan the inner surface of the thermoformed aligners. The digital scans were post-processed using Trios 3Shape software and converted into STL files. Group 3 aligners were digitally designed in MeshMixer with a thickness of 0.5 mm, extending 1 mm above the gingival margin, and sprayed with CAD/CAM spray prior to scanning. Samples were scanned using a 3Shape E3 laboratory scanner, and the resulting data were processed into STL format.	superimposition, allowing for the assessment of the precision of the aligner scan relative to the maxillary dental arch.	MC 0.0052 0.0004* 0.0716 RMS 0.0332* 0.0044* 0.5644 Significant differences according to the permutation t-test ($p \leq 0.05$, permuted 5,000 times).

Koletsi *et al.,*, 2022 Switzerland (English)	**Group 1 (G1):** Invisalign® CON: Invisalign® aligners, manufactured by Align Technology, San Jose, CA, USA, fabricated using SmartTrack material. Not used by patients. *N = 12 samples.* **Group 2 (G2):** Invisalign® Used: Invisalign® aligners, manufactured by Align Technology, San Jose, CA, USA, fabricated using SmartTrack material. Retrieved after 7 days of intraoral use by patients. *N = 12 samples.* **Group 3 (G3):** 3D-printed CON: Aligners printed in 3D using TC-85DAC resin (Graphy, Seoul, South Korea), fabricated with the Moonray S100 3D printer (Sprintray, Los Angeles, CA, USA). Not used by patients. *N = 12 samples.* **Group 4 (G4):** 3D-printed Used: Aligners printed in 3D using TC-85DAC resin (Graphy, Seoul, South Korea), fabricated with the Moonray S100 3D printer (Sprintray, Los Angeles, CA, USA). Retrieved after 7 days of intraoral use by patients. *N = 12 samples.* **Note:** All patients followed the same hygiene regimen and aligner care instructions. They were instructed to wear the aligners for more than 20 hours per day and to brush them once daily. The 3D printed aligners were fabricated in successive layers with a nominal thickness	**Optical Profilometry** A small area of approximately 4 × 4 mm was excised using a scalpel from the lingual surface of the central incisor region, and the internal side (which was in contact with the tooth) was analyzed. An optical profilometer (Wyko NT-1100, Tucson, AZ, USA) equipped with a nominal 20x magnification lens was used. The acquisition area was a rectangle measuring 231 × 303 µm. To eliminate the effect of waviness, a Gaussian regression filter was applied with a short-wavelength cutoff of 0.025 mm, and the following surface roughness parameters were determined: ● Arithmetic mean deviation (Sa); ● Root mean square deviation (Sq); ● Maximum surface height (Sz); ● Core void volume indicating the surface volume (Sc); ● Surface void volume (Sv). The bearing area curve was plotted by sweeping a horizontal plane from the highest peak to the deepest valley across the surface.	**Descriptive Statistics for Roughness Parameters for All Tested Groups (n = 12 in All Groups)** **Roughness Parameter** | **Invisalign CON Median,(IQR)** | **Invisalign Used** | **3D Printed CON** | **3D Printed Used** Sa (nm) | 124 (106–143) | 131 (104–164) | 54 (36–66) | 295 (264–464) Sq (nm) | 182 (161–200) | 203 (166–247) | 138 (77–162) | 499 (373–822) Sz (nm) | 3671 (2981–5260) | 9002 (3452–12.153) | 5995 (4192–8414) | 12.842 (10.656–20.836) Sc (nm³/nm²) | 204 (174–247) | 219 (168–261) | 66 (49–96) | 425 (394–597) Sv (nm³/nm²) | 20 (17–22) | 22 (12–34) | 13 (7–18) | 62 (40–113) IQR = Interquartile Range **Quantile Regression for the Examined Roughness Parameters (n = 48) (Part 1)** **Predictor Variables** | | **Coefficient β** | **95% CI** | **P Valor** | | **Sa (nm)*** | | Control | Invisalign | Reference | | | 3D Printed | -67 | -147 a 12 | 0.10 Used | Invisalign | Reference | | | 3D Printed | 169 | 89-248 | <0.001 | | **Sq (nm)*** | | Control | Invisalign | Reference | | | 3D Printed | -46 | -208 a 117 | 0.57 Used | Invisalign | Reference | | | 3D Printed | 315 | 152 a 477 | <0.001 | | **Sz (nm)⁺** | | Material | Invisalign | Reference | | | 3D Printed | 2739 | -1043 a 6520 | 0.15 Uso intra oral | Não | Reference | | | Sim | 5660 | 1879 a 9441 | 0.004 | | **Sc (nm³/nm²)*** | | Control | Invisalign | Reference | | | 3D Printed | -149 | -251 a -47 | 0.005 Used | Invisalign | Reference | | | 3D Printed | 233 | 131 a 335 | <0.001 | | **Sv(nm³/nm²)*** | | Control | Invisalign | Reference | | | 3D Printed | -6 | -32 a 19 | 0.63 Used | Invisalign | Reference | | | 3D Printed | 43 | 17-68 | 0.002 **Quantile Regression for the Examined Roughness Parameters (n = 48) (Part 2)** **Predictor Variables** | | Coefficient β | **95% CI** | **p-value** | | **Sa (nm)*** | | Invisalign | Control | Reference | |

	of 100 µm over 70 minutes, using 405 nm blue-violet light and digital light processing (DLP) technology. Excess resin was removed via centrifugation for 4 minutes. The aligners were then post-cured for 12 minutes on both the cervical and incisal sides in a Cure M post-curing unit (Graphy, Seoul, South Korea).		Used 12 -68 a 91 0.77 3D Aligner Control Reference Used 248 168 a 327 <0.001 **Sq (nm)*** Invisalign Control Reference Used 25 -138 a 187 0.76 3D Aligner Control Reference Used 385 223 a 548 <0.001 **Sc (nm^3/nm^2)*** Invisalign Control Reference Used -9 -110 a 93 0.87 3D Aligner Control Reference Used 373 271 a 475 <0.001 **Sv(nm^3/nm^2)*** Invisalign Control Reference Used 7 -19 a 32 0.59 3D Aligner Control Reference Used 56 30-81 <0.001 **Key Findings:** Strong evidence was found that intraoral use of 3D printed aligners was associated with an increase in all tested parameters (P < 0.001). Significant differences were observed when comparing recovered 3D printed aligners and the corresponding Invisalign® aligners in all parameters except Sz. The 3D printed aligners exhibited considerably higher values in the roughness parameters.
Kuntz *et al.*, 2024 France (English)	**Group 1 (G1):** Eighteen Invisalign® aligners, manufactured by Align Technology Inc., San Jose, California, USA. The material used was based on the SmartTrack™ system, derived from polyurethane with additives. The average thickness of the aligners was 0.75 mm. **Group 2 (G2):** Eighteen Suresmile® aligners, manufactured by Dentsply Sirona Inc., Charlotte, North Carolina, USA. The material used for fabrication was Essix™ ACE, a PET-G derivative. The average thickness of the	**Aligner Aging** Each aging cycle consisted of 20 seconds in a cold bath followed by 20 seconds in a hot bath. Considering the clinical recommendation to replace aligners every 14 days, aging of the samples was monitored for a maximum period of 14 days. Aging intervals of 1, 5, 7, 10, and 14 days corresponded to 50, 250, 350, 500, and 700 cycles, respectively. Each aging group consisted of 3 Accusmile® aligners, 3	**Young's Modulus at D0 in N** **Day** **Brand** **Elastic Modulus (GPa)** **Statistical Difference** D0 Accusmile® 7,38 ± 1,83 Different from Angel® and Invisalign® D0 Angel® 3,4 ± 1,05 Different from Accusmile® D0 Invisalign® 3,81 ± 1,29 Different from Accusmile® **Young's Modulus at D14 in N** **Day** **Brand** **Elastic Modulus (GPa)** **Statistical Difference** D14 Accusmile® 7,33 ± 1,93 Higher than Angel®, Invisalign®, Suresmile® D14 Angel® 3,15 ± 0,39 Lower than Accusmile®, GRAPHY®, Suresmile® D14 Invisalign® 4,6 ± 9,84 Lower than Accusmile®, GRAPHY® D14 Suresmile® 4,63 ± 1,98 Lower than Accusmile®, GRAPHY® D14 GRAPHY® 6,0 Lower than Accusmile® **Yield Strength (YS) (in N) and Maximum Elastic Stress MES (in MPa)** **Day** **Brand** **Value** **Statistical Differences** **Observations**

	aligners was 0.8 mm. **Group 3 (G3):** Eighteen Angel® aligners, manufactured by AngelAligner®, China. The material used was a three-layer thermoplastic composite. The average thickness of the aligners was 0.75 mm. **Group 4 (G4):** Eighteen Accusmile/Fas® aligners, manufactured by Forestadent Bernhard Foerster GmbH, Pforzheim, Germany. The material used was PET-G. The average thickness of the aligners was 0.8 mm. **Group 5 (G5):** Eight GRAPHY® aligners, manufactured by Graphy Inc., Seoul, Republic of Korea. The material used for direct 3D printing was Tera Harz TC-85, a shape-memory polymer. The average thickness of the aligners was 0.75 mm. **Note:** Each aligner was sectioned into five parts: anterior and lateral portions (for tensile testing), and segments from the second molars (for microscopic examination using a scanning electron microscope).	Angel® aligners, 1 GRAPHY® aligner, 3 Invisalign® aligners, and 3 Suresmile® aligners, except for groups D7 and D14, which included 2 GRAPHY® aligners. **Tensile Tests** Uniaxial tensile tests were performed using the LLOYD Instruments® LRX Plus traction dynamometer (Technical Engineering Hall, School of Dentistry, University of Lorraine, Nancy, France). The cut samples were fixed between the two ends of the machine, which applied a tensile force at a speed of 5 mm/min for 4 minutes or until rupture, using a 2 kN force sensor at a constant temperature of 20 °C. At the end of the test, each sample was ruptured, and a second measurement to evaluate method error could not be performed. Each aging group (D1, D5, D7, D10, and D14) was compared to the control group D0. The variables evaluated to determine the mechanical strength of the materials were: a) Young's Modulus (E), expressed in GPa. b) Yield Strength (YS), expressed in N, and Maximum Elastic Stress (MES), expressed in MPa.	**(MPa)** D0 Accusmile® 70,59 ± 18,8^{AB} — Higher than Angel® and Invisalign® — Highest YS among the brands D0 Angel® 52,9 ± 5,53^{A} — Lower than Accusmile® — Lowest YS along with Invisalign® D0 Invisalign® 51 ± 7,13^{B} — Lower than Accusmile® — Lowest YS along with Angel® D14 Angel® 42,97 ± 6,87 — Significant reduction from day 5 (P = .003) — Aging affected the resistance The Yield Strength (YS) did not show significant differences between Accusmile®, GRAPHY®, Invisalign®, and Suresmile® over the days, with P-values of .38, .93, .89, and .05, respectively. **Ultimate Tensile Strength (UTS) (in N)** Accusmile® 386.4 ± 56.58 Angel® 203 ± 27.22 Invisalign® 170 ± 82.74 Suresmile® 259.5 ± 26.46 GRAPHY® 261.8 ± 54.5 No statistically significant differences were observed within each group between D0 and subsequent days. **Scanning Electron Microscopy (SEM) Observations** The surface conditions of the Accusmile®, Angel®, Invisalign®, and Suresmile® aligners were relatively homogeneous at D0. However, at D14, a more abrasive surface condition was observed, with scratches, porosities, tearing phenomena, and even more significant cracks. In contrast, the directly printed GRAPHY® aligners showed material application lines corresponding to the printing technique, as well as deposits that seemed to peel off the surface. These deposits were heterogeneous and of the same composition as the aligner material. By D14, the deposits had disappeared, but cracks were observed crossing the aligner surface.

<table>
<tr>
<td></td>
<td></td>
<td>c) Ultimate Tensile Strength (UTS), expressed in N, and Maximum Stress (MS), expressed in MPa.

Scanning Electron Microscopy (SEM) Sample Preparation:

● Cleaning with ethanol: removal of impurities and dehydration.
● Ultrasonication: removal of residual contaminants.
● Drying: complete drying of the samples.
● Gold sputter-coating: to render the samples conductive.

Observations were carried out using the JEOL JSM-6010LA Analytical Scanning Electron Microscope at the Jean Lamour Institute, Campus Artem, Nancy, France. Observations were performed at an accelerating voltage of 10 kV, with 50× magnification to evaluate surface condition, in addition to systematic magnifications of 250×, 500×, 1000×, and 2500×.</td>
<td></td>
</tr>
<tr>
<td>Lee et al.,, 2022 South Korea (English)</td>
<td>Group 1 (G1): Thermoformed aligners fabricated from PETG (Easy-Vac Gasket, 3A MEDES, Korea), with a thickness of 0.75 mm. The aligners were vacuum thermoformed over a standardized model using the Thermoformingcaster (Ministar</td>
<td>Static Mechanical Property Test (Tensile Test)
Dogbone-shaped specimens (3.2 × 9.5 mm) were prepared for static mechanical testing in accordance with</td>
<td>Thickness Change
<table>
<tr><th>Parameter</th><th>Material</th><th>Average Thickness After Process (mm)</th><th>Variation Relative to Initial Thickness</th></tr>
<tr><td>Thermoforming</td><td>PETG</td><td>0,41</td><td>54.7% of initial thickness (0.75 mm)</td></tr>
<tr><td>3D Printing</td><td>TC-85</td><td>0,56</td><td>12% above the defined thickness (0.5 mm)</td></tr>
</table>
</td>
</tr>
</table>

	S, Scheu-Dental GmbH, Germany), following the manufacturer's recommended conditions. *N = 10 samples.* **Group 2 (G2):** Three-dimensionally printed aligners fabricated using GR30860 and GR3060 resins (TC-85, Graphy Inc., Korea), which are oligomeric resins containing bis(2,4,6-trimethylbenzoyl)-phenylphosphine oxide (Irgacure 819, BASF, Germany) as photoinitiator. Specimens were designed according to specific physical evaluation standards for each test, with a defined thickness of 0.5 mm. The printing angle was set at 90° relative to the horizontal plane to ensure that the support structures were placed only on the sides of the specimens. Aligners were printed using a DLP-type 3D printer (Uniz 4K, Uniz, USA), with a layer thickness of 100 µm. Residual liquid resin was removed from the surface of the specimens using a soft scraper, and the specimens were photo-cured twice for 25 minutes under nitrogen (N_2), using UV light (wavelength: 385–405 nm) in a post-curing chamber (CureM U102H, Graphy Inc., Korea). *N = 10 samples.*	ASTM D638-5. Six specimens per group were subjected to static tensile testing at 25 °C and 55% humidity using a universal testing machine (AllroundLine Z010, 2 kN load cell, Zwick, Germany). The crosshead speed was set at 5 mm/min, and each specimen was elongated at a constant rate until complete fracture. The static mechanical properties of each material were evaluated by comparing yield strength and elastic modulus using the Mann-Whitney test with statistical software (IBM SPSS Statistics for Windows, version 20.0, IBM Co., USA). **Thermomechanical Cycling Property Test (Stress Relaxation and Creep Test)** Specimen dimensions for thermomechanical cycling and DMA tests were defined considering the maximum drive motor capacity of the DMA equipment (Q800, TA Instruments, USA), which is 18 N: 3 × 10 mm for PETG and 5 × 10 mm for TC-85. Three specimens were tested for each material. Repetitive creep behavior and stress relaxation of	**Static Mechanical Properties** **Property** / **Material** / **Value** / **Deformation (%)** / **Observations** Yield Strength / PETG / 44,20 MPa / 3,92* / TC-85 / 32,31 MPa / 4,65* / Significant statistical difference ($p < 0.01$) Elastic Modulus / PETG / 1479,54 MPa / — / Significantly higher stiffness ($p < 0.01$) TC-85 / 1186,40 MPa / — Elongation to Fracture / PETG / — / 232,93 TC-85 / — / 62,55 **Thermomechanical Cycle Properties** **Property** / **Temperature** / **Material** / **Initial Static Force (N)** / **Stress Relaxation** / **Strain Recovery** / **Observations** Stress Relaxation and Creep / 37 °C / TC-85 / 18,00 / Rapid, decreasing to 1.0 N / Increased with repeated cycles / Residual force increased; recovery rate improved with cycles PETG / 13,00 / Gradual, decreasing to 11.3 N / Instant recovery of 80%; 20% gradual / Recovery rate and residual force increased slightly Stress Relaxation and Creep / 80 °C / TC-85 / 0,13 / Minimal decay / Constant recovery even with repeated cycles / Residual static force remained constant PETG / 0,12 / Rapid, decreasing to 0.01 N / Gradual recovery / Residual static force increased; post-recovery tension negative

		each material were assessed using DMA in stress relaxation mode. As the mechanical behavior of materials changes dynamically around the glass transition temperature (Tg), two experimental temperatures were selected through preliminary tests: 37 °C, to mimic the oral cavity temperature, and 80 °C, to simulate the temperature of hot food or beverages. A cycle of 1% elongation for 60 minutes followed by 60 minutes of recovery was repeated 13 times. Stress relaxation and strain recovery patterns over time were evaluated. **Dynamic Mechanical Analysis (Temperature Sweep Test)** Three specimens were tested per material. To investigate the thermal dynamics of each material, DMA was performed from −30 °C to 130 °C using tensile mode, with a frequency of 1 Hz and strain rate of 0.1%. The heating rate was set at 5 °C/min. Storage modulus, loss modulus, and loss tangent were recorded as a function of temperature. **Shape Memory Property**	**DMA** **Property** / **Parameter** / **Material** / **Value** / **Observations** DMA (37 °C) / Storage Modulus / TC-85 / 713,60 MPa / More viscous behavior compared to PETG PETG / 1262 MPa / More solid behavior Loss Modulus / TC-85 / 111,60 MPa PETG / 5,58 MPa Loss Tangent (tan δ) / TC-85 / 0,16 / Tg defined as the peak of the loss tangent PETG / 0,004 Glass Transition Temperature (Tg) / TC-85 / 69,45 °C PETG / 101,8 °C **Shape Memory Property** **Property** / **Material** / **Initial Condition** / **Strain Recovery** / **Observations** Shape Memory Property / TC-85 / Bent at 80 °C / 50% in 1 min, 90% in 10 min, 96% in 60 min / Recovered shape over time at 37 °C PETG / Bent at 80 °C / 0% / Remained deformed, no shape recovery **Effect of Shape Memory and Shape Recovery Rate Over Time for TC-85** **Elapsed Time** / **0** / **10 sec.** / **30 sec.** / **1 min.** / **5 min.** / **10 min.** / **60 min.** Curvature Angle (°) / 177.00 ± 3.92 / 146.27 ± 3.92 / 107.23 ± 7.05 / 79.43 ± 6.45 / 31.53 ± 5.48 / 20.32 ± 5.49 / 6.90 ± 2.68 Shape Recovery Rate (%) / 17.36 ± 2.06 / 17.36 ± 2.06 / 39.42 ± 3.90 / 39.42 ± 3.90 / 82.19 ± 3.09 / 88.52 ± 3.10 / 96.11 ± 1.50

		Test Specimens for the shape memory property test were prepared as rectangular strips measuring 10 × 50 mm. The average specimen thickness was determined by measuring thickness at three points (center and both ends) with a digital caliper (GAU-178.00, Eurotool, Inc., USA). A bending test was chosen to qualitatively investigate and directly visualize this property. A U-shaped mold was prepared and standardized for this purpose. The central axis of the mold measured 4 mm. Specimens were bent into a U-shape using the mold at 80 °C—above the Tg of TC-85—and held in this position for 5 minutes. The bent specimens were then rapidly cooled to 24 °C and held for another 5 minutes. After removal of the external force, the initial bending angle (θ_initial) of each specimen was recorded. The specimens were then immersed in a water bath at 37 °C, and their shape recovery was recorded on video at 30 FPS for 1 hour. The initial bending angle (θ_initial) and the bending angle (θ_t) at 10 s, 30 s, 1 min, 5 min, 10	

<table>
<tr>
<td></td>
<td></td>
<td>min, and 60 min were measured using software (GeoGebra, Markus Hohenwarter). The shape recovery rate at 37 °C was also determined using the same program.</td>
<td></td>
</tr>
<tr>
<td>Park et al.,, 2023 South Korea (English)</td>
<td>Group 1 (TS): Single-layer thermoformed aligners fabricated from PETG sheets produced by Scheu-Dental, Iserlohn, Germany, with a thickness of 0.75 mm. N = 10 samples.

Group 2 (TM): Multilayer thermoformed aligners composed of copolyester outer layers and a thermoplastic elastomeric core, produced by Scheu-Dental, Iserlohn, Germany, with a thickness of 0.75 mm. N = 10 samples.

Group 3 (PA): 3D-printed aligners fabricated from photopolymerizable polyurethane resin (TC-85), cleaned using 99.5% isopropyl alcohol for 1 minute, with a thickness of 0.5 mm. N = 10 samples.

Group 4 (PC): 3D-printed aligners fabricated from photopolymerizable polyurethane resin (TC-85), cleaned using centrifugation at 500 rpm for 6 minutes, with a thickness of 0.5 mm. N = 10 samples.

Note:
A standardized model of the maxillary dental</td>
<td>Thickness and Gap Measurement Method Using Micro-CT
Thermoformed aligners were immediately fitted onto the standardized model at room temperature, while 3D-printed aligners were inserted after being gently immersed in warm water at 80 °C, following the manufacturer’s clinical protocol. The 3D-printed samples were then dried at 37 °C to restore their original shape and strength. All aligners were scanned using a high-resolution micro-CT scanner (Skyscan1173, Bruker, MA, USA) at 40 kV, 200 µA, and a resolution of 34.9 µm. A total of 40 micro-CT scans were obtained. The target dental areas (anterior teeth: maxillary right central incisor and canine; posterior teeth: maxillary right first premolar and molar) were reoriented using Dataviewer software (version 1.5.6.2, Bruker, MA, USA). Slices were obtained using a horizontal plane based on</td>
<td>Median Thickness and Gap Width for Aligners Using Different Manufacturing Protocols
<table>
<tr><th></th><th colspan="4">Median (IQR) (µm)</th><th></th><th></th></tr>
<tr><th>Variable</th><th>TS (n = 10)</th><th>TM (n = 10)</th><th>PA (n = 10)</th><th>PC (n = 10)</th><th>p-value</th><th>Post-hoc</th></tr>
<tr><td>Thickness (µm)</td><td>504,68 (460,68–558,40)</td><td>509,54 (467,66–548,80)</td><td>614,24 (559,27–687,53)</td><td>687,53 (639,54–749,48)</td><td>0,001*</td><td>PC > PA > TS, TM</td></tr>
<tr><td>Gap Width (µm)</td><td>69,80 (0–115,17)</td><td>52,35 (0–89,87)</td><td>69,80 (17,45–107,32)</td><td>69,80 (34,90–131,75)</td><td>0,001*</td><td>PA, PC > TM</td></tr>
</table>
*The p-values were calculated using the Kruskal-Wallis test, followed by post-hoc comparisons using the Mann-Whitney U test with a Bonferroni adjustment for the alpha level. p < 0.01

● No significant difference in gap width was observed between the TS and TM groups.

Median Translucency Parameter for CAs Using Different Manufacturing Protocols
<table>
<tr><th>Variable</th><th>TS (n = 10)</th><th>TM (n = 10)</th><th>PA (n = 10)</th><th>PC (n = 10)</th><th>p-value</th><th>Post-hoc</th></tr>
<tr><td>Translucency Parameter</td><td>67,82 (67,64–68,05)</td><td>66,15 (65,84–66,45)</td><td>10,76 (9,17–15,81)</td><td>66,19 (65,44–66,36)</td><td>0,001*</td><td>TS, PC, TM > PA</td></tr>
</table>
*The p-values were calculated using the Kruskal-Wallis test for multiple comparisons, followed by post-hoc comparisons using the Mann-Whitney U test with a Bonferroni adjustment for the alpha level. p < 0.01

Group Comparisons for Median Thickness Depending on Tooth Type and Location
<table>
<tr><th></th><th colspan="4">Median (IQR)(µm)</th></tr>
<tr><th>Tooth Type/Location</th><th>TS (n = 10)</th><th>TM (n = 10)</th><th>PA (n = 10)</th><th>PC (n = 10)</th></tr>
<tr><td>Anterior Tooth</td><td>537.46 (451.08–588.94</td><td>518.27 (460.68–563.64)</td><td>668.34 (621.22–759.08)</td><td>710.22 (670–95-770.42)</td></tr>
<tr><td>Posterior Tooth</td><td>499.07 (464.17–544.44</td><td>509.54 (467.66–548.80)</td><td>568.87 (533.97–613.37)</td><td>654.38 (615.11–727.67)</td></tr>
<tr><td>p-value</td><td>0.021*</td><td>0.639</td><td>0.001**</td><td>0.001**</td></tr>
<tr><td>Post-hoc</td><td>Anterior > Posterior</td><td></td><td>Anterior > Posterior</td><td></td></tr>
<tr><td>Gingival palate</td><td>513.03 (488.60–547.06)</td><td>516.52 (499.07–543.57)</td><td>588.07 (547.93–660.48)</td><td>673.57 (652.63–721.56)</td></tr>
<tr><td>Palatine</td><td>551.42 (502.56–</td><td>547.93 (505.18–</td><td>615.99 (560.15–</td><td>689.28 (615.11–</td></tr>
</table>
</td>
</tr>
</table>

	arch of Korean adults with normal occlusion (CON2001-UL-SP-FEM-32, Nissin Dental, Kyoto, Japan) was scanned using an intraoral scanner (D250, 3Shape, Copenhagen, Denmark) to generate an STL file. Based on this file, a standardized model with dimensions of 60 mm × 50 mm × 20 mm was printed using a DLP 3D printer (Asiga MAX™, Asiga, Alexandria, Australia) (S-100, Graphy Inc., Seoul, South Korea). For thermoformed aligners, a uniform base was created to ensure constant model height relative to the teeth. The model was centered on the platform with the mid-palatal suture aligned at the 12 o'clock position. This orientation was maintained throughout the thermoforming process. After fabrication, the aligners were removed and the gingival margins were trimmed and polished. The 3D-printed aligners were designed using computer-aided design software (Deltaface, Coruo, Limoges, France), with a thickness of 0.5 mm, an offset of 50 µm, and positioned at a 30° angle for minimal tilt and reduced support. Printing was performed using a DLP 3D printer (SprintRay Pro 95, SprintRay, Los Angeles, CA) with a layer thickness of 50 µm. After printing, the samples were post-cured twice for 25 minutes under nitrogen and UV light (385–405 nm) in a post-curing chamber (CureM U102H, Graphy Inc., Seoul, South	the model's base and perpendicular to the line connecting the mesial and distal contact points of each tooth. These were saved by applying a volume of interest (VOI). The images were analyzed using CTAn software (version 2.5, Bruker, MA, USA) at 300× magnification. Minimum thickness and gap width were measured by projecting a perpendicular line from each reference point tangent. A total of 960 measurement points on the tooth surfaces were included. **Translucency Measurement Method Using a Spectrophotometer** A spectrophotometer (CM-3500d, Konica Minolta, Tokyo, Japan) was used to calculate the CIELab coordinates of specimens placed against white and black backgrounds. The spectrophotometer aperture size was 3 mm, and 10 samples with a 3 mm diameter were prepared from thermoformed specimens (0.75 mm thickness) and 3D-printed specimens (0.5 mm thickness). **3D Gap Visualization** Using 3D Slicer software (version 5.0.3,	595.92) Incisal/Occlusal: 588.07 (560.43–606.97); 550.26 (527.86–579.34); 706.15 (636.35–793.10); 763.15 (716.32–789.61) vestibule: 474.64 (453.70–498.20); 471.15 (457.19–506.05); 579.34 (538.33–629.07); 645.65 (614.24–676.19) Gingival vestibule: 443.23 (429.27–445.85); 453.70 (419.67–478.13); 610.75 (541.82–663.10); 694.51 (652.63–749.48) p-value: 0.001**; 0.001**; 0.001**; 0.001** Post-hoc: *Bg < Bu < Pg < Pa < In/Oc*; *Bg < Bu < Pg < Pa,In/Oc*; *Bu,Pg,Bg < Pa < In/Oc* P values were calculated using the Mann–Whitney U test for comparisons by tooth type. P values were calculated using the Kruskal–Wallis test for multiple comparisons by tooth location, followed by post hoc comparisons using the Mann–Whitney U test with a Bonferroni adjustment of the alpha level. *p < 0.05; **p < 0.01. **Group Comparisons for Median Gap Width Depending on Tooth Type and Location** **Mediana (IQR)(µm)** Tooth Type/Location: **TS (n = 10)**; **TM (n = 10)**; **PA (n = 10)**; **PC (n = 10)** Anterior Tooth: 73.29 (0–122.15); 62.82 (0–102.96); 76.78 (24.43–115.17); 71.55 (0–162.29) Posterior Tooth: 69.80 (17.45–95.98); 45.37 (0–69.80); 63.41 (2.62–94.23); 69.80 (45.37–118.37) p-value: 0.677; 0.045*; 0.079; 0.083 Post-hoc: Anterior > Posterior Gingival palate: 99.47 (69.80–145.71); 80.27 (21.81–134.37); 89.00 (21.81–189.33); 129.13 (69.80–233.83) Palatine: 94.23 (61.95–124.77); 68.06 (34.90–107.32); 48.86 (0–99.47); 80.27 (59.33–135.24) Incisal/Occlusal: 105.87 (73.29–135.82); 74.46 (52.35–105.86); 55.84 (0–76.78); 40.72 (0–114.88) vestibule: 0 (0–17.45); 0 (0–17.45); 52.35 (19.20–75.04); 38.39 (0–61.95) Gingival vestibule: 8.73 (0–67.18); 17.45 (0–69.8); 115.17 (81.14–164.03); 99.47 (69.80–172.76) p-value: 0.001**; 0.001**; 0.001**; 0.001** Post-hoc: *Bu,Bg < Pa,Pg,In/Oc*; *Bu,Bg < Pa,In/Oc,Pg*; *Pa < Bu,In/Oc < Pg,Bg*; *Bu,In/Oc < Pa,Bg,Pg* P values were calculated using the Mann–Whitney U test for comparisons by tooth type. P values were calculated using the Kruskal–Wallis test for multiple comparisons by tooth location, followed by post hoc comparisons using the Mann–Whitney U test with a Bonferroni adjustment of the alpha level. *p < 0.05; **p < 0.01.

	Korea). Final cleaning was performed with running water and ultrasonic treatment for 3 minutes at 76–80 °C.	http://www.slicer.org), micro-CT Digital Imaging and Communications in Medicine (DICOM) files of the central incisors were analyzed. Manual segmentation was performed to obtain 3D information on the space between the tooth and the aligners. Manually segmented regions of interest were rendered in 3D and exported as STL files. The STL files representing the gap width between the tooth and aligners were morphometrically compared using Geomagic Control X software (version 2018.0.1, 3D Systems, SC, USA).	

Sari, Turkey (English)	2024	**Group 1 (G1):** CA Pro thermoformed aligners + dry condition, no liquid exposure (control group). *N = 10 samples.* **Group 2 (G2):** CA Pro thermoformed aligners + orange juice, stored in an oven at 37 °C for 24 hours. *N = 10 samples.* **Group 3 (G3):** CA Pro thermoformed aligners + soy sauce, stored in an oven at 37 °C for 24 hours. *N = 10 samples.* **Group 4 (G4):** CA Pro thermoformed aligners + red wine, stored in an oven at 37 °C for 24 hours. *N = 10 samples.* **Group 5 (G5):** CA Pro thermoformed aligners + Coca-Cola, stored in an oven at 37 °C for 24 hours. *N = 10 samples.* **Group 6 (G6):** CA Pro thermoformed aligners + tea, stored in an oven at 37 °C for 24 hours. *N = 10 samples.* **Group 7 (G7):** CA Pro thermoformed aligners + coffee, stored in an oven at 37 °C for 24 hours. *N = 10 samples.* **Group 8 (G8):** Invisalign thermoformed aligners + dry condition, no liquid exposure (control group). *N = 10 samples.* **Group 9 (G9):** Invisalign thermoformed aligners + orange juice, stored in an oven	**Cyclic Loading Test** A Kistler 9272A dynamometer (Kistler Group, Winterthur, Switzerland), with an upper measurement limit of 400 N and a sensitivity of 0.001 N, was mounted on a perpendicular table. The experimental setup also included a Thorlabs LTS150/M device (Thorlabs, Inc., Newton, New Jersey, USA), capable of precise movement along the x, y, and z axes to determine deformation depth. This component of the mechanism consisted of a 0.8 mm diameter loading probe with a blunt tip. The tip of the loading probe was aligned with the central fossa of the tooth. A force was applied to the samples at a speed of 0.1 mm/s to reach a deformation depth of 1 mm. The force was applied to each sample 50 times, and the magnitude of the force required to achieve 1 mm deformation was recorded for the 1st, 5th, 10th, and 50th loading cycles for each specimen.	‘ **1st Load Force Values** **Aligner** | **Control** | **Orange Juice** | **Soy Sauce** | **Red Wine** | **Coca** | **Tea** | **Coffee** | ***p* (Ω)** **Mean ± SD** | **Mean ± SD** | **Mean ± SD** | **Mean ± SD** | **Mean ± SD** | **Mean ± SD** | **Mean ± SD** | **Mean ± SD** CA PRO: 34.15 ± 3.20^{Aa} | 31.33 ± 0.62^{Aa} | 31.37 ± 0.77^{Aa} | 31.35 ± 0.72^{Aa} | 31.34 ± 0.71^{Aa} | 31.36 ± 0.68^{Aa} | 31.29 ± 0.44^{Aa} | 0.167 INVISALIGN: 46.02 ± 1.00^{Ab} | 39.7 ± 0.84^{Bb} | 39.9 ± 0.33^{Bb} | 40.53 ± 1.27^{Ba} | 41.85 ± 0.84^{BCb} | 44.97 ± 0.46^{ACb} | 44.34 ± 0.92^{ACb} | 0.019* GRAPHY TC-85: 43.4 ± 0.38^{Ab} | 38.69 ± 0.41^{Bb} | 38.75 ± 0.20^{Bb} | 41.26 ± 0.77^{ABa} | 42.04 ± 0.22^{Ab} | 41.94 ± 0.16^{ABb} | 39.55 ± 0.16^{Bc} | 0.024* *p*(θ): 0.016* | 0.018* | 0.014* | 0.012* | 0.013* | 0.010* | 0.011* *The p-values were calculated using the Friedman test; θ, Kruskal-Wallis test; DP, standard deviation. Letters A and B represent statistical differences between groups in the same line. Different lowercase letters indicate statistical differences between groups in the same column. p < 0.01. **5th Load Force Values** **Aligner** | **Control** | **Orange Juice** | **Soy Sauce** | **Red Wine** | **Coca** | **Tea** | **Coffee** | ***p* (Ω)** **Mean ± SD** | **Mean ± SD** | **Mean ± SD** | **Mean ± SD** | **Mean ± SD** | **Mean ± SD** | **Mean ± SD** | **Mean ± SD** CA PRO: 31.60 ± 2.18^{Aa} | 29.01 ± 0.66^{Aa} | 29.09 ± 0.34^{Aa} | 29.04 ± 0.47^{Aa} | 29.03 ± 0.62^{A} | 28.99 ± 0.51^{Aa} | 29.02 ± 0.10^{Aa} | 0.172 INVISALIGN: 42.66 ± 0.93^{Ab} | 36.7 ± 0.77^{Bb} | 36.8 ± 0.61^{B} | 39.23 ± 0.50^{ABb} | 38.79 ± 0.78^{ABa} | 41.69 ± 0.43^{Ab} | 41.1 ± 0.85^{ABb} | 0.023* GRAPHY TC-85: 42.84 ± 0.37^{Ab} | 38.22 ± 0.45^{Bb} | 38.25 ± 0.20^{Bb} | 40.73 ± 0.76^{ABb} | 41.49 ± 0.22^{ABa} | 41.39 ± 0.16^{ABb} | 39.03 ± 0.16^{Bb} | 0.026* *p*(θ): 0.010* | 0.012* | 0.011* | 0.012* | 0.013* | 0.008* | 0.009 *The p-values were calculated using the Kruskal-Wallis test for multiple comparisons, followed by post-hoc comparisons using the Mann-Whitney U test with a Bonferroni adjustment. p < 0.01.

	at 37 °C for 24 hours. *N = 10 samples.* **Group 10 (G10):** Invisalign thermoformed aligners + soy sauce, stored in an oven at 37 °C for 24 hours. *N = 10 samples.* **Group 11 (G11):** Invisalign thermoformed aligners + red wine, stored in an oven at 37 °C for 24 hours. *N = 10 samples.* **Group 12 (G12):** Invisalign thermoformed aligners + Coca-Cola, stored in an oven at 37 °C for 24 hours. *N = 10 samples.* **Group 13 (G13):** Invisalign thermoformed aligners + tea, stored in an oven at 37 °C for 24 hours. *N = 10 samples.* **Group 14 (G14):** Invisalign thermoformed aligners + coffee, stored in an oven at 37 °C for 24 hours. *N = 10 samples.* **Group 15 (G15):** 3D-printed Graphy TC-85 aligners + dry condition, no liquid exposure (control group). *N = 10 samples.* **Group 16 (G16):** 3D-printed Graphy TC-85 aligners + orange juice, stored in an oven at 37 °C for 24 hours. *N = 10 samples.* **Group 17 (G17):** 3D-printed Graphy TC-85 aligners + soy sauce, stored in an oven at 37 °C for 24 hours. *N = 10 samples.*		**10th Load Force Values** **Aligner** | **Control** | **Orange Juice** | **Soy Sauce** | **Red Wine** | **Coca** | **Tea** | **Coffee** | ***p* (Ω)** **Mean ± SD** | **Mean ± SD** | **Mean ± SD** | **Mean ± SD** | **Mean ± SD** | **Mean ± SD** | **Mean ± SD** | **Mean ± SD** CA PRO | 29 ± 2.17^{Aa} | 26.64 ± 0.61^{Aa} | 26.55 ± 0.76^{Aa} | 26.63 ± 0.60^{Aa} | 26.57 ± 0.37^{Aa} | 26.58 ± 0.65^{Aa} | 26.58 ± 0.83^{Aa} | 0.169 INVISALIGN | 40.48 ± 0.88^{Ab} | 34.72 ± 0.74^{Bb} | 35.01 ± 0.58^{Bb} | 37.23 ± 0.49^{ABb} | 36.82 ± 0.74^{Bb} | 39.56 ± 0.41^{ABb} | 39.00 ± 0.81^{ABb} | 0.029* GRAPHY TC-85 | 42.12 ± 0.36^{Ab} | 37.53 ± 0.28^{Bc} | 37.61 ± 0.19^{Bc} | 40.04 ± 0.75^{Ac} | 40.8 ± 0.22^{Ac} | 40.7 ± 0.16^{Ab} | 38.38 ± 0.15^{Bb} | 0.033* *p*(θ) | 0.009* | 0.010* | 0.009* | 0.007* | 0.007* | 0.008* | 0.011* **The p-values were calculated using the Kruskal-Wallis test for multiple comparisons, followed by post-hoc comparisons using the Mann-Whitney U test with a Bonferroni adjustment. p < 0.01. **50th Load Force Values** **Aligner** | **Control** | **Orange Juice** | **Soy Sauce** | **Red Wine** | **Coca** | **Tea** | **Coffee** | ***p* (Ω)** **Mean ± SD** | **Mean ± SD** | **Mean ± SD** | **Mean ± SD** | **Mean ± SD** | **Mean ± SD** | **Mean ± SD** | **Mean ± SD** CA PRO | 26.44 ± 0.15^{Aa} | 24.29 ± 0.55^{Aa} | 24.21 ± 0.44^{Aa} | 24.28 ± 0.56^{Aa} | 24.20 ± 0.48^{Aa} | 24.24 ± 0.56^{Aa} | 24.25 ± 0.36^{aA} | 0.166 INVISALIGN | 26.75 ± 0.8^{Aa} | 23.12 ± 0.49^{Ba} | 23.08 ± 0.64^{Ba} | 24.6 ± 0.32^{Ba} | 24.33 ± 0.49^{Ba} | 26.14 ± 0.27^{Aa} | 25.77 ± 0.53^{ABab} | 0.027* GRAPHY TC-85 | 41.35 ± 0.36^{Ab} | 36.92 ± 0.19^{Bb} | 36.88 ± 0.35^{Bb} | 39.32 ± 0.74^{ABa} | 40.06 ± 0.21^{Ab} | 39.96 ± 0.15^{ABb} | 37.68 ± 0.15^{Bb} | 0.018*

	Group 18 (G18): 3D-printed Graphy TC-85 aligners + red wine. *N = 10 samples* **Group 19 (G19):** 3D-printed Graphy TC-85 aligners + Coca-Cola, stored in an oven at 37 °C for 24 hours. *N = 10 samples.* **Group 20 (G20):** 3D-printed Graphy TC-85 aligners + tea, stored in an oven at 37 °C for 24 hours. *N = 10 samples.* **Group 21 (G21):** 3D-printed Graphy TC-85 aligners + coffee, stored in an oven at 37 °C for 24 hours. *N = 10 samples.* **Note:** CA Pro aligners were manufactured by Henry Schein, Langen, Germany. A 3D maxillary model was produced using the Phrozen Sonic Mini 8K printer and thermoformed with the Ministar S device. The CA Pro sheets were thermoformed onto 3D-printed models at 70 °C under 4-bar pressure. A straight cut was made along the gingival margin. Invisalign aligners were produced by Align Technology, Santa Clara, California, USA, using the same patient's digital model, with the gingival margin defined by the company. The aligners were designed to produce no dental movement. Graphy TC-85 aligners were designed with a final thickness of 0.75 mm using Blue Sky Plan software (Libertyville, IL, USA) and fabricated via direct 3D printing using the Ackuretta [SOL] printer (Ackuretta, Taipei		*p*(θ) 0.006* 0.008* 0.007* 0.005* 0.004* 0.006* 0.007* *The p-values were calculated using the Kruskal-Wallis test for multiple comparisons, followed by post-hoc comparisons using the Mann-Whitney U test with a Bonferroni adjustment. $p < 0.01$.

<table>
<tr>
<td></td>
<td>City, Taiwan) with 100 µm layer thickness. No trimming was required as the gingival margin was digitally defined. After printing, the samples were rinsed with 97% isopropyl alcohol and air-dried to eliminate residual resin or alcohol. They were then cured twice for 25 minutes under UV light (wavelength: 385–405 nm). The right upper first molar region of each aligner sample was sectioned using an abrasive disc along the mesial and distal proximal contact lines. Sections were embedded in 2 mm-thick acrylic resin blocks cast in 3D-printed square molds (height: 12 mm; base: 12 mm × 12 mm), with occlusal surfaces oriented parallel to the horizontal plane.</td>
<td></td>
<td></td>
</tr>
<tr>
<td>Sayahpour et al.,, 2024
Germany
(English)</td>
<td>Group 01 (G1): DP-Clin: Three-dimensionally printed aligner, retrieved after 1 week of intraoral use. N = 10 samples.

Group 02 (G2): INV-Clin: Invisalign aligner, retrieved after 1 week of intraoral use. N = 10 samples.

Group 03 (G3): DUR-Clin: In-house thermoformed aligner, retrieved after 1 week of intraoral use. N = 10 samples.</td>
<td>Instrumented Indentation Test (IIT)
The mechanical properties evaluated were: Martens hardness (HM), indentation modulus (EIT), elastic index (ηIT), and indentation relaxation (RIT).

Sample Preparation and Mechanical Testing
Recovered aligners underwent a</td>
<td>Martens Hardness (HM), Indentation Modulus (EIT), Elasticity Index (ηIT), and Indentation Relaxation (RIT) of Internal Aligners (DUR), Directly Printed Aligners (DP), and Invisalign™ (INV)
<table>
<tr><th>Group Ctr</th><th></th><th>HM (N/mm²)</th><th></th><th>EIT (MPa)</th><th></th><th>ηIT (%)</th><th></th><th>RIT (%)</th><th></th></tr>
<tr><td>DUR</td><td>Mean ± SD</td><td>109 ± 2,88[A,B]</td><td>p< 0,001*</td><td>2753,73 ± 70,42[D,E]</td><td>p< 0,001**</td><td>35.3 ± 0.96[A,B]</td><td>p< 0,001*</td><td>17.92 ± 2.28[D,E]</td><td>p 0,001**</td></tr>
<tr><td></td><td>Median (IQR)</td><td>108 (4,5)</td><td></td><td>2754,90 (89,93)</td><td></td><td>35,05 (1,4)</td><td></td><td>18,05 (2,3)</td><td></td></tr>
<tr><td>DP</td><td>Mean ± SD</td><td>73,3 ± 11,8[A]</td><td></td><td>3285,23 ± 171,5[D,F]</td><td></td><td>20.8 ± 3.1[A]</td><td></td><td>78.46 ± 6.42[D,F],</td><td></td></tr>
<tr><td></td><td>Median (IQR)</td><td>75,0 (20,9)</td><td></td><td>3241 (251,9)</td><td></td><td>21,1 (4,94)</td><td></td><td>79,15 (6,2)</td><td></td></tr>
<tr><td>INV</td><td>Mean ± SD</td><td>74,0 ±</td><td></td><td>1717,0 ±</td><td></td><td>19.13 ±</td><td></td><td>29.73 ±</td><td></td></tr>
</table>
</td>
</tr>
</table>

Group 04 (G4): DP-Ctr: Three-dimensionally printed aligner, unused, serving as control group. *N = 10 samples.*

Group 05 (G5): INV-Ctr: Invisalign aligner, unused, serving as control group. *N = 10 samples.*

Group 06 (G6): DUR-Ctr: In-house thermoformed aligner, unused, serving as control group. *N = 10 samples.*

Note:

The 3D-printed aligners (groups DP-Clin and DP-Ctr) were designed with a thickness of 0.5 mm and an offset of 100 µm. They were oriented at 90° relative to the print platform, with the posterior section facing the build plate. Printing was performed in successive layers of 100 µm using the SprintRay Pro55 S 3D printer (SprintRay, Los Angeles, CA, USA) and the Tera Harz TC-85 DAC resin (Graphy, Seoul, South Korea). After printing, excess resin was removed by centrifugation at 600 rpm for 6 minutes. Subsequently, the aligners were post-cured for 20 minutes under nitrogen, level 2, using the Tera Harz Cure THC 2 UV curing system (Graphy, Seoul, South Korea).

For the thermoformed DUR group, 3D dental models were printed vertically using the Formlabs SLA Form 3 printer (Formlabs, Milbury, OH, USA) with a 100 gentle, non-chemical, and non-abrasive cleaning procedure, including submersion rinsing and plaque removal using a soft-bristle toothbrush. The buccal surface of the lower right first molars of the aligners was selected for specimen preparation due to its relatively flat geometry, which allows for more precise evaluation. Specimens were embedded in acrylic resin (Verso Cit-2, Struers, Ballerup, Denmark), with their occlusal surfaces aligned parallel to the horizontal plane. The samples were then ground using SiC papers up to 4000 grit under water cooling and polished with a 1 µm water-based diamond suspension (NapR1 DiaPro, Struers) on a grinding/polishing machine (Dap-V, Struers, Ballerup, Denmark).

Specimens were loaded using a Vickers indenter, applying two different load regimes with a universal hardness testing machine (ZHU0.2/Z2.5, Zwick Roell, Ulm, Germany). HM, EIT, and ηIT were automatically determined from the force–depth indentation curves, applying a maximum load of 4.9 N for a contact time of 2 seconds. For RIT, a

	SD	4,99[B]	216,22[E,F]	3.53[B]	2.51[E,F]
	Median (IQR)	74,0 (6,8)	1747,0 (292,25)	19,45 (2,83)	29,6 (2,1)

IQR = Interquartile Range; SD = Standard Deviation.
*Tested using Kruskal-Wallis. *ANOVA. A, B, C: Pairwise material comparisons Kruskal-Wallis < 0.05; A: DP—DUR, B: DUR—INV, C: DP—INV. D, E, F: Pairwise material comparisons ANOVA < 0.05; D: DP—DUR, E: DUR—INV, F: DP—INV.

Martens Hardness (HM), Indentation Modulus (EIT), Elasticity Index (ηIT), and Indentation Relaxation (RIT) of Internal Aligners (DUR), Directly Printed Aligners (DP), and Invisalign™ (INV)

Group Clin		HM (N/mm²)		EIT (MPa)		ηIT (%)		RIT (%)	
DUR	Mean ± SD	107.7 ± 1.3[A, B]	p< 0,001*	2736.54 ± 50.59[D,E]	p< 0,001**	34.83 ± 0.68[D,E]	p< 0,001**	19.06 ± 1.71[D,E]	p 0,001**
	Median (IQR)	108 (1.3)		2736.05 (63.95)		35.10 (1.08)		19.1 (2.8)	
DP	Mean ± SD	87.5 ± 18.1[A]		3134.06 ± 158.73[D,F]		24.76 ± 3.31[D,F]		65.32 ± 9.39[D,F],	
	Median (IQR)	97.3 (31.4)		3241 (251,9)		21,1 (4,94)		63.4 (9.4)	
INV	Mean ± SD	75.1 ± 3.6[B]		1809.30 ± 134.96[E,F]		19.36 ± 1.24[E,F]		29.36 ± 1.44[E,F]	
	Median (IQR)	74.5 (5.5)		1786.0 (232.5)		19.2 (1.78)		30.39 (2.3)	

IQR = Interquartile Range; SD = Standard Deviation.
*Tested using Kruskal-Wallis. *ANOVA. A, B, C: Pairwise material comparisons Kruskal-Wallis < 0.05; A: DP—DUR, B: DUR—INV, C: DP—INV. D, E, F: Pairwise material comparisons ANOVA < 0.05; D: DP—DUR, E: DUR—INV, F: DP—INV.

Pairwise Comparisons Between Martens Hardness (HM), Indentation Modulus (EIT), Elasticity Index (ηIT), and Indentation Relaxation (RIT) for Internal Aligners (DUR), Directly Printed Aligners (DP), and Invisalign™ (INV) in Unused (Ctr) and Recovered (Clin) Categories

Variable		Pairwise Comparisons		p-value
HM (N/mm²)	**Ctr**	DP	DUR	< 0,001*
		DP	INV	0,988
		DUR	INV	< 0,001*
	Clin	DP	DUR	< 0,001*
		DP	INV	0,267
		DUR	INV	< 0,001*
ηIT (%)	**Ctr**	DP	DUR	< 0,001*
		DP	INV	0,636
		DUR	INV	< 0,001*
	Clin	DP	DUR	< 0,001**
		DP	INV	0,001**
		DUR	INV	< 0,001**

	µm layer thickness and Formlabs Draft Resin V2. After printing, the models were washed in isopropyl alcohol for 10 minutes (Form Wash, Formlabs), then dried and cured using the Form Cure device (Formlabs) for 5 minutes at 0°C. The aligners were fabricated from 0.75 mm thick DURAN+ thermoplastic sheets (Scheu-Dental, Iserlohn, Germany) using the Biostar Thermoforming Unit (Scheu-Dental). The INV group aligners were retrieved from patients undergoing orthodontic treatment with Invisalign™ aligners made from SmartTrack (LD30) material (Align Technology, Inc., Santa Clara, CA, USA).	tetragonal indentation depth pulse with a constant depth of 50 µm was applied for 120 seconds, and the RIT value was measured by monitoring the force decrease from the beginning to the end of the constant indentation depth period.	**EIT (MPa)**	**Ctr**	DP	DUR	< 0,001**
					DP	INV	< 0,001**
					DUR	INV	< 0,001**
				Clin	DP	DUR	< 0,001**
					DP	INV	< 0,001**
					DUR	INV	< 0,001**
			RIT (%)	**Ctr**	DP	DUR	< 0,001**
					DP	INV	< 0,001*
					DUR	INV	< 0,001**
				Clin	DP	DUR	< 0,001**
					DP	INV	< 0,001**
					DUR	INV	< 0,001**
			*Tested using Kruskal-Wallis. **ANOVA. Significance is defined as $p < 0.05$.				
			Pairwise Comparisons Between Martens Hardness (HM), Indentation Modulus (EIT), Elasticity Index (ηIT), and Indentation Relaxation (RIT) for Used (Clin) vs. Unused (Ctr) in Each Aligner Group (DUR, DP, INV)				
			Variable	**Pairwise Comparisons**			**value**
			HM (N/mm²)	DP	DP		0,059
				DUR	DUR		0,554
				INV	INV		0,578
			EIT (MPa)	DP	DP		0,056
				DUR DUR	DUR		0,539
				INV	INV		0,267
			ηIT (%)	DP	DP		0,012*
				DUR	DUR		0,223
				INV	INV		0,544
			RIT (%)	DP	DP		0,002*
				DUR DUR			0,223
				INV INV			0,690
			*Tested using Student's t-test. **Mann-Whitney U test was used for comparisons of Martens Hardness (HM) in DP and DUR groups and Elastic Index (ηIT) in the INV group. $p < 0.05$.				

Sharif, Germany (English)	2024	**Group 1 (G1):** Tera Harz TC-85 (TC-85) aligner, manufactured by Graphy AG (Seoul, South Korea), with a thickness of 0.6 mm. It was fabricated via 3D printing using a DLP-type printer (Uniz NBEE; Uniz, CA, USA) with a layer thickness of 100 µm, followed by UV light photopolymerization (wavelength: 405 nm) under nitrogen conditions for 25 minutes using a dedicated post-curing unit (Tera Harz Cure; Graphy, South Korea). Its composition consists of urethane acrylate oligomers and acrylic monomers. *N = 18 samples.* **Group 2 (G2):** Zendura FLX™ (ZF) aligner, manufactured by Bay Materials (Fremont, CA, USA), with a thickness of 0.75 mm. The production process involves thermoforming by heating at 220 °C for 50 seconds, followed by molding under 5.8 bar of pressure and cooling for 60 seconds using a thermoforming unit (Biostar®; Scheu-Dental GmbH, Iserlohn, Germany) (Code: 162). The aligner consists of a tri-layer sheet with a thermoplastic polyurethane elastomeric core. *N = 18 samples.* **Note:** The specimens were produced in two configurations: rectangular strips (for three-point bending tests) and full anatomical aligners (for 3D force measurements). For the rectangular strips, ZF	This study employed the Orthodontic Measurement and Simulation System (OMSS) biomechanical setup for three-dimensional force measurements and mechanical testing of orthodontic aligners. The OMSS consists of a measurement unit coupled to a sensor capable of replicating 3D tooth movements while simultaneously recording force/displacement or moment/rotation relationships. The device operates in a dry chamber with controlled temperature, allowing tests under various thermal conditions. **Three-Point Bending Test (3PB)** The OMSS was configured with a 24 mm span and a load application rate of 5 mm/min. Each specimen was subjected to a 2 mm vertical deflection, and the maximum force at this deflection was recorded. Tests were conducted at 20 °C, 25 °C, 30 °C, 37 °C, and 40 °C, with a permitted temperature variation of ±0.5 °C. A total of 30 specimens per material were tested,	**Maximum Bending Force Measured in Two Deflection Cycles of 2 mm for Two Different Aligner Materials, Zendura FLX (right) and Tera Harz TC-85 (left), at Various Temperatures** **Material** / **Temperature (°C)** / **Load Cycle 1 (N)** / **Load Cycle 2 (N)** Zendura FLX / 20 / 2,30 / 2,29 Zendura FLX / 25 / 2,13 / 2,08 Zendura FLX / 30 / 2,23 / 2,24 Zendura FLX / 37 / 1,73 / 1,71 Zendura FLX / 40 / 2,08 / 2,04 Tera Harz TC-85 / 20 / 2,73 / 2,57 Tera Harz TC-85 / 25 / 2,70 / 2,44 Tera Harz TC-85 / 30 / 1,71 / 1,45 Tera Harz TC-85 / 37 / 0,87 / 0,57 Tera Harz TC-85 / 40 / 0,51 / 0,34 **Force and Moment Generated by Aligners Made of Zendura FLX and Tera Harz TC-85 Materials for Teeth 11, 13, and 15** **Tooth** / **Movement** / **Zendura FLX (N)** / **TC-85 (N)** 11 / Intrusion / 2,20 / 2,28 11 / Extrusion / -0,30 / -0,50 13 / Intrusion / 1,57 / 1,23 13 / Extrusion / -0,68 / -0,75 15 / Intrusion / 2,71 / 1,63 15 / Extrusion / -0,75 / -0,76 11 / Oral / 0,94 / 0,56 11 / Vestibular / -0,40 / -0,83 13 / Oral / 0,71 / 0,66 13 / Vestibular / -1,66 / -0,82 15 / Oral / 1,71 / 1,70 15 / Vestibular / -1,11 / -1,10 TC-85 / Mesial Rotation / 7,41 / 9,18 TC-85 / Distal Rotation / -4,98 / -8,58 Zendura / Mesial Rotation / 9,42 / 8,88 Zendura / Distal Rotation / -6,96 / -6,52

	thermoplastic sheets were thermoformed over a custom mold following the manufacturer's guidelines. This process resulted in sheet thinning from 0.75 mm to approximately 0.6 mm, confirmed using a digital caliper (Fisher Scientific International Inc., Hampton, NH, USA). The specimens were then cut into rectangular strips with dimensions of 50 × 10 × 0.6 mm using scissors, and the edges were polished with a polishing machine. In contrast, TC-85 specimens were directly 3D printed in rectangular strip format with the same dimensions using 3D image processing software (3-matic 16.0; Materialise, Leuven, Belgium) (Figure 1). The anatomical aligners were created from a digital model of a maxillary arch derived from a 3D dataset (Digimation Corp., St. Rose, Louisiana, USA). This model was exported as an STL file and processed in two ways. First, it was printed using a DLP 3D printer (P20+; Straumann AG, Basel, Switzerland) with P pro resin (Straumann AG, Basel, Switzerland), and used for thermoforming the ZF sheets. Second, the digital model was used to design full anatomical aligners in the 3-matic software, which were 3D printed from TC-85. Each aligner had a straight trim line precisely 2 mm above the gingival margin.	with six assigned to each temperature (n = 6). Two load–unload cycles were applied, and the corresponding force–displacement curves were recorded for analysis. **Force and Moment Measurement Test** Three self-curing resin models (Technovit 4004) were fabricated, representing the maxillary arch with one movable tooth in each model: the upper right central incisor (Tooth 11), upper right canine (Tooth 13), and upper right second premolar (Tooth 15). The adjacent teeth were reduced to allow smooth insertion of the movable tooth, which was attached to the sensor while the model remained stabilized with the occlusal plane aligned parallel to the sensor axis. Eighteen aligners of each material were divided into three groups (n = 6) according to the tested tooth. Measurements involved movements along the X-axis (intrusion/extrusion) and Y-axis (oro-vestibular translation) at ±0.4 mm with 0.01 mm increments, and rotations around the X-axis at ±4° with 0.1° increments. Simulations were conducted at 37 °C	

<table>
<tr>
<td></td>
<td></td>
<td>in dry conditions, reflecting normal intraoral temperature. The OMSS was preheated to ensure thermal stability during testing, and both the aligners and the model with the removable tooth were preconditioned in the OMSS chamber. Force/translation and moment/rotation curves were recorded, with adjustments made after each measurement as needed.</td>
<td></td>
</tr>
<tr>
<td>Shirey et al.,, 2023 United States of America (English)</td>
<td>Group 1 (G1): Material: EX30 (Align Technology). Manufacturing method: thermoforming with single-layer rigid polyurethane. Manufacturer-declared thickness of 0.78 mm; minimum measured thickness of 0.35 mm (± 0.05 mm). N = 15 samples.

Group 2 (G2): Material: LD30 (Align Technology). Manufacturing method: thermoforming with multilayer polyurethane/co-polyester.Manufacturer-declared thickness of 0.76 mm; minimum measured thickness of 0.50 mm (± 0.00 mm). N = 15 samples.

Group 3 (G3): Material X (Envisiontec), not yet commercially available.</td>
<td>Elastic Modulus Test
Six samples were used, consisting of three dry and three wet specimens. Data were processed using a Dynamic Mechanical Analyzer RSA3 (Texas Instruments, Dallas, TX). The strain rate was set at 0.2 mm per second for a duration of 5 seconds. The elastic modulus was determined from the stress–strain curve using linear regression to calculate the best-fit line.

Tensile Strength Test
This test employed six samples, including three dry and three wet specimens. Tensile strength was</td>
<td>Elastic Modulus of Samples
<table><tr><th></th><th>Dry</th><th>Wet</th><th>% Change (Decrease)</th><th>p-value</th></tr><tr><td>EX30</td><td>103,2 ± 17,3 MPa[a]</td><td>114,4 ± 17,9 MPa[a]</td><td>10,9</td><td>>0,05</td></tr><tr><td>LD30</td><td>61,3 ± 9,18 MPa[b]</td><td>103,5 ± 11,4 MPa[a]</td><td>68,8</td><td><0,05</td></tr><tr><td>Material X</td><td>431,2 ± 16,0 MPa[c]</td><td>139,9 ± 34,6 MPa[a]</td><td>(67,6)</td><td><0,001</td></tr><tr><td>OD-Clear TF</td><td>38,4 ± 14,7 MPa[b]</td><td>38,3 ± 8,4 MPa[b]</td><td>(0,2)</td><td>>0,05</td></tr></table>Values with different superscript letters (a, b, or c) are significantly different.

Final Tensile Strength of Samples
<table><tr><th></th><th>Dry</th><th>Wet</th><th>% Change (Decrease)</th><th>p-value</th></tr><tr><td>EX30</td><td>64,41 ± 7,25 MPa[a]</td><td>61,43 ± 7,41 MPa[a]</td><td>(4,6)</td><td>>0,05</td></tr><tr><td>LD30</td><td>40,04 ± 5,00 MPa[b]</td><td>30,09 ± 1,50 MPa[b]</td><td>(24,9)</td><td><0,05</td></tr><tr><td>Material X</td><td>28,11 ± 3,75 MPa[c]</td><td>27,57 ± 4,09 MPa[b]</td><td>(1,9)</td><td>>0,05</td></tr><tr><td>OD-Clear TF</td><td>9,34 ± 1,96 MPa[d]</td><td>8,27 ± 0,93 MPa[c]</td><td>(11,5)</td><td>>0,05</td></tr></table>Values with different superscript letters (a, b, c, or d) are significantly different.</td>
</tr>
</table>

	Manufacturing method: direct 3D printing at a 20° angle using Envision One cDLM resin. Manufacturer-declared thickness of 0.35 mm; minimum measured thickness of 0.53 mm (± 0.05 mm). *N = 15 samples.* **Group 4 (G4):** Material: OD-Clear TF Tough and Foldable (3DResyns). Manufacturing method: direct 3D printing using AnyCubic stereolithography printer (Shenzhen, China), with a layer thickness of 0.50 µm and a print angle of 60°. Thickness: manufacturer-declared thickness of 0.50 mm; minimum measured thickness of 0.58 mm (± 0.10 mm). *N = 15 samples.* **Note:** During post-processing of the 3D-printed samples, aligners were removed from the build platform, washed for 30 minutes in 99% isopropyl alcohol using the Wash & Cure 2.0 machine (AnyCubic), dried, and subsequently post-cured in the same device for 15 minutes at room temperature. **Sample Origin Details:** Groups 1, 2, and 3: samples were produced using a calibrated plaster model (American Board of Orthodontics Calibration Casts Set III), which was scanned and the STL file was sent to Align Technologies and Envisiontec (Dearborn, MI). Group 4: samples were	determined using the Instron Universal Testing System (Instron, Norwood, MA). The strain rate was set at 2 mm per second until specimen failure. This test produced 350 data points per sample. **2% Stress Relaxation Test** Three wet specimens were prepared, with deformation maintained at 2% for a duration of 2 hours. Residual stress was calculated by dividing the peak stress generated during the first 0.1 seconds of the test by the residual stress measured at the end of the 2-hour period. **Wet Sample Preparation** Wet specimens were immersed in phosphate-buffered saline solution (Gibco, Waltham, MA), adjusted to pH 7.4, at a temperature of 37 °C for 7 days prior to testing. **Test Repetitions** Each variable was tested in triplicate to ensure reliability and consistency of the results obtained.	**Stress Relaxation of Wet Samples** **Initial Stress** / **Residual Stress** / **Residual Stress (%)** EX30: 2.83 ± 0.04 MPa / 1.70 ± 0.11 MPa / 59,99 ± 3,02%[a] LD30: 1.04 ± 0.14 MPa / 0.54 ± 0.10 MPa / 52,57 ± 12,28%[a] Material X: 5.59 ± 0.75 MPa / 0.38 ± 0.09 MPa / 6,98 ± 2,64% [b] OD-Clear TF: 3.12 ± 1.33 MPa / 0.13 ± 0.05 MPa / 4,39 ± 0,84%[b] Values with different superscript letters (a, b, c, or d) are significantly different ($p < 0.05$).

<table>
<tr>
<td></td>
<td>designed using Blue Sky Bio software (Grayslake, IL) to create a series of passive 3D-printed aligners.</td>
<td></td>
<td></td>
</tr>
<tr>
<td>Simunovic, 2024
Croatia
(English)</td>
<td>Group 01 (G1): Thermoformed aligner ClearCorrect. Manufactured from polyurethane by Straumann, Basel, Switzerland. N = 4 samples.

Group 02 (G2): Thermoformed aligner Invisalign®. Manufactured from polyurethane by Align Technology, San Jose, CA, USA. N = 4 samples.

Group 03 (G3): 3D-printed aligner. Fabricated from Tera Harz TC-85 resin by Graphy, Seoul, Republic of Korea. N = 4 samples.

Group 04 (G4): 3D-printed aligner Clear-A. Fabricated by Senertek, Izmir, Turkey. N = 4 samples.

Beverage Preparation
Standard commercial brands of the following beverages were used:

• Coca-Cola® (Coca-Cola HBC Hrvatska, Zagreb, Croatia).
• Black coffee (Franck Jubilarna Original, Franck d.d., Zagreb, Croatia).
• Black tea (Franck d.d., Zagreb, Croatia).
• Red Bull® (Red Bull GmbH, Fuschl am See, Austria).

Note:</td>
<td>Color Change Evaluation
A standard compact VITA Easyshade colorimeter was used to assess color change, which was evaluated across five intervals: T0 (before immersion), T1 after 24 h, T2 after 48 h, T3 after 72 h, and T4 after 7 days. All measurements were performed in the same room under a standardized light source. Color change was measured using the CIE Lab* color system of the Commission Internationale de l'Éclairage (CIE). Measurements were taken on the flat labial surface of the upper teeth from tooth 15 to tooth 25.

Color Change Classification
Color change classification was determined using the National Bureau of Standards (NBS) system to express color differences. The ΔE* value was converted into NBS units to relate the magnitude of the color change to clinical relevance. The NBS classification values are as</td>
<td>ATR-FTIR spectroscopy was performed before and after exposure to different beverages. The spectra were recorded in different areas of the aligners, including the incisor, canine, and molar regions.
Category — Observations
TeraHarz TC85 and Clear-A — Exclusively composed of polyurethane (PU). - Significant variations in spectra depending on the sampling position, possibly related to uneven polymerization. - Treated samples did not show bands indicating absorption of components from the tested beverages.
Exposure to Beverages (Invisalign) — Red Bull: No spectral differences compared to the control sample. Tea: Appearance of a weak band at 730 cm^{-1}. Coffee and Coca-Cola: Significant deviations, including: - Development of a strong band at 730 cm^{-1}. - New peaks and low resolution in the vibrational modes of C–O–C bonds (~1350–1000 cm^{-1}). - Reduction in intensity of bands at 1596 cm^{-1} (C=C vibration) and 1527 cm^{-1} (N-H bending). - Decrease in hydrogen bonding: - Increased intensity of the non-hydrogen-bonded carbonyl band (1714 cm^{-1}). - Broad N–H vibration band not hydrogen-bonded (3560–3400 cm^{-1}). - Reduction in hydrogen-bonded bands.
Conclusion — Variations in the spectra of TeraHarz TC85 and Clear-A aligners exposed to beverages did not allow for conclusive comparisons. - Changes were mainly attributed to irregular polymerization of the materials.

FTIR Peak Identification for Invisalign Samples
Polyurethane Layers | Poly (ethylene terephthalate glycol) Layer
Wavenumber (cm^{-1}) | Vibration | Wavenumber (cm^{-1}) | Vibration
3316 | v N-H | 2927 | vas C–H (CH2)
2939 | vas C–H (CH2) | 2855 | vs C–H (CH2)
2855 | vs C–H (CH2) | 1714 | v C=O
1726 | v C=O (free) | 1407 | δ CH2
1698 | v C=O (ligação de hidrogênio) | 1375 | δwg CH2
1596 | v C=C (aromático) | 1262 | v (C=O)–O
1524 | δ N–H, v C–C, v C–N | 1244 |
1218 | v C–O | 1096 | vs C–O
1104 | v C–O–C (grupo éster) | 1017 | δip C–H
1063 | | 956 | δ C–H (anel ciclohexileno)
726 | δoop C–H
v = stretching, δ = bending, s = symmetric, as = asymmetric, oop = out of plane, ip = in-plane, wg = wagging.</td>
</tr>
</table>

	Tea was prepared by placing one tea bag into 2 dL of hot water (90 °C), allowing it to steep for 3 minutes. Coffee was prepared by adding 2 heaping teaspoons of ground coffee to 1 dL of boiling water, mixing and gently heating until foam appeared. All beverages were allowed to cool to room temperature. The aligner samples were stored in a culture incubator (Ivoclar Vivadent, Schaan, Liechtenstein) at a temperature of 37 °C. To compensate for evaporation, the immersion solutions were renewed every 24 hours throughout the experiment.	follows: 0.1–0.5, extremely slight change; 0.5–1.5, slight change; 1.5–3.0, noticeable change; 3.0–6.0, marked change; 6.0–12.0, extremely marked change; ≥12.0, change to a different color. **ATR-FTIR Analysis** Fourier-transform infrared (FTIR) spectra in the range of 4000–400 cm^{-1} were collected using a Bruker Alpha FTIR spectrometer (Bruker Optics, Ettlingen, Germany) equipped with an ATR accessory. Each spectrum was the result of 10 continuous scans acquired at a resolution of 4 cm^{-1}. OPUS v7.0 software was used for instrument control and spectral processing.	**Color Change** Coffee caused the most significant color change (mean = 15.156), followed by black tea (9.052) and Coca-Cola (4.374), with significant differences between them ($p < 0.001$). Tera Harz TC85 aligners showed the greatest color change, while ClearCorrect was the least affected. **Descriptive Statistics (Mean and Standard Deviation (SD)) of ΔE at 5 Time Points and Across Different Beverages and Brands*** **Manufacturing Method** The manufacturing method has a significant effect on color stability, with thermoformed aligners showing less color change compared to 3D-printed aligners. **Differences Between Brands** Post-hoc analyses revealed specific brand impacts, with Tera Harz TC85 showing the greatest average color change, significantly different from ClearCorrect, which exhibited the smallest change ($p < 0.001$ for all brand comparisons).

Brand	Beverage	*ΔE (24 h)** *Média*	SD	*ΔE (48 h)** *Média*	SD	*ΔE (72 h)** *Média*	SD	*ΔE (7 Dias)** *Média*	SD
Invisalign	Coffee	10.64	2.43	13.38	2.3	16.95	2.68	20.06	2.61
	Black tea	2.89	0.96	2.71	0.73	3.69	1.58	4.75	2.34
	Coca-Cola	2.16	0.97	3.55	1.84	3.19	1.1	3.42	1.5
	Red Bull	4.74	1.9	4.66	1.69	4.01	1.55	6.87	6.52
ClearCorrect	Coffee	2.51	1.06	3.28	0.66	4.27	0.94	4.28	1.46
	Black tea	2.86	1.62	2.94	0.94	3.19	0.88	2.99	1.07
	Coca-Cola	3.43	0.85	3.79	1.15	3.91	0.77	3.62	1.04
	Red Bull	3.18	1.47	5.27	1.9	4.6	1.97	4.86	2.18
Clear-A	Coffee	15.02	4.72	19.45	1.76	19.72	1.12	23.38	2.12
	Black tea	6.54	1.82	8.45	1.71	12.48	1.98	17	1.93
	Coca-Cola	5.24	2.72	5.1	2.6	6.06	2.61	4.36	2.93
	Red Bull	5.48	2.14	4.82	3.28	3.57	2.29	4.92	2.81
Tera Harz TC85	Coffee	17.14	4.76	22.48	2.44	23.56	1.72	26.38	2.39
	Black tea	9.77	2.77	15.46	2.65	22.06	2.1	27.04	1.58
	Coca-Cola	3.89	1.57	6	2.77	6.79	2.11	5.49	2.05
	Red Bull	4.3	2.59	4.74	2.33	3.6	2.38	3.73	1.92

Average Color Change ΔE Between Brands

Manufacturing Method	*Average Color Change (ΔE)**	*Mean Difference (ΔE)**	p
Thermoformed Aligners	5.208		
3D-Printed Aligners	11.376	6.168	p < 0,001
Overall Average (for all samples)	8.292		

Average ΔE Color Change Between Brands

Brand (I)	Brand (I)	Mean Difference (I–J)	95% CI Lower	95% CI Upper	p-value
Invisalign	ClearCorrect	3.041	2.027	4.055	<0.001
Invisalign	Clear-A	−3.371	−4.386	−2.357	<0.001
Invisalign	Tera Harz TC85	−5.924	−6.938	−4.909	<0.001
ClearCorrect	Invisalign	−3.041	−4.055	−2.027	<0.001
ClearCorrect	Clear-A	−6.413	−7.427	−5.398	<0.001
ClearCorrect	Tera Harz TC85	−8.965	−9.979	−7.951	<0.001
Clear-A	Invisalign	3.371	2.357	4.386	<0.001
Clear-A	ClearCorrect	6.413	5.398	7.427	<0.001
Clear-A	Tera Harz TC85	−2.552	−3.566	−1.538	<0.001
Tera Harz TC85	Invisalign	5.924	4.909	6.938	<0.001
Tera Harz TC85	ClearCorrect	8.965	7.951	9.979	<0.001
Tera Harz TC85	Clear-A	2.552	1.538	3.566	<0.001

Differences Between Beverages

The beverage impact was further corroborated by significant average differences in pairwise comparisons, especially between coffee and other beverages ($p < 0.001$), showing a strong association between the beverage type and color change ($F(3, 144) = 356.181$, $p < 0.001$, $\eta p^2 = 0.881$).

Average ΔE Color Change Between Beverages

Beverage (I)	Beverage (I)	Mean Difference (I–J)	95% CI Lower	95% CI Upper	p-value
Coffee	Black tea	6.103	5.089	7.117	<0.001
Coffee	Coca-Cola	10.781	9.767	11.796	<0.001
Coffee	Red Bull	10.571	9.557	11.586	<0.001
Black tea	Coffee	−6.103	−7.117	−5.089	<0.001
Black tea	Coca-Cola	4.678	3.664	5.692	<0.001
Black tea	Red Bull	4.468	3.454	5.482	<0.001
Coca-Cola	Coffee	−10.781	−11.796	−9.767	<0.001
Coca-Cola	Black tea	−4.678	−5.692	−3.664	<0.001
Coca-Cola	Red Bull	−0.210	−1.224	0.804	1.000
Red Bull	Coffee	−10.571	−11.586	−9.557	<0.001
Red Bull	Black tea	−4.468	−5.482	−3.454	<0.001
Red Bull	Black tea	0.210	−0.804	1.224	1.000

Repeated Measures of ΔE Color Change

The repeated measures analysis revealed a progressive and significant increase in color change (ΔE*) from one time point to another ($p < 0.001$ after Bonferroni adjustment). The multivariate analysis confirmed this effect with a large effect size ($\eta p^2 = 0.692$), indicating a strong and significant impact of time on color change.

Time Point	*Mean Difference (ΔE)**	p-value
T0 - T1	Progressive Increase	<0.001
T1 - T2	Progressive Increase	<0.001
T2 - T3	Progressive Increase	<0.001
T3 - T4	Progressive Increase	<0.001

The contribution of each parameter (L*, a*, and b*) to the cumulative color change (ΔE*) of aligners from four brands exposed to different beverages.

Brand	Beverage	*L (Mean ± SD)**	*a (Mean ± SD)**	*b (Mean ± SD)**	*ΔE (Mean ± SD)**
Invisalign	Café	0.26 ± 0.04	0.06 ± 0.01	0.68 ± 0.04	20.06 ± 2.61
	Black tea	0.45 ± 0.18	0.15 ± 0.10	0.40 ± 0.15	4.75 ± 2.34
	Coca-Cola	0.33 ± 0.15	0.17 ± 0.15	0.50 ± 0.20	3.42 ± 1.50
	Red Bull	0.34 ± 0.27	0.10 ± 0.08	0.56 ± 0.26	6.87 ± 6.52
ClearCorrect	Coffee	0.35 ± 0.15	0.17 ± 0.08	0.49 ± 0.17	4.28 ± 1.46
	Black tea	0.17 ± 0.13	0.23 ± 0.12	0.60 ± 0.15	2.99 ± 1.07
	Coca-Cola	0.28 ± 0.19	0.15 ± 0.08	0.57 ± 0.20	3.62 ± 1.04
	Red Bull	0.15 ± 0.12	0.06 ± 0.04	0.79 ± 0.15	4.86 ± 2.18
Clear-A	Coffee	0.37 ± 0.07	0.08 ± 0.02	0.54 ± 0.06	23.38 ± 2.12
	Black tea	0.57 ± 0.11	0.15 ± 0.01	0.28 ± 0.11	17.00 ± 1.93
	Coca-Cola	0.46 ± 0.21	0.17 ± 0.17	0.37 ± 0.18	4.36 ± 2.93
	Red Bull	0.49 ± 0.22	0.07 ± 0.03	0.44 ± 0.22	4.92 ± 2.81
Tera Harz TC85	Coffee	0.35 ± 0.08	0.11 ± 0.02	0.54 ± 0.08	26.38 ± 2.39
	Black tea	0.44 ± 0.06	0.16 ± 0.02	0.40 ± 0.05	27.04 ± 1.58
	Coca-Cola	0.76 ± 0.11	0.08 ± 0.06	0.16 ± 0.11	5.49 ± 2.05
	Red Bull	0.52 ± 0.32	0.10 ± 0.19	0.38 ± 0.24	3.73 ± 1.92

() indicate statistically significant differences in the highest proportion (bolded numbers) in the group, highlighting the dominant factor contributing to color change for each beverage-brand combination.*

Color Change Classification:

The Tera Harz TC85 aligners were most affected by both coffee and black tea, showing NBS values that suggest drastic color transformations. Invisalign and ClearCorrect aligners were relatively more resistant, although coffee still resulted in "remarkable changes" for ClearCorrect and "extremely remarkable changes" for Invisalign. Black tea, Coca-Cola, and Red Bull also caused perceptible color changes among the brands, with the impact of Red Bull ranging from "perceptible" to "remarkable changes."

Color Change Classification Between Brands and Beverages

Brand	Beverage	Average ΔE*
Invisalign	Coffee	18.45
	Black Tea	4.37
	Coca-Cola	3.14
	Red Bull	6.32
ClearCorrect	Coffee	3.94

			Black Tea 2.75 Coca-Cola 3.33 Red Bull 4.47 Clear-A Coffee 21.51 Black Tea 15.64 Coca-Cola 4.01 Red Bull 4.53 Tera Harz TC85 Coffee 24.27 Black Tea 24.87 Coca-Cola 5.05 Red Bull 3.43
Souman, 2023 United States of America (English)	**Group 01 (G1):** Thermoformed aligners fabricated using the BioSTAR® MiniSTAR® thermoforming machine (Scheu-Group, Iserlohn, Germany), with 0.040" (1.016 mm) PET-G plastic sheets. *N = 26 samples.* **Group 02 (G2):** Directly 3D-printed aligners, digitally designed with a thickness of 1.016 mm and fabricated using Digiline® aligner resin on the JUELL® 3D Printer (Park Dental Research Group, Ardmore, OK, USA). *N = 26 samples.* **Note:** From each intraoral scan performed using the TRIOS® scanner (3Shape, Copenhagen, Denmark), a virtual treatment plan for clear aligner therapy was created using the Orchestrate 3D software (version 7.0). Based on this plan, both a set of thermoformed aligners and a set of directly 3D-printed aligners were produced for both the upper and lower arches. Although the aligner sets were generated at the same treatment phase, the individual	**Thickness Comparison Test** Following fabrication, the aligners were scanned using a RayScan micro-computed tomography (micro-CT) system (RayScan, Meersburg, Germany) and converted into STL files. These files were imported into Geomagic® Control X™ software (Artec 3D, Luxembourg, Germany), version 2020.0.1. The "Initial Alignment" tool was used, followed by "Enhanced Alignment Accuracy with Feature Recognition" for preliminary positioning and sample superimposition. Final overlay was refined using the "Best Fit Alignment" tool to ensure precise comparison. The "Comparison Point" tool in Geomagic® Control X™ was employed to measure aligner thickness perpendicularly at 27 predefined anatomical	**General Average Thickness Comparisons** **Arch** **N** **Direct Printing Mean (SD) mm** **Thermoforming Mean (SD) mm** **Mean Difference (SD) mm** **p-value** Maxilla 351 1.10 (0.087) 0.524 (0.128) 0.578 (0.008) <0.001* Mandible 351 1.10 (0.091) 0.555 (0.115) 0.546 (0.008) <0.001* Total 702 1.10 (0.089) 0.540 (0.122) 0.560 (0.012) <0.001* **Location-Specific Average Thickness Comparisons** **Measurement Location** **N** **Direct Printing Mean (SD) mm** **Thermoforming Mean (SD) mm** **Mean Difference (SD) mm** **p-value** Gingival Vestibular Zenith 130 1.086 (0.072) 0.418 (0.122) 0.674 (0.012) <0.001* Gingival Lingual Zenith 130 1.063 (0.081) 0.563 (0.099) 0.505 (0.013) <0.001* Facial Axis Point 130 1.078 (0.081) 0.483 (0.096) 0.599 (0.011) <0.001* Lingual Axis Point 130 1.063 (0.073) 0.610 (0.069) 0.453 (0.010) <0.001* Incisal Edges 78 1.182 (0.072) 0.606 (0.116) 0.574 (0.014) <0.001* Cuspid Tips 104 1.176 (0.077) 0.597 (0.084) 0.577 (0.012) <0.001* **Tooth-Specific Average Thickness Comparisons** **Tooth** **N** **Direct Printing Mean (SD) mm** **Thermoforming Mean (SD) mm** **Mean Difference (SD) mm** **p-value** Right Central Incisor 130 1.096 (0.091) 0.528 (0.146) 0.569 (0.015) <0.001* Left Central Incisor 130 1.092 (0.090) 0.538 (0.144) 0.555 (0.015) <0.001* Left Canine 130 1.094 (0.083) 0.534 (0.118) 0.560 (0.012) <0.001* Left First Premolar 156 1.105 (0.088) 0.543 (0.088) 0.564 (0.010) <0.001* Left First Molar 156 1.115 (0.092) 0.552 (0.115) 0.560 (0.012) <0.001*

	aligner stages varied among patients.	landmarks on the external surface. **Reference Points for Measurement** *Right Central Incisor* • Buccal gingival zenith • Facial axis point • Incisal edge • Lingual axis point • Lingual gingival zenith *Left Central Incisor* • Buccal gingival zenith • Facial axis point • Incisal edge • Lingual axis point • Lingual gingival zenith *Left Canine* • Buccal gingival zenith • Facial axis point • Incisal cusp • Lingual axis point • Lingual gingival zenith *Left First Premolar* • Buccal gingival zenith • Facial axis point • Buccal cusp	

		• Lingual cusp Lingual axis point Lingual gingival zenith **Definitions Used in the Study** *Gingival Zenith:* *Maxillary arch:* Highest point of the gingival margin. *Mandibular arch:* Lowest point of the gingival margin. *Facial Axis Point:* Visual center of the clinical crown on the buccal surface. *Lingual Axis Point:* Visual center of the clinical crown on the lingual surface.	
Spangler *et al.*,, 2023 United States of America (English)	**Group 01 (G1):** 3D-printed aligners for patients without dental crowding, fabricated using Dental LT Clear resin from Formlabs Inc. The aligner thickness was set at 0.65 mm. *N = 10 samples.* **Group 02 (G2):** 3D-printed aligners for patients with moderate dental crowding (4–6 mm), fabricated using Dental LT Clear resin from Formlabs Inc. The aligner thickness was set at 0.65 mm. *N = 10 samples.* **Group 03 (G3):** 3D-printed aligners for patients with severe dental crowding (6.1–10.0 mm), fabricated using Dental LT Clear resin from Formlabs Inc. The aligner thickness was set at 0.65 mm. *N = 10 samples.*	**Mean and RMS Deviation by Crowding Severity and Manufacturing Method** A cone-beam computed tomography (CBCT) scan was obtained for both 3D-printed and vacuum-formed aligners in each case within each group. The scan parameters were set to a field of view of 16 cm × 10 cm, voxel size of 0.3 mm, scan time of 4.8 seconds, exposure time of 2.0 seconds, 120 kVp, 5 mA, and 283, 582, or 291 mGy/cm². The digital images generated by CBCT were converted into STL file models using 3D Slicer software (3D Slicer; National Institutes of Health, Bethesda, MD).	**Summary Statistics for Mean Deviation and RMS by Malocclusion Degree and Manufacturing Method** **Malocclusion Degree** — **Mean Deviation (mm)** — **RMS** **3D Printed Aligners** No Malocclusion — 0.12 ± 0.01 — 0.15 ± 0.02 Moderate Malocclusion — 0.11 ± 0.01 — 0.15 ± 0.02 Severe Malocclusion — 0.11 ± 0.01 — 0.15 ± 0.02 **Thermoformed Aligners** No Malocclusion — 0.13 ± 0.03 — 0.17 ± 0.04 Moderate Malocclusion — 0.13 ± 0.02 — 0.17 ± 0.03 Severe Malocclusion — 0.13 ± 0.02 — 0.17 ± 0.03 Values are presented as mean ± standard deviation. RMS, root mean square.

	Group 04 (G4): Thermoformed aligners for patients without dental crowding, fabricated with Invisacryl Ultra, produced by Great Lakes Dental Technologies, Tonawanda, NY. *N = 10 samples.* **Group 05 (G5):** Thermoformed aligners for patients with moderate dental crowding (4–6 mm), fabricated with Invisacryl Ultra, produced by Great Lakes Dental Technologies, Tonawanda, NY. *N = 10 samples.* **Group 06 (G6):** Thermoformed aligners for patients with severe dental crowding (6.1–10.0 mm), fabricated with Invisacryl Ultra, produced by Great Lakes Dental Technologies, Tonawanda, NY. *N = 10 samples.* **Note:** Digital intraoral scans of patients from the orthodontic graduate clinic database at Virginia Commonwealth University were evaluated for mandibular anterior crowding, from canine to canine. Previously acquired digital scans from an iTero scanner (Align Technology, San Jose, California) were imported into 3Shape software (Copenhagen, Denmark) in STL file format. The 3Shape Appliance Designer software was used to digitally design a customized aligner for each case. Samples from each group were randomly printed in sets of six,	These STL models were manually trimmed in Meshmixer software (Autodesk, Inc., San Rafael, CA), and the intaglio surfaces were extracted. The STL files of the intaglio surfaces of both printed and vacuum-formed aligners were individually compared to the original STL file of the examined dental arch. Files were initially aligned using the Transform Alignment tool. Three corresponding anatomical landmarks were selected to establish alignment, and the surfaces were superimposed using the best-fit alignment model in Geomagic Control X software (3D Systems, Rock Hill, SC), with a maximum alignment tolerance of 0.5 mm and a sampling rate of 25%. Deviations between the CBCT-derived models and the original reference STL were recorded, and the mean absolute discrepancy (accuracy) was calculated. Overall trueness was determined using the root mean square (RMS) value, which accounts for the absolute differences between reference and measured values at each point on the model.	

<table>
<tr>
<td></td>
<td>at a 30° angle, using the Form-3B stereolithography printer (Formlabs Inc). Post-processing followed the manufacturer's instructions and included rinsing in 96% isopropyl alcohol for 5 minutes, air drying, and UV curing for 20 minutes at 80 °C.
Additionally, the patients' original STL files were sent to a local dental laboratory, where current commercial technology was simulated for the fabrication of clear aligners. The process involved 3D printing of a resin model for each individual case (Juell 3D printer and 3D printing resin; Park Dental Research, Ardmore, OK), followed by vacuum thermoforming of the aligner.</td>
<td></td>
<td></td>
</tr>
<tr>
<td>Wendl, Wendl, and Proff, 2025
Germany
(English)</td>
<td>Group 01 (G1): CA® Pro Clear Aligner (Scheu Dental GmbH, Germany), a thermoformed aligner composed of a three-layer sheet with a dual-shell structure made of copolyester and a thermoplastic elastomeric core.

Group 02 (G2): Erkodur-al (Erkodent Erich Kopp GmbH, Germany), a thermoformed aligner made of copolyester.

Group 03 (G3): SMP aligner, a thermoformed aligner with shape-memory properties, developed in collaboration with the University of Leoben, composed of PPC (polypropylene carbonate) and TPU (thermoplastic</td>
<td>Development of a Finite Element Model
To analyze the forces acting on the malpositioned tooth, a finite element model was developed in which the entire tooth surface (represented by the nodes of the surface mesh) was rigidly connected to a central evaluation node. This approach enabled the calculation of forces and moments exerted by the aligner at a single reference point, with the possibility of spatial adjustment as needed.
Digital models of the malocclusion and</td>
<td>Forces and Moments at the Central Node.
<table>
<tr><th>Manufacturer</th><th>Thickness</th><th>Fx (N)</th><th>Fy (N)</th><th>Fz (N)</th><th>F_{res}</th><th>Mx (N·mm)</th><th>My (N·mm)</th><th>Mz (N·mm)</th><th>M_{res} (N·mm)</th></tr>
<tr><td>SMP aligner</td><td>0.40 mm</td><td>-7.8</td><td>-5.3</td><td>0.79</td><td>9.5</td><td>-2.4</td><td>24.0</td><td>-3.7</td><td>24.4</td></tr>
<tr><td></td><td>0.50 mm</td><td>-11.5</td><td>-6.6</td><td>1.0</td><td>13.3</td><td>-1.7</td><td>36.4</td><td>-6.5</td><td>37.0</td></tr>
<tr><td></td><td>0.60 mm</td><td>-15.9</td><td>-10.1</td><td>1.6</td><td>18.9</td><td>-3.3</td><td>52.6</td><td>-6.9</td><td>53.0</td></tr>
<tr><td>CA® pro clear</td><td>0.40 mm</td><td>-10.8</td><td>-11.8</td><td>0.9</td><td>15.8</td><td>-11.5</td><td>30.6</td><td>-2.3</td><td>32.7</td></tr>
<tr><td></td><td>0.50 mm</td><td>-15.0</td><td>-13.2</td><td>0.8</td><td>20.0</td><td>-3.2</td><td>45.4</td><td>0.5</td><td>45.5</td></tr>
<tr><td></td><td>0.60 mm</td><td>-22.4</td><td>-15.4</td><td>0.9</td><td>27.2</td><td>-4.2</td><td>72.8</td><td>-9.6</td><td>73.6</td></tr>
<tr><td>Erkodur-al</td><td>0.40 mm</td><td>0.6</td><td>-3.1</td><td>-0.1</td><td>3.1</td><td>7.0</td><td>-5.2</td><td>11.4</td><td>14.4</td></tr>
<tr><td></td><td>0.50 mm</td><td>1.4</td><td>-3.5</td><td>-0.3</td><td>3.8</td><td>12.4</td><td>-9.7</td><td>16.8</td><td>23.0</td></tr>
<tr><td></td><td>0.60 mm</td><td>1.0</td><td>-6.0</td><td>-0.6</td><td>6.1</td><td>10.7</td><td>-1.4</td><td>13.5</td><td>17.3</td></tr>
<tr><td>Graphy</td><td>0.40 mm</td><td>-2.8</td><td>-1.8</td><td>0.1</td><td>3.4</td><td>-5.1</td><td>8.2</td><td>-0.4</td><td>9.7</td></tr>
<tr><td></td><td>0.50 mm</td><td>-5.0</td><td>-4.4</td><td>0.0</td><td>6.6</td><td>-12.1</td><td>14.6</td><td>3.9</td><td>19.4</td></tr>
<tr><td></td><td>0.60 mm</td><td>-8.4</td><td>-6.9</td><td>-0.6</td><td>10.9</td><td>-19.8</td><td>25.1</td><td>4.6</td><td>32.3</td></tr>
</table>
F_{res} and M_{res} represent the forces and moments resulting from the sum of the forces and moments acting in all three spatial directions.</td>
</tr>
</table>

	polyurethane). **Group 04 (G4):** 3D-printed aligner made of Tera Harz TC-85 (Graphy Inc., South Korea), fabricated from vinyl ether urethane resin with shape-memory characteristics. **Note:** Thermoforming was performed using the Ministar device (Scheu Dental GmbH, Germany), following the manufacturer's specifications. The Graphy aligners (TC-85 DAC Tera Harz) were 3D printed using the UNIZ NBee printer (USA) after design planning in the UNIZ Dental software. After printing, while still flexible, the aligners were removed from the platform with their support structures and centrifuged (Tera Harz spinner, Graphy Inc.) to activate the shape-memory function. The supports were removed, and the aligners were UV-cured under nitrous oxide using the Tera Harz Cure 2 unit (Graphy Inc.), achieving transparency. A plaster model (Ernst Hinrichs GmbH, Germany) was fabricated to reproduce the clinical condition of a patient with malocclusion, where the upper right central incisor (tooth 11) was mesially rotated by 10°. This tooth was separated from the dental arch of the plaster model, manually repositioned to its ideal position, and fixed in place using pink wax (Beauty Pink, Integra Miltex GmbH,	the various aligners were obtained via scanning and stored as triangulated meshes (STL format). As these files represented only surface geometry (without volumetric data), remeshing was required to convert the triangular mesh into quadrilateral elements. This process optimized computational efficiency by reducing the degrees of freedom without compromising geometric resolution (average element size: 0.25 mm). Both the malocclusion model and the aligners were truncated to include only anatomically relevant regions.	

	Germany). Both the malocclusion model and the corrected model were digitally scanned. The aligners were scanned while still fitted to the models and, after removal, their inner and outer surfaces were scanned using contrast spray (Zirko Scanspray, Zirkonzahn S.R.L., Italy). All scans were standardized and performed using the MedIT i500 3D scanner (MedIT, South Korea). The digital models of the dental arches and aligners were exported as STL files using the MeshLab software (ISTI–CNR, Italy).		

Table 5 – Bias analysis

Author, year	Was the study's objective clearly stated?	Was the sample size justified?	Was the number of samples in each group similar in each test?	Were those who assessed the results blinded to the treatment allocation?	Were the baseline conditions similar across different groups? (according to the brands or whether the aligners were received or retrieved)	Were the groups treated identically, except for the named interventions?	Were the experimental procedures similar across different groups?	Were the operators blinded to the grouping?	Was the experimental protocol clearly described?	Were the results measured in the same way for all groups?	Were the result data complete, with no missing values?	Were all measured results adequately reported?	Blinded to the assessment of the results	Were all the reported results adequately explained in the methods?	Was appropriate statistical analysis used?	Any other inconsistencies or sources of bias?	Scoring
Atta *et al.,*, 2024	1	0	0	0	1	1	1	0	1	1	1	0	0	1	1	1	10/16
Bae *et al.,*, 2025	1	1	0	0	1	1	1	0	1	1	1	0	0	1	1	0	10/16
Bandic *et al.,*, 2024	1	0	0	0	1	1	1	0	1	1	1	1	0	1	1	1	11/16
Cremonine *et al.,*, 2025b	1	1	1	0	1	1	1	0	1	1	1	0	0	1	1	1	12/16
Cremonine, *et al.,*, 2025	1	1	1	0	1	1	1	0	1	1	1	1	0	1	1	1	13/16
Cremonini *et al.,*, 2024	1	0	1	0	1	1	1	0	1	1	1	1	0	1	1	1	12/16
Eslami *et al.,*, 2024	1	1	1	0	1	1	1	0	1	1	1	1	0	1	1	0	12/16
Hertan *et al.,*, 2022	1	0	1	0	1	1	1	0	1	1	1	1	0	1	1	1	12/16
Jidal *et al.,*, 2019	1	0	1	0	1	1	1	0	1	1	1	0	1	1	1	1	12/16
Jidal *et*	1	0	0	0	1	1	1	0	1	1	1	0	0	1	1	1	10/1

al.,, 2020																	6
Koening *et al.*,, 2022	1	1	1	0	1	1	1	0	1	1	1	1	0	1	1	0	12/16
Koletsi *et al.*,, 2022	1	0	1	0	1	1	1	0	1	1	1	1	0	1	1	1	12/16
Kuntz *et al.*,, 2024	1	0	0	0	1	1	1	0	1	1	1	0	0	1	1	1	10/16
Lee *et al.*,, 2022	1	0	0	0	1	1	1	0	1	1	1	0	0	1	1	1	10/16
Park *et al.*,, 2023	1	0	1	0	1	1	1	0	1	1	1	1	0	1	1	0	11/16
Sari *et al.*,, 2024	1	1	1	0	1	1	1	0	1	1	1	1	0	1	1	1	13/16
Sayahpour *et al.*,, 2024	1	1	1	0	1	1	1	0	1	1	1	1	0	1	1	1	13/16
Sharif *et al.*,, 2024	1	1	1	0	1	1	1	0	1	1	1	1	0	1	1	1	13/16
Shirey *et al.*,, 2023	1	1	0	0	1	1	1	0	1	1	1	1	0	1	1	1	12/16
Simonovic *et al.*,, 2024	1	1	1	1	1	1	1	0	1	1	1	1	1	1	1	0	14/16
Souman, 2023	1	1	1	0	1	1	1	0	1	1	1	1	0	1	1	0	12/16
Spangler *et al.*,, 2023	1	1	1	0	1	1	1	0	1	1	1	0	0	1	1	0	11/16
Wendl, *et al.*,, 2025	1	0	1	0	1	1	1	0	1	1	1	1	0	1	1	1	12/16

Graph 01 – Bias Relationship by Article

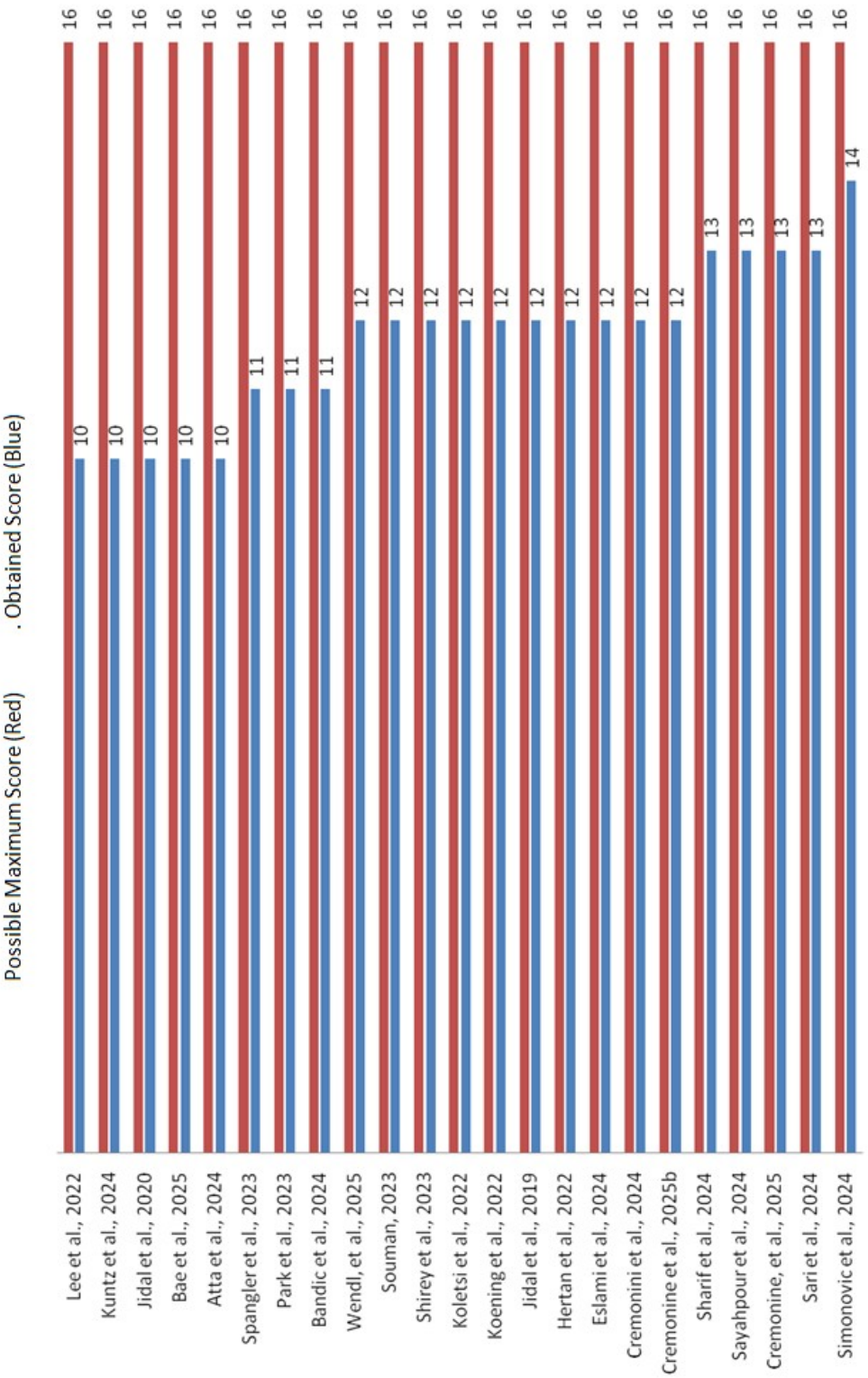

Graph 02 – Bias Relationship by Analyzed Category

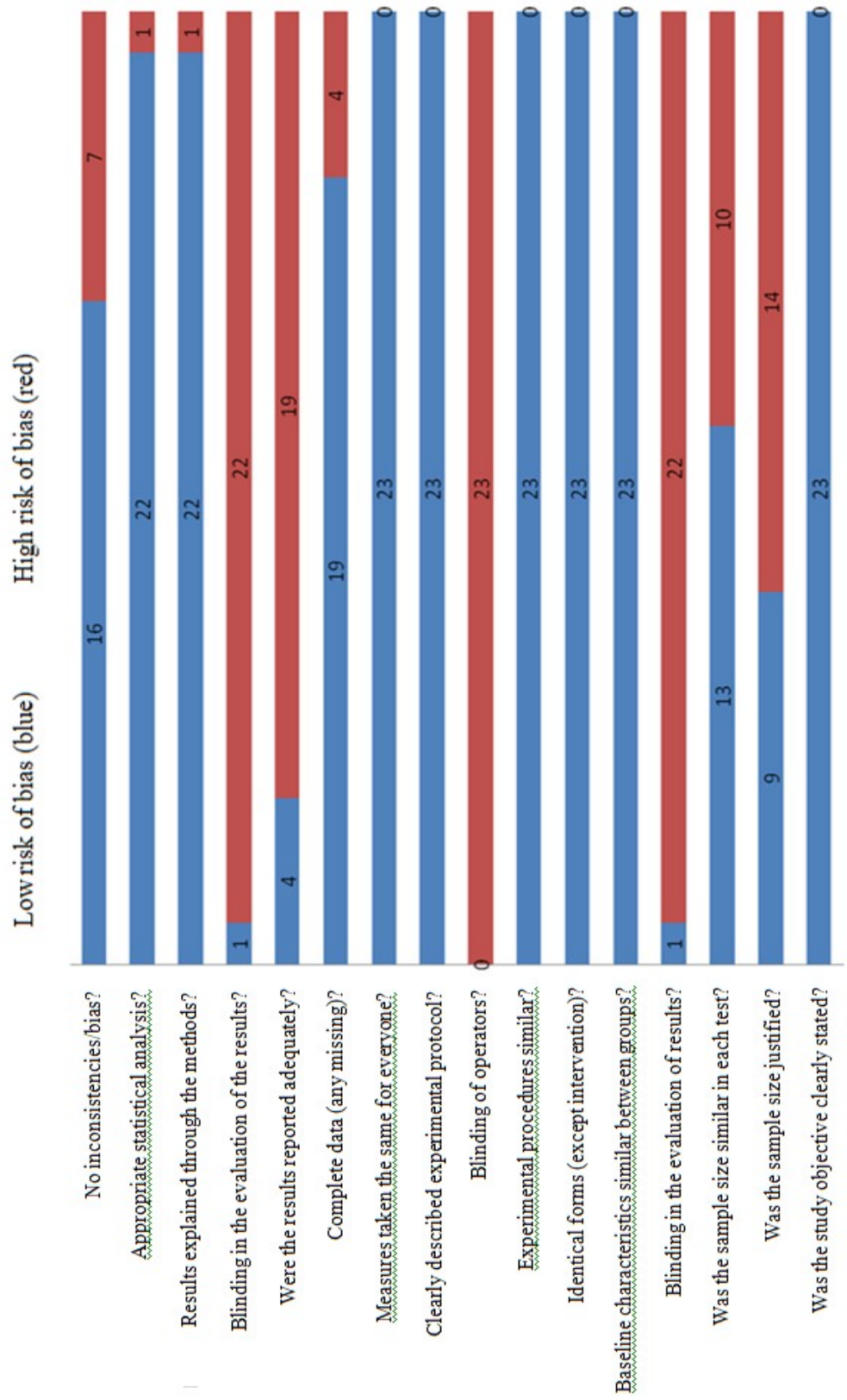

Data extracted from the meta-analysis of roughness

Sa variable of unused thermoformed and 3D-printed aligners

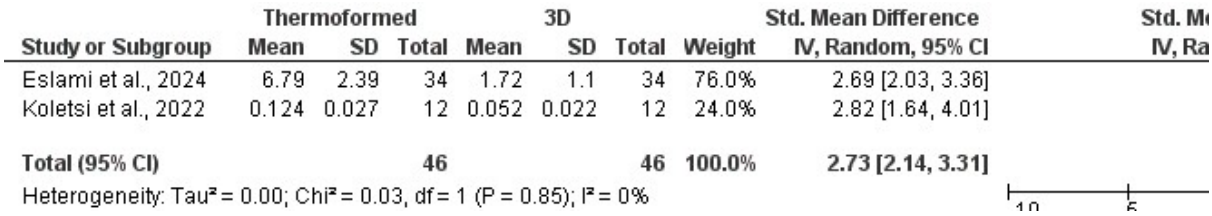

	Thermoformed			3D				Std. Mean Difference	Std. M
Study or Subgroup	Mean	SD	Total	Mean	SD	Total	Weight	IV, Random, 95% CI	IV, Ra
Eslami et al., 2024	6.79	2.39	34	1.72	1.1	34	76.0%	2.69 [2.03, 3.36]	
Koletsi et al., 2022	0.124	0.027	12	0.052	0.022	12	24.0%	2.82 [1.64, 4.01]	
Total (95% CI)			**46**			**46**	**100.0%**	**2.73 [2.14, 3.31]**	
Heterogeneity: Tau² = 0.00; Chi² = 0.03, df = 1 (P = 0.85); I² = 0%									

Sq variable of unused thermoformed and 3D-printed aligners

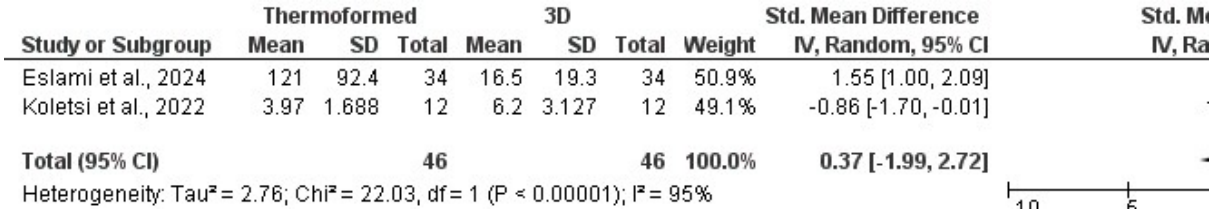

	Thermoformed			3D				Std. Mean Difference	Std. M
Study or Subgroup	Mean	SD	Total	Mean	SD	Total	Weight	IV, Random, 95% CI	IV, Ra
Eslami et al., 2024	121	92.4	34	16.5	19.3	34	50.9%	1.55 [1.00, 2.09]	
Koletsi et al., 2022	3.97	1.688	12	6.2	3.127	12	49.1%	-0.86 [-1.70, -0.01]	
Total (95% CI)			**46**			**46**	**100.0%**	**0.37 [-1.99, 2.72]**	
Heterogeneity: Tau² = 2.76; Chi² = 22.03, df = 1 (P < 0.00001); I² = 95%									

Sv variable of unused thermoformed and 3D-printed aligners

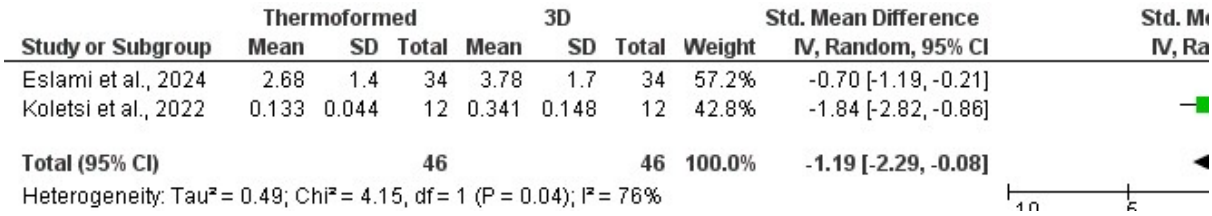

	Thermoformed			3D				Std. Mean Difference	Std. M
Study or Subgroup	Mean	SD	Total	Mean	SD	Total	Weight	IV, Random, 95% CI	IV, Ra
Eslami et al., 2024	2.68	1.4	34	3.78	1.7	34	57.2%	-0.70 [-1.19, -0.21]	
Koletsi et al., 2022	0.133	0.044	12	0.341	0.148	12	42.8%	-1.84 [-2.82, -0.86]	
Total (95% CI)			**46**			**46**	**100.0%**	**-1.19 [-2.29, -0.08]**	
Heterogeneity: Tau² = 0.49; Chi² = 4.15, df = 1 (P = 0.04); I² = 76%									

Sz variable of unused thermoformed and 3D-printed aligners

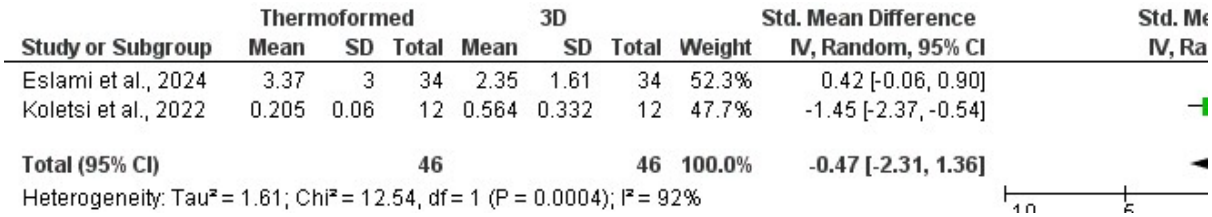

	Thermoformed			3D				Std. Mean Difference	Std. M
Study or Subgroup	Mean	SD	Total	Mean	SD	Total	Weight	IV, Random, 95% CI	IV, Ra
Eslami et al., 2024	3.37	3	34	2.35	1.61	34	52.3%	0.42 [-0.06, 0.90]	
Koletsi et al., 2022	0.205	0.06	12	0.564	0.332	12	47.7%	-1.45 [-2.37, -0.54]	
Total (95% CI)			**46**			**46**	**100.0%**	**-0.47 [-2.31, 1.36]**	
Heterogeneity: Tau² = 1.61; Chi² = 12.54, df = 1 (P = 0.0004); I² = 92%									

Sa variable of used thermoformed and 3D-printed aligners

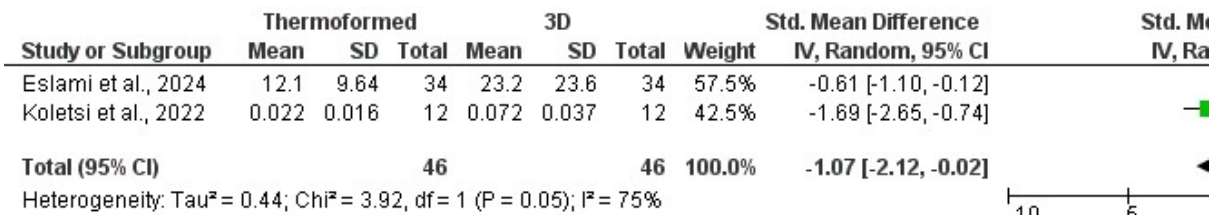

	Thermoformed			3D				Std. Mean Difference	Std. M
Study or Subgroup	Mean	SD	Total	Mean	SD	Total	Weight	IV, Random, 95% CI	IV, Ra
Eslami et al., 2024	12.1	9.64	34	23.2	23.6	34	57.5%	-0.61 [-1.10, -0.12]	
Koletsi et al., 2022	0.022	0.016	12	0.072	0.037	12	42.5%	-1.69 [-2.65, -0.74]	
Total (95% CI)			**46**			**46**	**100.0%**	**-1.07 [-2.12, -0.02]**	
Heterogeneity: Tau² = 0.44; Chi² = 3.92, df = 1 (P = 0.05); I² = 75%									

Sq variable of used thermoformed and 3D-printed aligners

	Thermoformed			3D				Std. Mean Difference	Std. M
Study or Subgroup	Mean	SD	Total	Mean	SD	Total	Weight	IV, Random, 95% CI	IV, Ra
Eslami et al., 2024	24.5	18.8	34	42.1	32.8	34	75.1%	-0.65 [-1.14, -0.16]	
Koletsi et al., 2022	8.202	6.445	12	14.778	7.54	12	24.9%	-0.91 [-1.75, -0.06]	
Total (95% CI)			**46**			**46**	**100.0%**	**-0.71 [-1.14, -0.29]**	
Heterogeneity: Tau² = 0.00; Chi² = 0.26, df = 1 (P = 0.61); I² = 0%									

Sv variable of used thermoformed and 3D-printed aligners

	Thermoformed			3D				Std. Mean Difference	Std. M
Study or Subgroup	Mean	SD	Total	Mean	SD	Total	Weight	IV, Random, 95% CI	IV, Ra
Eslami et al., 2024	76.4	67.7	34	9.59	13.3	34	51.1%	1.35 [0.82, 1.88]	
Koletsi et al., 2022	3.97	1.688	12	6.2	3.127	12	48.9%	-0.86 [-1.70, -0.01]	
Total (95% CI)			**46**			**46**	**100.0%**	**0.27 [-1.89, 2.44]**	
Heterogeneity: Tau² = 2.31; Chi² = 18.94, df = 1 (P < 0.0001); I² = 95%									

Sz variable of used thermoformed and 3D-printed aligners

	Thermoformed			3D				Std. Mean Difference	Std. M
Study or Subgroup	Mean	SD	Total	Mean	SD	Total	Weight	IV, Random, 95% CI	IV, Ra
Eslami et al., 2024	10.4	4.89	34	2.35	1.61	34	54.5%	2.19 [1.58, 2.79]	
Koletsi et al., 2022	0.181	0.028	12	0.125	0.062	12	45.5%	1.12 [0.25, 2.00]	
Total (95% CI)			**46**			**46**	**100.0%**	**1.70 [0.67, 2.74]**	
Heterogeneity: Tau² = 0.42; Chi² = 3.83, df = 1 (P = 0.05); I² = 74%									

Data extracted from the meta-analysis of dimensional variation Expected and found

Thickness in thermoformed and 3D-printed aligners.

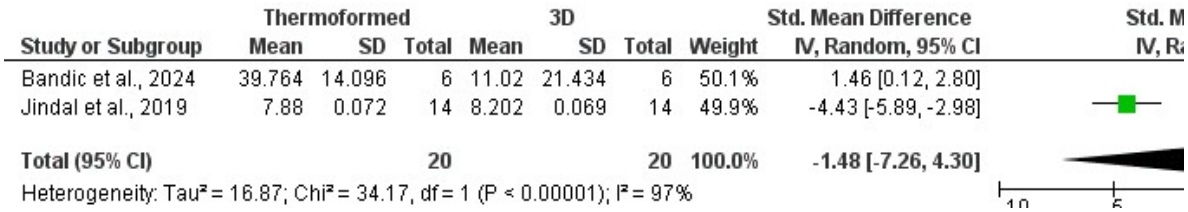

Study or Subgroup	Thermoformed Mean	SD	Total	3D Mean	SD	Total	Weight	Std. Mean Difference IV, Random, 95% CI	Std. M IV, Ra
Bandic et al., 2024	39.764	14.096	6	11.02	21.434	6	50.1%	1.46 [0.12, 2.80]	
Jindal et al., 2019	7.88	0.072	14	8.202	0.069	14	49.9%	-4.43 [-5.89, -2.98]	
Total (95% CI)			**20**			**20**	**100.0%**	**-1.48 [-7.26, 4.30]**	

Heterogeneity: Tau² = 16.87; Chi² = 34.17, df = 1 (P < 0.00001); I² = 97%

6. CONSIDERAÇÕES FINAIS

A análise crítica dos estudos in vitro incluídos nesta revisão sistemática destacou diferenças significativas entre alinhadores ortodônticos transparentes produzidos por termoformagem e aqueles fabricados por impressão tridimensional (3D). Os alinhadores termoformados apresentaram maior dureza superficial e resistência à flexão pontual, mas sofreram considerável perda de espessura, e apresentaram menor precisão geométrica, o que pode comprometer a previsibilidade de movimentos dentários mais complexos. Além disso, demonstraram menor capacidade de recuperação de forma e menor controle sobre a distribuição interna das forças.

Em contraste, os alinhadores impressos em 3D destacaram-se pela superioridade em estabilidade dimensional, precisão morfológica, recuperação elástica, resistência à tração e potencial de personalização anatômica, especialmente quando combinados com gradientes de espessura, margens anatômicas e materiais com temperatura de transição vítrea compatível com o ambiente intraoral. A metanálise indicou que os alinhadores impressos em 3D apresentam rugosidade superficial significativamente maior antes do uso, mas mantêm melhor preservação das características topográficas após o uso clínico, sugerindo maior resistência ao desgaste. Já os alinhadores termoformados tendem a suavizar a superfície durante o uso, o que pode melhorar o conforto, mas comprometer a estabilidade do movimento ao longo do tempo. Quanto à variação dimensional entre a espessura planejada e a espessura real, não foram encontradas diferenças estatisticamente significativas entre os dois métodos, embora tenha sido observada alta heterogeneidade entre os estudos avaliados.

No entanto, os alinhadores impressos em 3D ainda enfrentam desafios relacionados à retenção de força prolongada e desgaste superficial, embora esses fatores não tenham mostrado comprometimento estrutural significativo nos estudos analisados.

Considerando as limitações metodológicas observadas nos estudos incluídos, como tamanhos de amostra pequenos, variabilidade nos protocolos experimentais e falta de validação clínica, recomenda-se cautela ao extrapolar os resultados. No entanto, os dados disponíveis sugerem que a impressão 3D representa uma tecnologia promissora e em expansão, com o potencial de redefinir

os padrões biomecânicos, estéticos e funcionais na ortodontia com alinhadores transparentes.

Estudos futuros devem focar na integração dos dados laboratoriais com as respostas clínicas reais, avaliando os movimentos dentários controlados por alinhadores com diferentes geometrias, materiais e ciclos de uso, a fim de fortalecer a base científica para decisões terapêuticas mais precisas e individualizadas.

REFERÊNCIAS

ABREU, L. G. Orthodontics in children and impact of malocclusion on adolescents' quality of life. **Pediatric Clinics of North America**, Philadelphia, v. 65, n. 5, p. 995-1006, set./out. 2018. Disponível em: https://pubmed.ncbi.nlm.nih.gov/30213359/. Acesso em: 12 jan. 2025.

AL-NADAWI, M.; KRAVITZ, N. D.; *et al.* Effect of clear aligner wear protocol on the efficacy of tooth movement. **Angle Orthodontist**, Appleton, v. 91, n. 2, p. 157-163, mar./abr. 2021. Disponível em: https://pubmed.ncbi.nlm.nih.gov/33296455/. Acesso em: 03 mar. 2025.

ALBERTINI, P.; COLOMBO, M.; *et al.* Advances in orthodontic aligner materials: a critical review of property testing methodologies. **Materials Science and Engineering C**, Amsterdam, v. 134, p. 112683, jan. 2022. Disponível em: https://pmc.ncbi.nlm.nih.gov/articles/PMC9588987/. Acesso em: 28 jan. 2025.

ALEXANDROPOULOS, A.; AL JABBARI, Y. S.; *et al.* Chemical and mechanical characteristics of contemporary thermoplastic orthodontic materials. **Australian Orthodontic Journal**, Sydney, v. 31, n. 2, p. 165-170, jul./dez. 2015. Disponível em: https://pubmed.ncbi.nlm.nih.gov/26999889/. Acesso em: 10 mar. 2025.

ALHASYIMI, A. A.; AYUB, A.; *et al.* Effectiveness of the attachment design and thickness of clear aligners during orthodontic anterior retraction: finite element analysis. **European Journal of Dentistry**, Stuttgart, v. 18, n. 1, p. 174-181, jan./fev. 2024. Disponível em: https://pubmed.ncbi.nlm.nih.gov/36963425/. Acesso em: 10 mar. 2025.

ALLISON, P. J.; LOCKER, D.; FEINE, J. S. Quality of life: a dynamic construct. **Social Science & Medicine**, Oxford, v. 45, n. 2, p. 221-230, jul. 1997. Disponível em: https://pubmed.ncbi.nlm.nih.gov/9225410/. Acesso em: 10 mar. 2025..

ARSLAN AVAN, B.; BODUR, O. C.; *et al.* An in-vitro assessment of bisphenol A release from thermoplastic orthodontic appliances exposed to various beverages. **BMC Oral Health**, London, v. 25, n. 1, p. 750, 2025. Disponível em: https://pubmed.ncbi.nlm.nih.gov/40399894/. Acesso em: 12 jan. 2025..

ATTA, I.; BOURAUEL, C.; *et al.* Physiochemical and mechanical characterisation of orthodontic 3D printed aligner material made of shape memory polymers (4D aligner material). **Journal of the Mechanical Behavior of Biomedical Materials**, Amsterdam, v. 150, p. 106337, jan. 2024. Disponível em: https://pubmed.ncbi.nlm.nih.gov/38154364/. Acesso em: 27 abr. 2025.

BAE, B. G.; KIM, Y. H.; *et al.* A study on the compressive strength of three-dimensional direct printing aligner material for specific designing of clear aligners. **Scientific Reports**, London, v. 15, n. 1, p. 2489, 2025. Disponível em: https://pubmed.ncbi.nlm.nih.gov/39833361/. Acesso em: 05 mai. 2025.

BANDIĆ, R.; VODANOVIĆ, K.; *et al.* Thickness variations of thermoformed and 3D-printed clear aligners. **Acta Stomatologica Croatica**, Zagreb, v. 58, n. 2, p. 145-155, abr./jun. 2024. Disponível em: https://pubmed.ncbi.nlm.nih.gov/39036327/ Acesso em: 18 mai. 2024.

BOLLEN, A. M.; HUJOEL, P. P.; *et al.* Secular trends in adult orthodontic patients: a review of 25 years of practice. **American Journal of Orthodontics and Dentofacial Orthopedics**, St. Louis, v. 117, n. 5, p. 559-562, maio 2000. Disponível em: https://pubmed.ncbi.nlm.nih.gov/18005830/. Acesso em: 9 set. 2024.

GARCIA-FERNANDEZ, C. A.; GOMEZ-BARREIRO, S.; *et al.* Comparative study of dynamic glass transition temperature of orthodontic materials. **Polymer Testing**, Amsterdam, v. 29, n. 8, p. 1002-1006, out. 2010. Disponível em: https://www.researchgate.net/publication/229334910_Comparative_study_of_the_dynamic_glass_transition_temperature_by_DMA_and_TMDSC. Acesso em: 20 mai. 2025.

GÖRANSON, E.; SONESSON, M.; *et al.* Malocclusions and quality of life among adolescents: a systematic review and meta-analysis. **European Journal of Orthodontics**, Oxford, v. 45, n. 3, p. 295-307, jun. 2023. Disponível em: https://pubmed.ncbi.nlm.nih.gov/36995692/. Acesso em: 14 jun. 2025.

GRANT, J.; FOLEY, P.; *et al.* Forces and moments generated by 3D direct printed clear aligners of varying labial and lingual thicknesses during lingual movement of maxillary central incisor: an in vitro study. **Progress in Orthodontics**, Milan, v. 24, n. 1, p. 23, jan. 2023. Disponível em: https://pubmed.ncbi.nlm.nih.gov/37423974/. Acesso em: 3 fev. 2025.

HAHN, W.; ENGELKE, B.; *et al.* Initial forces and moments delivered by removable thermoplastic appliances during rotation of an upper central incisor. **Angle Orthodontist**, Appleton, v. 80, n. 2, p. 239-246, mar./abr. 2010. Disponível em: https://pubmed.ncbi.nlm.nih.gov/19905847/. Acesso em: 22 mai. 2025.

HAOULILI, N.; KRAVITZ, N. D.; *et al.* Has Invisalign improved? A prospective follow-up study on the efficacy of tooth movement with Invisalign. **American Journal of Orthodontics and Dentofacial Orthopedics**, St. Louis, v. 158, n. 3, p. 420-425, set. 2020. Disponível em: https://pubmed.ncbi.nlm.nih.gov/32620479/. Acesso em: 1 jun. 2025.

HENNESSY, J.; AL-AWADHI, E. A. Clear aligners generations and orthodontic tooth movement. **Journal of Orthodontics**, London, v. 43, n. 1, p. 68-76, mar. 2016. Disponível em: https://pubmed.ncbi.nlm.nih.gov/25939782/. Acesso em: 9 set. 2024.

HERTAN, E.; MCCRAY, J.; *et al.* Force profile assessment of direct-printed aligners versus thermoformed aligners and the effects of non-engaged surface patterns. **Progress in Orthodontics**, Milan, v. 23, n. 1, p. 49, jan. 2022. Disponível em: https://pubmed.ncbi.nlm.nih.gov/36443390/. Acesso em: 11 fev. 2025.

ILIADI, A.; KOLETSI, D.; *et al.* Safety considerations for thermoplastic-type appliances used as orthodontic aligners or retainers: a systematic review and meta-

analysis of clinical and in-vitro research. **Materials**, Basel, v. 13, n. 8, p. 1876, ago. 2020. Disponível em: https://pubmed.ncbi.nlm.nih.gov/32295303/. Acesso em: 5 mar. 2025.

JINDAL, P.; JUNEJA, M.; *et al.* Mechanical and geometric properties of thermoformed and 3D printed clear dental aligners. **American Journal of Orthodontics and Dentofacial Orthopedics**, St. Louis, v. 156, n. 5, p. 694-701, nov. 2019. Disponível em: https://www.ajodo.org/article/S0889-5406(19)30457-3. Acesso em: 22 jan. 2024.

JINDAL, P.; WORCESTER, F.; *et al.* Mechanical behaviour of 3D printed vs thermoformed clear dental aligner materials under non-linear compressive loading using FEM. **Journal of the Mechanical Behavior of Biomedical Materials**, Amsterdam, v. 112, p. 104045, fev. 2020. Disponível em: https://pubmed.ncbi.nlm.nih.gov/31677678/ Acesso em: 15 fev. 2025.

JOFFE, L. Invisalign: early experiences. **Journal of Orthodontics**, London, v. 30, n. 4, p. 348-352, dez. 2003. Disponível em: https://pubmed.ncbi.nlm.nih.gov/14634176/. Acesso em: 30 mar. 2025.

KESLING, H. D. The philosophy of the tooth positioning appliance. **American Journal of Orthodontics and Oral Surgery**, St. Louis, v. 31, n. 6, p. 297-306, jun. 1945. Disponível em: https://www.sciencedirect.com/science/article/pii/0096634745901013?via%3Dihub. Acesso em: 12 set. 2024.

KIYAK, H. A. Does orthodontic treatment affect patients' quality of life? **Journal of Dental Education**, Chicago, v. 72, n. 8, p. 886-894, ago. 2008. Disponível em: https://pubmed.ncbi.nlm.nih.gov/18676797/. Acesso em: 18 dez. 2024.

KO, J.; BLOOMSTEIN, R. D.; *et al.* Effect of build angle and layer height on the accuracy of 3-dimensional printed dental models. **American Journal of Orthodontics and Dentofacial Orthopedics**, St. Louis, v. 160, n. 3, p. 451-458 e452, set. 2021. Disponível em: https://pubmed.ncbi.nlm.nih.gov/34456006/ Acesso em: 22 fev. 2025.

KOENIG, N.; CHOI, J. Y.; *et al.* Comparison of dimensional accuracy between direct-printed and thermoformed aligners. **Korean Journal of Orthodontics**, Seoul, v. 52, n. 4, p. 249-257, out. 2022. Disponível em: https://pubmed.ncbi.nlm.nih.gov/35466087/ Acesso em: 30 mai. 2025.

KOHLDA, N.; IIJIMA, M.; *et al.* Effects of mechanical properties of thermoplastic materials on the initial force of thermoplastic appliances. **Angle Orthodontist**, Appleton, v. 83, n. 4, p. 476-483, jul./ago. 2013. Disponível em: https://pubmed.ncbi.nlm.nih.gov/23035832/. Acesso em: 18 set. 2024

KOLETSI, D.; PANAYI, N.; *et al.* In vivo aging-induced surface roughness alterations of Invisalign(®) and 3D-printed aligners. **Journal of Orthodontics**, London, v. 50, n. 4, p. 352-360, dez. 2023. Disponível em: https://pubmed.ncbi.nlm.nih.gov/36573484/. Acesso em: 9 fev. 2025.

KUMAR, S. M. Cytotoxicity of 3D printed materials: an in vitro study. **Journal of Clinical Orthodontics**, Chicago, v. 53, n. 7, p. 420-427, jul. 2019. Disponível em: https://www.semanticscholar.org/paper/Cytotoxicity-of-3D-Printed-Materials%3A-An-In-Vitro-Kumar/66a1b505e12155cf45a6ebf38a51784ce5846b2c. Acesso em: 12 mar. 2025.

KUNTZ, L.; ARANDA, L.; *et al.* Effects of aging on the tensile strength and surface condition of orthodontic aligners: a comparative study of five models. **European Journal of Orthodontics**, Oxford, v. 46, n. 6, p. 653-662, nov. 2024. Disponível em: https://pubmed.ncbi.nlm.nih.gov/39540439/. Acesso em: 15 jan. 2025.

LANDIS, J. R.; KOCH, G. G. The measurement of observer agreement for categorical data. **Biometrics**, Washington, v. 33, n. 1, p. 159-174, mar. 1977. Disponível em: https://pubmed.ncbi.nlm.nih.gov/843571/. Acesso em: 20 fev. 2025.

LEE, S. Y.; KIM, H.; *et al.* Thermo-mechanical properties of 3D printed photocurable shape memory resin for clear aligners. **Scientific Reports**, London, v. 12, n. 1, p. 6246, jul. 2022. Disponível em: https://pubmed.ncbi.nlm.nih.gov/35428796/. Acesso em: 11 abr. 2025.

LEVRINI, L.; MANGANO, A.; *et al.* Periodontal health status in patients treated with the Invisalign(®) system and fixed orthodontic appliances: a 3 months clinical and microbiological evaluation. **European Journal of Dentistry**, Heidelberg, v. 9, n. 3, p. 404-410, jul./set. 2015. Disponível em: https://pubmed.ncbi.nlm.nih.gov/26430371/ Acesso em: 28 mar. 2025.

LINJAWI, A. I.; ABUSHAL, A. M. Adaptational changes in clear aligner fit with time. **Angle Orthodontist**, Appleton, v. 92, n. 2, p. 220-225, mar./abr. 2022. Disponível em: https://pubmed.ncbi.nlm.nih.gov/35168255/. Acesso em: 5 jan. 2025.

LOMBARDO, L.; ARREGHINI, A.; *et al.* Predictability of orthodontic movement with orthodontic aligners: a retrospective study. **Progress in Orthodontics**, Milan, v. 18, n. 1, p. 35, jan. 2017. Disponível em: https://pubmed.ncbi.nlm.nih.gov/29130127/. Acesso em: 9 mar. 2025.

LOW, B.; LEE, W.; *et al.* Ultrastructure and morphology of biofilms on thermoplastic orthodontic appliances in 'fast' and 'slow' plaque formers. **European Journal of Orthodontics**, Oxford, v. 33, n. 5, p. 577-583, out. 2011. Disponível em: https://pubmed.ncbi.nlm.nih.gov/21187528/. Acesso em: 14 mai. 2025.

MALEKI, E.; BAGHERIFARD, S.; *et al.* Correlation of residual stress, hardness and surface roughness with crack initiation and fatigue strength of surface treated additive manufactured AlSi10Mg: experimental and machine learning approaches. **Journal of Materials Research and Technology**, Amsterdam, v. 24, p. 3265-3283, set. 2023. Disponível em: https://www.sciencedirect.com/science/article/pii/S2238785423006555?dgcid=rss_sd_all&. Acesso em: 7 mai. 2025.

MASPERO, C.; TARTAGLIA, G. M. 3D Printing of Clear Orthodontic Aligners: Where We Are and Where We Are Going. **Materials**, Basel, v. 13, p. 1234, fev. 2020. Disponível em: https://pubmed.ncbi.nlm.nih.gov/33217905/. Acesso em: 10 mar. 2025.

MILOVANOVIĆ, A.; SEDMAK, A.; *et al.* The effect of time on mechanical properties of biocompatible photopolymer resins used for fabrication of clear dental aligners. **Journal of the Mechanical Behavior of Biomedical Materials**, Amsterdam, v. 119, p. 104494, dez. 2021. Disponível em: https://pubmed.ncbi.nlm.nih.gov/33813333/. Acesso em: 15 jan. 2025.

MOHER, D.; LIBERATI, A.; *et al.* Preferred reporting items for systematic reviews and meta-analyses: the PRISMA statement. **PLoS Medicine**, San Francisco, v. 6, n. 7, p. e1000097, jul. 2009. Disponível em: https://pubmed.ncbi.nlm.nih.gov/19621072/. Acesso em: 22 fev. 2025.

MONISHA, J.; PETER, E. Efficacy of clear aligner wear protocols in orthodontic tooth movement - a systematic review. **European Journal of Orthodontics**, Oxford, v. 46, n. 3, p. 201-214, jun. 2024. Disponível em: https://pubmed.ncbi.nlm.nih.gov/38666743/. Acesso em: 28 abr. 2025.

MOSHIRI, M.; KRAVITZ, N.; *et al.* Invisalign eighth-generation features for deep-bite correction and posterior arch expansion. **Seminars in Orthodontics**, Philadelphia, v. 27, p. 45-54, jan. 2021. Disponível em: https://www.researchgate.net/publication/354455947_Invisalign_eighth-generation_features_for_deep-bite_correction_and_posterior_arch_expansion.. Acesso em: 9 mai. 2025.

NAKORNNOI, T.; SRIRODJANAKUL, W.; *et al.* The biomechanical effects of clear aligner trimline designs and extensions on orthodontic tooth movement: a systematic review. **BMC Oral Health**, London, v. 24, n. 1, p. 1523, dez. 2024. Disponível em: https://pubmed.ncbi.nlm.nih.gov/39707339/. Acesso em: 12 mai. 2025.

PAPADOPOULOU, A. K.; CANTELE, A.; *et al.* Changes in roughness and mechanical properties of Invisalign(®) appliances after one- and two-weeks use. **Materials**, Basel, v. 12, n. 15, p. 2456, ago. 2019. Disponível em: https://pubmed.ncbi.nlm.nih.gov/31357697/. Acesso em: 20 set. 2024.

PAPADOPOULOU, A. K.; ZAFIRIADIS, M. A.; LEKKAS, D. Clinical effectiveness of clear aligner therapy: a systematic review. **Progress in Orthodontics**, Milan, v. 16, n. 1, p. 1-11, mar. 2015. Disponível em: https://pubmed.ncbi.nlm.nih.gov/30264270/. Acesso em: 20 set. 2024.

PARK, S. Y.; CHOI, S. H.; *et al.* Comparison of translucency, thickness, and gap width of thermoformed and 3D-printed clear aligners using micro-CT and spectrophotometer. **Scientific Reports**, London, v. 13, n. 1, p. 10921, jun. 2023. Disponível em: https://pubmed.ncbi.nlm.nih.gov/37407694/. Acesso em: 28 mai. 2025.

PHAN, X.; LING, P. H. Clinical limitations of Invisalign. **Journal of the Canadian Dental Association**, Ottawa, v. 73, n. 3, p. 263-266, mar. 2007. Disponível em: https://pubmed.ncbi.nlm.nih.gov/17439714/. Acesso em: 5 fev. 2025.

RASZEWSKI, Z.; CHOJNACKA, K.; *et al.* Mechanical properties and biocompatibility of 3D printing acrylic material with bioactive components. **Journal of Functional Biomaterials**, Basel, v. 14, n. 1, p. 25, jan. 2022. Disponível em: https://pubmed.ncbi.nlm.nih.gov/36662060/. Acesso em: 18 mar. 2025.

RIBEIRO, L. G.; ANTUNES, L. S.; *et al.* Impact of malocclusion treatments on oral health-related quality of life: an overview of systematic reviews. **Clinical Oral Investigations**, Berlin, v. 27, n. 3, p. 907-932, mar. 2023. Disponível em: https://pubmed.ncbi.nlm.nih.gov/36602588/. Acesso em: 12 abr. 2025.

ROSSINI, G.; PARRINI, S.; *et al.* Efficacy of clear aligners in controlling orthodontic tooth movement: a systematic review. **Angle Orthodontist**, Appleton, v. 85, n. 5, p. 881-889, set. 2015. Disponível em: https://pubmed.ncbi.nlm.nih.gov/25412265/. Acesso em: 20 mai. 2025.

RYU, J. H.; KWON, J. S.; *et al.* Effects of thermoforming on the physical and mechanical properties of thermoplastic materials for transparent orthodontic aligners. **Korean Journal of Orthodontics**, Seoul, v. 48, n. 5, p. 316-325, out. 2018. Disponível em: https://pubmed.ncbi.nlm.nih.gov/30206530/ Acesso em: 28 jan. 2025.

SAFAVI, M.; BORDBAR-KHIABANI, A.; *et al.* Additive Manufacturing: An Opportunity for the Fabrication of Near-Net-Shape NiTi Implants. **Journal of Manufacturing and Materials Processing**, Basel, v. 6, p. 65, jul. 2022. Disponível em: https://www.researchgate.net/publication/361329478_Additive_Manufacturing_An_Opportunity_for_the_Fabrication_of_Near-Net-Shape_NiTi_Implants. Acesso em: 10 mai. 2025.

SARI, T.; CAMCI, H.; *et al.* Evaluation of mechanical changes to clear aligners caused by exposure to different liquids. **Australasian Orthodontic Journal**, Sydney, v. 40, p. 75-86, mar. 2025. Disponível em: https://www.researchgate.net/publication/361329478_Additive_Manufacturing_An_Opportunity_for_the_Fabrication_of_Near-Net-Shape_NiTi_Implants. Acesso em: 15 mai. 2025.

SAYAHPOUR, B.; ZINELIS, S.; *et al.* Effects of intraoral aging on mechanical properties of directly printed aligners vs. thermoformed aligners: an in vivo prospective investigation. **European Journal of Orthodontics**, Oxford, v. 46, n. 1, p. 35-44, jan. 2024. Disponível em: https://pubmed.ncbi.nlm.nih.gov/37936263/. Acesso em: 20 fev. 2025.

SCHÜNEMANN, H. B.; GUYATT, G.; OXMAN, A. GRADE handbook for grading quality of evidence and strength of recommendations. **GRADE Working Group**, Oxford, 2013. Disponível em: https://gdt.gradepro.org/app/handbook/handbook.html. Acesso em: 5 jan. 2025.

SHARIFA, M.; BOURAUELA, C.; *et al.* Force system of 3D-printed orthodontic aligners made of shape memory polymers: an in vitro study. **Virtual and Physical Prototyping**, London, v. 19, p. e2361857, jan. 2024. Disponível em: https://www.researchgate.net/publication/381326003_Force_system_of_3D-printed_orthodontic_aligners_made_of_shape_memory_polymers_an_in_vitro_study. Acesso em: 12 fev. 2025.

SHIREY, N.; MENDONCA, G.; *et al.* Comparison of mechanical properties of 3-dimensional printed and thermoformed orthodontic aligners. **American Journal of Orthodontics and Dentofacial Orthopedics**, St. Louis, v. 163, n. 5, p. 720-728, maio 2023. Disponível em: https://pubmed.ncbi.nlm.nih.gov/37142355/. Acesso em: 8 jun. 2025.

ŠIMUNOVIĆ, L.; ČEKALOVIĆ AGOVIĆ, S.; *et al.* Color and chemical stability of 3D-printed and thermoformed polyurethane-based aligners. **Polymers**, Basel, v. 16, n. 8, p. 1245, abr. 2024. Disponível em: https://pubmed.ncbi.nlm.nih.gov/38674987/. Acesso em: 20 mai. 2025.

SOUMAN, O. Comparison of thickness between thermoformed and printed orthodontic aligners. **Loma Linda University Electronic Theses, Dissertations & Projects**, Loma Linda, p. 2665, 2023. Disponível em: https://scholarsrepository.llu.edu/etd/2665/. Acesso em: 15 mai. 2025.

SPANGLER, T.; AMMOUN, R.; *et al.* The effect of crowding on the accuracy of 3-dimensional printing. **American Journal of Orthodontics and Dentofacial Orthopedics**, St. Louis, v. 164, n. 6, p. 879-888, dez. 2023. Disponível em: https://scholarsrepository.llu.edu/etd/2665/ Acesso em: 10 mai. 2025.

SRIVASTAVA, R.; JYOTI, B.; *et al.* Sequential removal orthodontics: an alternative approach. **International Journal of Contemporary Medicine Surgery and Radiology**, New Delhi, v. 22, p. 32-36, fev. 2017. Disponível em: https://www.researchgate.net/publication/320798825_Sequential_Removal_Orthodontics_An_Alternative_Approach. Acesso em: 5 jan. 2025.

SUTER, F.; ZINELIS, S.; *et al.* Roughness and wettability of aligner materials. **Journal of Orthodontics**, London, v. 47, n. 3, p. 223-231, set. 2020. Disponível em: https://pubmed.ncbi.nlm.nih.gov/32615846/. Acesso em: 20 fev. 2025.

WAJEKAR, N.; PATHAK, S.; *et al.* Rise & review of Invisalign clear aligner system. **IP Indian Journal of Orthodontics and Dentofacial Research**, Pune, v. 8, p. 7-11, jan. 2022. Disponível em: https://www.researchgate.net/publication/359621700_Rise_review_of_invisalign_clear_aligner_system. Acesso em: 15 mar. 2025.

WANG, Y.; ZHOU, S.; *et al.* Comparison of treatment effects between clear aligners and fixed appliances in patients treated with miniscrew-assisted molar distalization. **European Journal of Orthodontics**, Oxford, v. 46, n. 3, p. 245-256, jun. 2024. Disponível em: https://pubmed.ncbi.nlm.nih.gov/38733349/. Acesso em: 28 mai. 2025.

WANG, Z.; LIU, J.; *et al.* The study of thermal, mechanical and shape memory properties of chopped carbon fiber-reinforced TPI shape memory polymer composites. **Polymers**, Basel, v. 9, n. 11, p. 1234, nov. 2017. Disponível em: https://pubmed.ncbi.nlm.nih.gov/30965901/. Acesso em: 5 mai. 2025.

WEIR, T. Clear aligners in orthodontic treatment. **Australian Dental Journal**, Sydney, v. 62 Suppl 1, p. 58-62, jun. 2017. Disponível em: https://pubmed.ncbi.nlm.nih.gov/28297094/. Acesso em: 12 mai. 2025.

WENDL, T.; WENDL, B.; *et al.* An analysis of initial force and moment delivery of different aligner materials. **Biomedizinische Technik (Berl)**, Berlin, v. 70, n. 3, p. 259-267, mar. 2025. Disponível em: https://pubmed.ncbi.nlm.nih.gov/40019868/. Acesso em: 15 mai. 2025.

ZHENG, M.; LIU, R.; *et al.* Efficiency, effectiveness and treatment stability of clear aligners: a systematic review and meta-analysis. **Orthodontics & Craniofacial Research**, Oxford, v. 20, n. 3, p. 127-133, set. 2017. Disponível em: https://pubmed.ncbi.nlm.nih.gov/28547915/. Acesso em: 20 mar. 2025.

ZINELIS, S.; PANAYI, N.; *et al.* Comparative analysis of mechanical properties of orthodontic aligners produced by different contemporary 3D printers. **Orthodontics & Craniofacial Research**, Oxford, v. 25, n. 3, p. 336-341, set. 2022. Disponível em: https://pubmed.ncbi.nlm.nih.gov/34569692/. Acesso em: 12 mai. 2025.